

ScholarWorks@GSU

The Effects Of Environmental Pollutants On Adipogenesis In The 3T3-L1 Model

| | |
|---------------|--|
| Authors | Wang, Jing |
| Citation | Wang, Jing. 2015. "The Effects Of Environmental Pollutants On Adipogenesis In The 3T3-L1 Model." Georgia State University. https://doi.org/10.57709/7899703 |
| DOI | https://doi.org/10.57709/7899703 |
| Download date | 2026-04-12 22:26:10 |
| Link to Item | https://hdl.handle.net/20.500.14694/1959 |

THE EFFECTS OF ENVIRONMENTAL POLLUTANTS ON ADIPOGENESIS IN THE 3T3-L1 MODEL

by

JING WANG

Under the Direction of Roberta Attanasio (PhD)

ABSTRACT

Humans are continuously exposed to mixtures of environmental pollutants. Polycyclic aromatic hydrocarbons (PAHs), such as 2-naphthol, and heavy metals, such as lead, are some of these pollutants. Results from epidemiological studies show associations between exposure to 2-naphthol, exposure to lead, and obesity. However, the individual and combined effects of 2-naphthol and lead on fat cell development (adipogenesis) have not been directly characterized in a biological system. In this study, we evaluated the effects of 2-naphthol and/or lead on adipogenesis using mouse 3T3-L1 cells.

Cells were exposed to different doses of 2-naphthol and/or lead. Induced terminal differentiation was evaluated by cell morphology, lipid production, and mRNA expression of

marker genes characteristic of either early adipocyte differentiation: CCAAT-enhancer-binding protein β (C/EBP β), insulin receptor substrate 2 (IRS2), and sterol responsive element binding protein 1 c (SREBP1c); or terminal differentiation: C/EBP α , peroxisome proliferator-activated receptor- γ (PPAR γ), and fatty acid binding protein 4 (aP2). Production of antimicrobial peptide cathelicidin (Camp), which is produced by differentiating adipocytes and modulates inflammation and immunity, was also evaluated.

Cell morphology changes and increased lipid accumulation indicated that, individually, 2-naphthol and lead induced 3T3-L1 differentiation; however, the highest dose of lead (10 μ M) showed the lowest induction level. During terminal differentiation, 2-naphthol and low doses of lead increased C/EBP α , PPAR γ , and aP2 expression, whereas 10 μ M lead suppressed PPAR γ and aP2. During early differentiation, 2-naphthol stimulated C/EBP β , IRS2, and SREBP1c expression, while lead upregulated C/EBP α and aP2. The 2-naphthol/10 μ M lead mixture induced a counterbalancing effect on 3T3-L1 adipogenesis, where 10 μ M lead suppressed 2-naphthol-induced adipogenesis. Moreover, 2-naphthol elevated Camp expression in a dose-dependent manner, whereas lead slightly increased Camp at lower doses but suppressed it at 10 μ M. The 2-naphthol/10 μ M lead mixture showed no effect on Camp expression.

In conclusion, 2-naphthol and low lead doses accelerate adipocyte differentiation and Camp production in 3T3-L1 cells; however, high doses of lead attenuate the induction. This effect of lead at high dose counterbalances the upregulation of adipocyte differentiation and Camp production by 2-naphthol. Together, these findings indicate that 2-naphthol and lead play potential roles in the development of inflammation and obesity.

INDEX WORDS: Polycyclic aromatic hydrocarbon, Heavy metal, Adipocyte differentiation,
Antimicrobial peptide

THE EFFECTS OF ENVIRONMENTAL POLLUTANTS ON ADIPOGENESIS IN THE 3T3-L1 MODEL

by

JING WANG

A Dissertation Submitted in Partial Fulfillment of the Requirements for the Degree of

Doctor of Philosophy

in the College of Arts and Sciences

Georgia State University

2015

Copyright by
Jing Wang
2015

THE EFFECTS OF ENVIRONMENTAL POLLUTANTS ON ADIPOGENESIS IN THE 3T3-L1 MODEL

by

JING WANG

Committee Chair: Roberta Attanasio

Committee: Franco Scinicariello

Phang-Cheng Tai

Sang-Moo Kang

Electronic Version Approved:

Office of Graduate Studies

College of Arts and Sciences

Georgia State University

December 2015

DEDICATION

To Mom, for her unconditional and unimaginable love to let me go and explore myself in a country that seemed a world away.

To Dad, for using the United Nations Educational, Scientific and Cultural Organization “reward” for curing cancer as motivation during my childhood, which led me to pursue research in the biological sciences – never tell him the truth, please!

To Dawang, for his companionship and patience over the years, and for waiting for me since we first met.

To Tetsuo-san’s sportsman and great basketball player, Mitsui Hisashi, for his spiritual encouragement throughout the way – my light in the dark.

ACKNOWLEDGEMENTS

This work is the culmination of the efforts of many individuals who have encouraged and helped me to achieve this goal.

I wish to give my deepest gratitude to my advisor, Dr. Roberta Attanasio. I am grateful to her for her strict validations and high research standard, which established my critical thinking about science and the correct way to do research. I feel very lucky to have an advisor who not only patiently guided me throughout the completion of my PhD career, but also revealed to me a variety of possible lifestyles with a PhD degree in America and in European countries.

I also give a heartfelt thanks to my committee members. I am extremely grateful to Dr. Franco Scinicariello for the abundant help and assistance given to me over the years. I give a special thanks to Dr. Phang-Cheng Tai, who recruited me to pursue this degree at GSU. I express my gratitude to Dr. Sang-Moo Kang, who continuously encouraged me and always congratulated me every step of the way, even for my small progresses.

I would like to acknowledge all my lab mates, both past and present, Dr. Feda Masseoud, Dr. Doan Nguyen, Anton Chesnokov, Alan Copenhaver, Rashash Sanghvi, Asia Bright and Rachel Mirpour, for their generous support and friendship.

A very special thanks to my friends, Nan Zhao, Jie Xu, Xiangyu Yao, Dan Cui, Lei Zhong, Wen Li, and Hesong Han. I am very glad that we shared so many important moments and precious memories along the way.

Finally, I'd be remiss if I did not acknowledge my family for their love and patience. Without the unimaginable support and understanding from my Mom, Dad and my husband, none of this would have been possible.

TABLE OF CONTENTS

| | |
|--|------------------|
| ACKNOWLEDGEMENTS..... | v |
| LIST OF TABLES..... | xiii |
| LIST OF FIGURES..... | xiv |
| LIST OF ABBREVIATIONS..... | xvi |
| 1 Chapter 1: Introduction | 1 |
| 1.1 Environmental pollution: an increasing global issue | 1 |
| 1.2 Environmental pollutants and their effects on health..... | 2 |
| <i>1.2.1 Types and sources of environmental pollutants.....</i> | <i>2</i> |
| <i>1.2.2 Diseases associated with environmental pollutants.....</i> | <i>6</i> |
| 1.3 Polycyclic aromatic hydrocarbon: 2-naphthol (2-NAP)..... | 7 |
| <i>1.3.1 Polycyclic aromatic hydrocarbons</i> | <i>7</i> |
| <i>1.3.2 Health effects of PAHs</i> | <i>8</i> |
| <i>1.3.3 2-NAP as an endocrine disruptor.....</i> | <i>9</i> |
| 1.4 Heavy metal: lead (Pb)..... | 10 |
| <i>1.4.1 Lead exposure in the human population</i> | <i>10</i> |
| <i>1.4.2 Health effects and mechanisms of lead toxicity.....</i> | <i>12</i> |
| 1.5 Obesity: a pandemic disease..... | 13 |
| 1.6 Antimicrobial peptides and adipocytes | 14 |

| | | |
|-------|---|----|
| 1.6.1 | <i>AMP definition and origin</i> | 14 |
| 1.6.2 | <i>Groups and mechanisms of action</i> | 15 |
| 1.6.3 | <i>Role of adipocytes in immunity</i> | 16 |
| 1.7 | Adipocyte differentiation | 18 |
| 1.7.1 | <i>Adipogenesis is a multiple-stage event</i> | 18 |
| 1.7.2 | <i>The transcriptional cascade of adipogenesis</i> | 20 |
| 1.7.3 | <i>Other factors that control adipogenesis</i> | 21 |
| 1.7.4 | <i>Mouse 3T3-L1 preadipocyte Model</i> | 22 |
| 1.8 | Research overview | 23 |
| 2 | Chapter 2: The polycyclic Aromatic Hydrocarbon 2-Naphthol Contributes to Adipocyte Differentiation in the Mouse 3T3-L1 Model | 25 |
| 2.1 | Summary | 25 |
| 2.2 | Introduction | 27 |
| 2.3 | Materials and methods | 28 |
| 2.3.1 | <i>Materials</i> | 28 |
| 2.3.2 | <i>Experimental design</i> | 28 |
| 2.3.3 | <i>Cell culture and differentiation</i> | 31 |
| 2.3.4 | <i>Oil Red O staining</i> | 32 |
| 2.3.5 | <i>XTT assays</i> | 33 |

| | | |
|-------|---|----|
| 2.3.6 | <i>Quantitative real-time reverse transcription-polymerase chain reaction (Real-Time PCR)</i> | 33 |
| 2.3.7 | <i>Statistical analysis</i> | 35 |
| 2.4 | Results | 35 |
| 2.4.1 | <i>Effect of 2-NAP on cell viability</i> | 35 |
| 2.4.2 | <i>Effect of 2-NAP on cell morphology and lipid accumulation</i> | 36 |
| 2.4.3 | <i>Effect of 2-NAP on adipogenic gene expression</i> | 42 |
| 2.4.4 | <i>Effect of 2-NAP on signaling and transcriptional cascade of adipogenesis</i> | 48 |
| 2.5 | Discussion | 55 |
| 3 | Chapter 3: The effect of lead on 3T3-L1 adipocyte differentiation is non-monotonic | 59 |
| 3.1 | Summary..... | 59 |
| 3.2 | Introduction | 61 |
| 3.3 | Materials and methods..... | 62 |
| 3.3.1 | <i>Materials</i> | 62 |
| 3.3.2 | <i>Experimental design</i> | 62 |
| 3.3.3 | <i>Cell culture and differentiation</i> | 65 |
| 3.3.4 | <i>Oil Red O staining</i> | 66 |
| 3.3.5 | <i>XTT assays</i> | 66 |

| | | |
|--------------|---|-----------|
| 3.3.6 | <i>Quantitative real-time reverse transcription-polymerase chain reaction</i> | |
| | <i>(Real-Time PCR)</i> | 67 |
| 3.3.7 | <i>Statistical analysis</i> | 68 |
| 3.4 | Results | 68 |
| 3.4.1 | <i>The induction of lead on lipid accumulation</i> | 68 |
| 3.4.2 | <i>Negative regulation of lead on cell proliferation</i> | 72 |
| 3.4.3 | <i>Effect of lead on adipogenic genes</i> | 75 |
| 3.4.4 | <i>Effect of lead on signaling and transcriptional cascade of adipogenesis</i> ... | 78 |
| 3.5 | Discussion | 89 |
| 4 | Chapter 4: High Concentration of Lead Suppresses Adipocyte Differentiation | |
| | Induced by 2-Naphthol in the 3T3-L1 Model | 93 |
| 4.1 | Summary | 93 |
| 4.2 | Introduction | 94 |
| 4.3 | Materials and Method | 95 |
| 4.3.1 | <i>Materials</i> | 95 |
| 4.3.2 | <i>Experimental design</i> | 96 |
| 4.3.3 | <i>Cell culture and differentiation</i> | 98 |
| 4.3.4 | <i>Quantitative real-time reverse transcription-polymerase chain reaction</i> | |
| | <i>(Real-Time PCR)</i> | 98 |

| | | |
|-------|---|-----|
| 4.3.5 | <i>Statistical analysis</i> | 99 |
| 4.4 | Results | 99 |
| 4.4.1 | <i>The co-effect of 2-NAP and lead on marker gene expressions of adipogenesis</i> 99 | |
| 4.5 | Discussion | 102 |
| 5 | Chapter 5: The effect of environmental pollutants on anti-microbial peptide production during adipocyte differentiation | 105 |
| 5.1 | Summary | 105 |
| 5.2 | Introduction | 106 |
| 5.3 | Materials and methods..... | 108 |
| 5.3.1 | <i>Materials</i> | 108 |
| 5.3.2 | <i>Experimental design</i> | 109 |
| 5.3.3 | <i>Cell culture and differentiation</i> | 111 |
| 5.3.4 | <i>Quantitative real-time reverse transcription-polymerase chain reaction (Real-Time PCR)</i> | 111 |
| 5.3.5 | <i>Statistical analysis</i> | 112 |
| 5.4 | Results | 113 |
| 5.4.1 | <i>The effect of 2-NAP and lead on Camp production</i> | 113 |
| 5.5 | Discussion | 116 |

6 Chapter 6: Conclusions 119

REFERENCES 125

LIST OF TABLES

| | |
|--|----|
| Table 2.1 Parameter settings for EnSpire multilabel plate reader. | 33 |
| Table 2.2 Primer/probe information for Real-Time RT-qPCR. | 35 |

LIST OF FIGURES

| | |
|--|----|
| Figure 1.1 Scheme of different stages of adipogenesis in 3T3-L1 cells. | 19 |
| Figure 2.1 Protocols for adipogenic differentiation and 2-naphthol exposure in 3T3-L1 cells.... | 30 |
| Figure 2.2 Effects of 2-NAP on 3T3-L1 cell viability. | 37 |
| Figure 2.3 Cell morphology change and lipid accumulation in 2-NAP treated 3T3-L1 cells..... | 40 |
| Figure 2.4 Quantification of lipid accumulation in 2-NAP treated 3T3-L1 cells. | 41 |
| Figure 2.5 Effects of 2-naphthol (Experiment 2-NAP D0-8) on adipogenic gene expression at day 8 of 3T3-L1 differentiation. | 45 |
| Figure 2.6 Effects of 2-naphthol in the presence of insulin (Insulin+2-NAP) on adipogenic gene expression at day 8 of 3T3-L1 differentiation..... | 46 |
| Figure 2.7 Effects of 2-naphthol on IRS2, SREBP1c, and adipogenic gene expression at day 2 of 3T3-L1 differentiation. | 51 |
| Figure 2.8 Effects of 2-naphthol in the presence or absence of insulin on adipogenic gene expression at day 5 and day 8 of 3T3-L1 differentiation. | 53 |
| Figure 3.1 Protocols for adipogenic differentiation and lead exposure in 3T3-L1 cells. | 64 |
| Figure 3.2 Effects of lead on cell morphology change and lipid accumulation. | 70 |
| Figure 3.3 Quantification of lipid accumulation in lead treated 3T3-L1 cells..... | 71 |
| Figure 3.4 Effects of lead on 3T3-L1 cell viability..... | 74 |
| Figure 3.5 Effects of lead on adipogenic gene expression at day 8 of 3T3-L1 differentiation. | 77 |
| Figure 3.6 Expression of marker genes of adipogenesis during differentiation of 3T3-L1 preadipocytes induced by the standard differentiation protocol. | 80 |

| | |
|--|-----|
| Figure 3.7 Effects of lead on marker gene expression during differentiation of 3T3-L1 preadipocytes in the presence of insulin..... | 82 |
| Figure 3.8 Effects of lead on marker gene expression during differentiation of 3T3-L1 preadipocytes in the absence of insulin. | 84 |
| Figure 3.9 Effects of lead on marker gene expression in insulin signaling pathway during differentiation of 3T3-L1 preadipocytes. | 88 |
| Figure 4.1 Protocols for adipogenic differentiation and chemical exposure in 3T3-L1 cells. | 97 |
| Figure 4.2 Effects of 2-naphthol in the presence of lead on adipogenic gene expression at day 8 of 3T3-L1 differentiation. | 101 |
| Figure 5.1 Protocols for adipogenic differentiation and chemical exposure in 3T3-L1 cells. | 110 |
| Figure 5.2 Effects of BPA on adipogenic gene and Camp expressions. | 114 |
| Figure 5.3 Effects of 2-NAP and lead on Camp expression..... | 115 |

LIST OF ABBREVIATIONS

PAH: polycyclic aromatic hydrocarbons

2-NAP: 2-Naphthol

CEBPs: CCAAT-enhancer-binding proteins

PPAR γ : peroxisome proliferator-activated receptor- γ

aP2: fatty acid binding protein 4 (also known as FABP4)

IRS: insulin receptor substrate

SREBP1c: sterol responsive element binding protein 1 c

AMP: antimicrobial peptides

Camp: cathelicidin

1 Chapter 1: Introduction

1.1 Environmental pollution: an increasing global issue

Environmental pollution is caused by human activities that produce excessive harmful by-products. Such production oversteps far beyond the capacity of the environment to process and neutralize them. Environmental pollution has been a growing global issue since the onset of the Industrial Revolution during the 19th century. Technological progress facilitated the exploitation of natural resources, such as coal and fuel, and their universal utilization throughout different industries. The development of natural sciences, especially chemistry, led to a novel model of developing new chemicals—search or create first, and understand later—which impacted the industry in the 20th century, and still does. In contrast, relatively little information has been generated on the effects of these chemicals on the environment and health.

In February 2015, the Centers for Disease Control and Prevention (CDC) updated the biomonitoring data of national exposure to environmental chemicals for the *Fourth National Report on Human Exposure to Environmental Chemicals, 2009*. This report presents exposure data for a total of 265 chemicals measured in blood and urine samples from participants in the National Health and Nutrition Examination Survey (NHANES) since 1999 (CDC 2015). Among these 265 environmental chemicals, several chemicals, such as bisphenol A (BPA), polychlorinated biphenyls (PCBs), and o,p'-Dichlorodiphenyltrichloroethane (DDT) had already been reported to have adverse effects on human health (Schug et al. 2011).

1.2 Environmental pollutants and their effects on health

1.2.1 Types and sources of environmental pollutants

Environmental pollutants exist in gaseous, solid, or liquid form, and are usually present in the environment as a mixture of different types of chemicals. Environmental pollutants can be simply categorized into three major types: soil pollutants, water pollutants and air pollutants.

- Soil pollutants, found on the earth's land surface, are mainly heavy metals, crude oil and coal tars, pesticides and herbicides, and organic or radioactive chemicals, deriving from mining, agricultural materials, and household and industrial waste.
- Water pollutants are contaminants that reach the water system including rivers, lakes, oceans, and other water sources.
- Air pollutants, which exist in the earth's atmosphere, are mainly generated by human activities, such as burning of fossil fuel and coal, smoking, industrial and vehicle exhausts, and certain household products. Carbon monoxide, lead, nitrogen dioxide, ozone, sulfur dioxide, and particulate matters are the most common air pollutants.

Based on the cellular mechanisms by which environmental pollutants exert their adverse health effects, environmental pollutants can be grouped into three categories:

1. Pro-oxidants and free radicals generators (e.g., ozone and nitrogen oxides)
2. Endocrine disruptors (e.g., BPA)
3. Heavy metal (e.g., cadmium)

1.2.1.1 Pro-oxidants and free radicals generators

Some environmental pollutants are potential oxidants, and are able to directly or indirectly oxidize tissue and cellular components, such as lipids, proteins and DNAs, or to

generate reactive oxygen species (ROS) and free radicals, resulting in oxidative stress and inflammation, which finally lead to harmful health effects. Ozone, nitrogen oxides, carbon monoxide, sulfur oxides, and particulate matter less than 2.5 and 10 μm in diameter ($\text{PM}_{2.5}$, PM_{10}) all belong to this category. The ROS or free oxygen and nitrogen radicals induced by ozone and nitrogen oxides are able to initiate lipid peroxidation from unsaturated and polyunsaturated fatty acids, and thiol proteins. This biological process produces various byproducts that may promote oxidative damage to the target tissues and modify the function of target proteins. Ozone and PM initiated redox state is able to activate nuclear factor- κB (NF κB), a transcription regulator that controls gene transcription of pro-inflammatory cytokines and proteins involved in inflammation and immune responses (Yang and Omaye 2009).

This category of environmental pollutants is mainly generated from the combustion of fossil fuels. Nitrogen oxides and volatile organic compounds are emitted from fuel-based transportation and stationary combustion sources, such as power plants. Carbon monoxide results from incomplete combustion, as well as from vehicle exhaust. Sulfur oxides are produced by combustion of coal and heavy oils or smelting metal ores that contain Sulphur. The major sources of PM are motor vehicles, industrial processes, fuel combustion by power plants, fires, and dust from natural wind (Kampa and Castanas 2008; Katsouyanni 2003; Poschl 2005).

1.2.1.2 Endocrine disruptors

Endocrine-disrupting chemicals (EDCs), also called endocrine disruptors, are a large group of natural or synthetic chemicals that show hormone-like activities. Because of these hormone-like characteristics, this group of chemicals is capable of interfering with endogenous hormone homeostasis (synthesis, secretion, transport, and metabolism) and physiological regulatory

functions of endocrine signaling pathways and systems. The adverse effects of EDCs on glands and hormone-regulated functions include complications of growth, reproduction, stress response, sex and gender development, and insulin function (Newbold 2010). EDCs are commonly found in many industrial and agricultural products, including coolants and lubricants such as polychlorinated biphenyls (PCBs); plasticizer like bisphenol A (BPA) and di-2-ethylhexyl phthalate; herbicides, fungicides and pesticides such as carbamates, endrin, lindane and dichlorodiphenyltrichloroethane (DDT). EDCs may also be present in household and everyday products—including detergents, flame retardants (i.e. polybrominated biphenyls), plastics, toys, pharmaceuticals, food, and solvents in cosmetics.

EDCs exert their endocrine disrupting effects by imitating or antagonizing the actions of steroid hormones, including testosterone, estrogen, thyroid hormone, progesterone, cortisol, lipids or fatty acids. Through binding to nuclear hormone receptors, EDCs can alter target gene transcription (Diamanti-Kandarakis et al. 2009; Janesick and Blumberg 2011). One example is the synthetic estrogen diethylstilbestrol (DES), used during the 1940s-1970s for pregnant women. Prenatal and developmental exposure to DES results in teratogenic or carcinogenic syndrome in the female reproductive tract. The DES toxic effect on gene expression and tissue differentiation is mediated by the estrogen receptor alpha (Couse et al. 2001).

EDCs can also act through mechanisms independent of nuclear receptors, interacting with nonsteroid receptors and coactivators in the transcriptional complex, as well as participating in steroid synthesis and metabolism pathways (Tabb and Blumberg 2006). For example, a study using a rat model demonstrated that 1,1-dichloro-2,2-bis(p-chlorophenyl)ethylene (the metabolite of DDT) increases the transcriptional activity of steroid and xenobiotic

receptor/rodent pregnane X receptor and constitutive androstane receptor, two nuclear receptors that are important to regulate hormone metabolism (Wyde et al. 2003).

Other mechanisms include direct impact on gene expression profiles during development and alterations of DNA methylation, both causing transgenerational effects (Anway and Skinner 2008; Moral et al. 2008). Prenatal exposure to BPA in rats alters the mammary glands morphology, changing the number of undifferentiated epithelial structures. Moreover, it also modifies the expression of genes at different ages, such as down-regulation of *Gad1*, a gene involved in cell communication, and up-regulation of several immune system genes like *Cd3d* and *Sipi* (Moral et al. 2008). Fetal BPA exposure triggers changes in methylated genomic DNA and alters gene expression patterns in postnatal and adult mammary glands, resulting in elevated level of histone methylation at the promotor region of the alpha-lactalbumin gene (Dhimolea et al. 2014).

1.2.1.3 Heavy metals

Heavy metals, such as arsenic, cadmium, lead, mercury, nickel, cesium, chromium and copper, naturally exist as components of earth's crust. Because of their non-biodegradable characteristics, heavy metals can persist in the environment for a long time, therefore they are widespread in air, soil, and water. Heavy metal-based consumer products including paint, glasses, ceramics, cosmetics, toys, certain spices, contaminated food, tobacco and cigarettes, are all considered potential sources of heavy metal exposure (CDC 2002; Meyer et al. 2008; Sainio et al. 2000; Woolf and Woolf 2005). Heavy metals are relatively poorly absorbed in the body; however, once absorbed, they accumulate in the body resulting in the disruption of normal cellular processes.

The adverse health effects of heavy metals are attributed to both their ability to generate free radicals leading to DNA damage, lipid peroxidation, and depletion of protein sulfhydryls (Valko et al. 2005), and the ability to substitute polyvalent cations such as zinc, calcium, copper and magnesium that are important for regulatory and enzymatic function in cells, including mediators in catalysis, charge carriers, as well as basic structural components of protein complex (Kampa and Castanas 2008). Cadmium is able to utilize the transport mechanisms developed for calcium, iron and magnesium, influencing the homeostasis of these essential metals (Jihen el et al. 2009). Based on this benefit, cadmium can be retained at a high concentration in smooth muscle cells, resulting in interrupted calcium cation flux as well as cytotoxic effects (Abu-Hayyeh et al. 2001; Prozialeck et al. 2008). As one of calcium-like metals, lead can compete with calcium for transport across cellular membranes, including endoplasmic reticulum and mitochondria membrane, leading to abnormal changes in cytosolic calcium ions (Alissa and Ferns 2011; Goldstein 1993).

1.2.2 Diseases associated with environmental pollutants

The toxicity of a chemical is related to its concentration as well as individual susceptibility. Thus, the presence of an environmental chemical in a person's blood and urine does not necessarily mean it is causing adverse effects on human health. However, a variety of epidemiological data has revealed that human exposure to environmental pollutants is associated with a wide range of diseases, including allergic diseases, arthritis and inflammatory diseases, autoimmune diseases, diabetes, neurodegenerative disorders such as Parkinson's disease, reproductive function disorders such as testicular dysgenesis syndrome, polycystic ovary syndrome, premature ovarian failure, as well as cancers.

1.3 Polycyclic aromatic hydrocarbon: 2-naphthol (2-NAP)

1.3.1 Polycyclic aromatic hydrocarbons

Polycyclic aromatic hydrocarbons (PAHs) are a family of organic chemicals which contain two or more fused aromatic (benzene) rings. The conjoined benzene rings are the basic PAH, which are also called the parent or unsubstituted PAHs. The derivatives or substituted PAHs contain substituted groups, such as nitrogen, sulfur, oxygen atoms, or alkyl chains, on exterior carbon atoms (Boehm 2006).

Based on the number of aromatic rings, PAHs can be simply divided into two groups: the low-molecular-weight PAHs consisting of two to three rings, and the high-molecular-weight compounds with four or more fused benzene rings (Law et al. 2002). Low-molecular-weight PAHs are most likely to exist in the air and are biodegradable (Law et al. 2002), whereas high-molecular-weight PAHs tend to exist in soils and sediments (Abbondanzi et al. 2005; Manoli and Samara 1999), thus persisting for a longer time in the environment.

1.3.1.1 Exposure sources to human

PAHs are ubiquitous environmental contaminants formed naturally or anthropogenically. Naturally-occurring PAHs are mainly from wildfires, volcanic eruptions, and thermal geological reactions (Maliszewska-Kordybach 1999), as well as from aromatization reactions that occurred in microorganisms and non-biological chemical processes (Boehm 2006). Anthropogenic PAHs result from incomplete combustion of organic matters. Fossil fuels, coal, wood, tobacco products, heating and power generation, industry waste, and fuel-based transportation, especially car emissions, are important sources of anthropogenic PAHs (ATSDR 1995). Indoor sources of PAHs

include incomplete combustion of fuels or natural gas for heating and cooking, tobacco related activities, burning of candles and incense, and overcooked food and grilled meat (ATSDR 1995).

PAHs are distributed widely in the environment including air, groundwater, drinking water, soil, sediments, rain, snow and fog. PAHs in water, air and soil have been detected as a mixture of compounds (Gan et al. 2009). Humans are exposed to PAHs mainly through air, drinking water, food, and to a lesser extent, through skin contact.

1.3.1.2 Metabolism of PAHs in the body

PAHs are relatively inert, and can be stored and accumulated in fat cells, livers and kidneys (Laher et al. 1984; Shu and Nichols 1979), but also can be metabolized. PAHs are primarily metabolized in liver (Kapitulnik et al. 1977; Kiefer et al. 1988; Monteith et al. 1987), and secondly in kidneys, but other organs, such as small intestines, thyroid, skin, lungs, and testes, are also able to metabolize PAHs (ATSDR 1995). In general, PAHs first bind to aromatic hydrocarbon receptors to activate phase I metabolic enzymes, e.g. cytochrome P450 enzymes (CYP). In the first step of PAH metabolism, CYPs oxidize PAHs into unstable and electrophilic intermediates, such as dihydrodiols, diol-epoxide, *ortho*-quinones, and radical cations. In the second step, these electrophilic intermediates can be further conjugated with cellular thiols, glutathione, sulfate, glucuronic acid, cysteine, or glycine by phase II conjugating enzymes, leading to the generation of hydrophilic metabolites. Finally, these water-soluble conjugates and hydroxylated metabolites are excreted from the body through feces and urine (Ramesh et al. 2004; Shimada 2006).

1.3.2 Health effects of PAHs

Once having been metabolically activated via xenobiotic-metabolizing enzymes, PAHs exert their adverse health effects on genetic materials and genetic processes including DNA

damage, DNA repair, mitosis and cell proliferation (ATSDR 1995). It has been reported by many studies *in vivo* and *in vitro* that both individual PAHs and PAH mixtures show a wide range of genotoxic effects including gene mutations, chromosome aberrations, sister chromatid exchange, and elevated level of induced DNA adducts (ATSDR 1995; Denissenko et al. 1996). PAHs are considered potential carcinogens. Studies using animal models have demonstrated the carcinogenicity of seven PAHs, including Benzo[a]pyrene, Benz[a]anthracene, Benzo[b]fluoranthene, Benzo[k]fluoranthene, Chrysene, Dibenz[a,h]anthracene, and Indeno[1,2,3-cd]pyrene (Nisbet and LaGoy 1992). Moreover, PAHs are also known to be immunotoxic. Benzo[a]pyrene is able to suppress humoral and cellular immune responses by inhibiting the activation of B/T lymphocytes *in vitro* (Davila et al. 1996; Romero et al. 1997). Prenatal exposure to a PAH mixture during gestation leads to increased weight and fat mass, higher expression of adipose genes, such as peroxisome proliferator-activated receptor γ and CCAAT/enhancer-binding proteins α , and lower DNA methylation of peroxisome proliferator-activated receptor γ in offspring and grand-offspring mice, indicating the impact of PAHs exposure on obesity and epigenetic changes in progeny (Yan et al. 2014).

1.3.3 2-NAP as an endocrine disruptor

2-Naphthol (2-NAP), or β -naphthol, (other names as 2-Hydroxynaphthalene; 2-Naphthalenol; Naphth-2-ol), is one of the important metabolites of naphthalene, which is the simplest PAH and contains two benzene rings. Urinary 2-NAP, as well as the other naphthalene metabolites 1-naphthol (1-NAP), have been used as a biomarker of PAH exposure, especially as a naphthalene biomarker.

Sharing the basic phenolic structure with endogenous steroid hormones, 2-NAP is considered a potential endocrine disruptor. Schultz and Sinks (Schultz and Sinks 2002) detected the estrogenic activity of 2-NAP to human estrogen receptor α (hER α) using the *Saccharomyces cerevisiae*-based *Lac-Z* reporter assay. In addition, Terasaki (Terasaki et al. 2007) demonstrated that 2-NAP is able to interact with hER α , and the relative affinity to 17 β -estradiol for 2-NAP is 0.0009% using yeast two-hybrid assays, thus indicating the estrogenic agonist activity of 2-NAP. Moreover, an epidemiological study with excessive PC game room users among young male Koreans, who were exposed to abnormal level of PAHs, shows significantly negative correlation between urinary 2-NAP and plasma testosterone concentrations, indicating an adverse impact on male hormone homeostasis (Kim et al. 2005). Furthermore, in another *in vitro* study, Sun's group generated an expression vector by fusing the ligand binding domain of human thyroid hormone receptor β (hTR β 1) with the DNA binding domain of Gal4. By transfecting this expression vector to a Gal4-responsive luciferase reporter system, they showed that treatment with 2-NAP inhibited the transcriptional activation of hTR β 1 induced by triiodothyronine (T3) (Sun et al. 2008). This *in vitro* study reveals the thyroid hormone antagonist activity of 2-NAP.

1.4 Heavy metal: lead (Pb)

1.4.1 Lead exposure in the human population

Lead, both in organic and inorganic forms, is exposed to humans primarily through the ingestion of contaminated food and water, inhalation of polluted air, and to a lesser extent via dermal contact. 30-40% of inhaled lead is absorbed into the blood stream via the respiratory tract. An average 10-15% of ingested lead is absorbed through the gastrointestinal tract in adults,

and up to 50% in infants and young children (Markowitz 2000; Philip and Gerson 1994). Absorbed lead accumulates in blood, soft tissues and bone. The estimated half-life of lead in these three compartments are 35 days, 40 days, and 20 to 30 years, respectively (ATSDR 2007). More than 95% of the total body burden of lead is stored in skeletal bone and teeth. Once absorbed, lead excretion from the body is extremely slow and occurs mainly through the urine (Philip and Gerson 1994).

Lead has been present in human environments for over 5000 years (Philip and Gerson 1994). The use of lead in human activities can be traced back to ancient Rome as a component of water pipes. In modern times, lead was used in paint, and in the 20th century in gasoline to improve their performance. However, these two applications of lead were banned in 1977 and 1990, respectively, due to health concerns. Nowadays, lead is still used in a wide variety of products such as batteries, cosmetics, ceramic glazes, and certain imported home remedies (ATSDR 2007).

Because of its wide distribution, exposure of humans to lead is inevitable. Leaded paint that remain in old houses built before 1978 and lead-contaminated house dusts are the major sources of lead exposure to children in the United States. Drinking water is contaminated by lead through corrosion of plumbing pipes, faucets and solder, especially in homes built before 1986 which are at higher risk of water contamination from lead plumbing materials. Food and beverages might be contaminated with lead during production, processing, packaging, and storage. Even its inclusion is prohibited in many products, lead is still used in commercial products, such as painted toys, furniture, toy jewelry, cosmetics, food and liquid containers, and plumbing materials (ATSDR 2007).

1.4.2 Health effects and mechanisms of lead toxicity

Based on the most recent report from the CDC, the geometric mean of lead concentration in blood has decreased to 1.12 µg/dL for the US population from NHNES 2009-2010 (CDC 2015), compared with more than 10 µg/dL in the 1970s (Mahaffey et al. 1982). The average blood lead level has declined, but the low exposure of lead during development and throughout the lifetime remains as a serious health issue.

In general, lead affects every system in the body. Children are the most vulnerable population to environmental lead exposure because of the high rate of absorption and retention as well as the routes and frequency of lead exposure. In children, presence of lead in blood is associated with a decrease in the intelligence quotient-IQ, impaired peripheral nerve function, decreased hearing acuity, and increased attention deficit hyperactivity disorder (ATSDR 2007). In the adult population, chronic exposure to low levels of lead results in adverse health effects on erythropoiesis, blood pressure, kidney function, and the central nervous system (Tchounwou et al. 2012).

The mechanisms at the basis of lead toxic effects are not fully characterized, but the abilities to 1) compete with or substitute for essential metallic cations such as calcium and zinc, 2) promote reactive oxygen species production and free radicals formation, and 3) directly interact with proteins such as sulfhydryl, carboxyl groups, phosphate, and amine are considered the major mechanisms of lead toxicity (ATSDR 2007; Flora et al. 2007; Hermes-Lima et al. 1991; Tchounwou et al. 2012). In addition, long term exposure to lead is demonstrated to reduce global DNA methylation of long interspersed nuclear elements-1, indicating epigenetic effects of lead exposure (Li et al. 2013; Wright et al. 2010).

1.5 Obesity: a pandemic disease

Obesity is an increasing problem all over the world. According to the World Health Organization's (WHO) global estimates, more than 600 million adults were obese, and 1.9 billion adults (39% of global population) were overweight in 2014. Childhood obesity is of particular concern. The WHO estimates that in 2013, 42 million of 0- to 5-year-old children were overweight or obese, with childhood obesity 30% higher in developing countries than in developed countries (WHO 2015). In the United States, more than 65% of adults are overweight or obese and 6.4% are extremely obese with body mass index (BMI) over 40 kg/m². Among children and adolescents aged from 2 to 19 years, 31.8% of them are overweight or obese, and 8.4% of 2- to 5-year-olds, 17.7% of 6- to 11-year-olds, and 20.5% of 12- to 19-year-olds are obese (Ogden et al. 2014).

Obesity is a medical condition where excessive body fat accumulates to an extent that causes adverse effects on health, with increasing risk of morbidity and mortality. In obese tissue, low-grade and chronic inflammation causes insulin resistance, which links obesity to multiple metabolic diseases including type 2 diabetes, cardiovascular diseases, autoimmune diseases, osteoarthritis, respiratory problems, nonalcoholic fatty liver dysfunction, and increased risk for cancer and cancer-related mortality (Collins 2005; Mokdad et al. 1999; Mokdad et al. 2003).

Obesity is caused by a complex interaction of multiple factors, such as genetic, behavioral and environmental, acting through psychological mediators that interrupt energy homeostasis. On one hand, genetic influences play a role through susceptibility genes, which increase the risk of developing a disease. Studies from monogenic animal models, as well as from rare obesity-associated syndromes with a familial inheritance, indicate the consistent link between obesity and single-gene disorders. On the other hand, different physical activity/exercise habits and

metabolic rate reveal a direct association between low energy expenditure and overweight/obesity. In addition, increased energy intake by a high calorie, high fatty diet and sedentary lifestyle represent root causes for the prevalence of overweight and obesity (Kopelman 2000). Although genetic/epigenetic influences are undoubtedly important, one of the most plausible explanations for the rapid increase in obesity over the past 50 years is the adverse effects of environmental pollutant exposure, in combination with unhealthy diet and lifestyle.

1.6 Antimicrobial peptides and adipocytes

1.6.1 AMP definition and origin

The host immune response of living organisms against pathogens and microbial infections involves the cooperation of cells in the innate and adaptive immunity. The production of antimicrobial peptides (AMPs) by resident cells during the lag phase between the onset of infections and the recruitment of additional leukocytes immediately protects the host organisms. This immediate antimicrobial response occurs within several minutes, thus serving as the first-line of host defense (Wiesner and Vilcinskas 2010).

AMPs are a group of small peptides and proteins that have direct antimicrobial activity; therefore, the production of AMPs is considered as the most ancient mechanism of host defense. AMPs are produced by almost all species, including bacteria, plants, insects, invertebrates, vertebrates, and mammals. Most AMPs exhibit a wide-spectrum of microbicidal activity to kill or neutralize bacteria, viruses, fungi, and parasites. AMPs are present in the skin, eye, mucosal surfaces of the respiratory system and the digestive system, bone marrow, and testes (Hancock and Scott 2000). Their expression can be either constitutive or inducible in different cell types,

such as epithelial cells, keratinocytes, Paneth cells, neutrophils, macrophages, monocytes, mast cells, as well as other leukocytes (Hancock and Scott 2000).

AMPs are small peptides that are encoded by the genome and synthesized by ribosomes. Eukaryotic AMPs usually comprise between 12 and 50 amino acids with no unusual post-transcriptional modifications (Wiesner and Vilcinskas 2010). Most of the eukaryotic AMPs exert wide-spectrum activity at high concentrations, while certain AMPs display a very restricted spectrum. Beside the direct antimicrobial activities, AMPs exert other biological functions such as recruiting neutrophils and macrophages, modulating cytokine production in leukocytes (De Yang et al. 2000; Huang et al. 1997), and promoting re-epithelialization (Tokumaru et al. 2005). To date, the Antimicrobial Peptide Database (APD, <http://aps.unmc.edu/AP/main.php>) has reported more than 2600 AMPs from different organisms.

1.6.2 Groups and mechanisms of action

On the basis of their molecular targets, structures, peptide properties (e.g., net charge), and sources, AMP can be categorized in different groups. However, three major groups are usually considered. The first group includes AMPs characterized on the basis of their biological function (antibacterial peptides, antiviral peptides, antifungal peptides, antiparasitic peptides, anticancer peptides, anti-protist peptides, insecticidal peptides, spermicidal peptides, chemotactic peptides, wound healing, antioxidant peptides, and protease inhibitors) (Hancock and Sahl 2006). The second group includes AMPs characterized on the basis of amino acid composition and three-dimensional structure, and consists of four classes: (1) α -helix structures, (2) β -sheet structures with disulfide bonds, (3) structures with both α -helix and β -strands, and (4) structures with neither α -helix or β -strands (Lai and Gallo 2009). The third group, recently

introduced, is defined on the basis of, a universal classification that takes into account the peptide bonding patterns: class I linear AMPs such as human cathelicidin, class II sidechain-connected peptides such as the human defensin family, class III polypeptides with side chain linked to the backbone (e.g., lassos), and class IV loop peptides such as cyclic defensins found in rhesus macaques (Wang 2015).

The mechanisms of action of AMPs have not been fully characterized, but different mechanisms of action for cationic AMPs directed against Gram-negative bacteria have been proposed. According to one of the proposed mechanisms, the positively charged AMPs adsorb onto negatively charged bacterial surfaces by electrostatic attraction, whereas, according to another, the amphipathic structures allow AMPs to aggregate or integrate into the lipid bilayer. In addition, the barrel-stave model (Rosado et al. 2008), worm-hole model (Yang et al. 2001), and the carpet model (Chang et al. 2008) have been proposed to explain how AMPs form pores and disrupt bacterial cell membranes (Wiesner and Vilcinskas 2010)). The insertion of AMPs into lipid bilayers finally leads to cell lysis and the loss of ion gradients and essential metabolites, eventually causing cell death.

1.6.3 Role of adipocytes in immunity

The adipose tissue is increasingly considered as an immunological active organ because of the presence of a variety of immune cells and the production of adipokines and pro- or anti-inflammatory cytokines and chemokines by mature adipocytes (Grant and Dixit 2015).

Adipocytes, by secreting adipokines (adipocytokines), cytokines and chemokines, cross-talk with immune cells and modulate their functions (Ouchi et al. 2011). On one hand, adipocytes interact with a variety of immune cells. It has been well established in animal models of obesity

that excessive mature adipocytes recruit neutrophils (Elgazar-Carmon et al. 2008), macrophages (Weisberg et al. 2003), and lymphocytes (Nishimura et al. 2009; Winer et al. 2011) into adipose tissue. In addition, mature adipocytes are able to mimic antigen presenting cells to promote T lymphocytes activation and proliferation. This action requires a direct contact through Major Histocompatibility Complex (MHC) class II molecules expressed on adipocytes as well as adipocyte-secreted pro-inflammatory cytokines (Poloni et al. 2015). On the other hand, adipokines, produced by mainly by adipocytes, regulate immune responses. Leptin induces the production of TNF- α , IL-6, and IL12 in CD4 T cells promoting pro-inflammatory immune responses (Loffreda et al. 1998). Adiponectin, on the other hand, plays an anti-inflammatory role in macrophages by suppressing the activation of NF κ B and TNF- α and IL-6 induction by LPS (Ajuwon and Spurlock 2005; Wulster-Radcliffe et al. 2004). Resistin, involved in glucose metabolism and insulin sensitivity, modulate inflammatory responses by upregulating the expression of adhesion molecules VCAM-1 and ICAM-1 on vascular endothelial cell surfaces (Kawanami et al. 2004).

A recent study focusing on skin infection by *Staphylococcus aureus* reveals one additional role of adipocytes in innate immunity: bacteria-induced differentiating adipocytes protect the animals by producing cathelicidin that directly kill the pathogens (Zhang et al. 2015). This study elucidates important properties of adipocyte at the site of infection. Firstly, presence of bacteria can induce preadipocytes to differentiate. Secondly, upon stimulation, adipocytes are capable of producing cathelicidin, but this response only appears in the differentiating adipocytes, not the fully mature adipocytes.

1.7 Adipocyte differentiation

In adipose tissue, mature adipocytes take up approximately one-third of the cellular composition. The remaining two-thirds are connective tissue, nerve tissue, endothelial precursor cells, mesenchymal stem cells, preadipocytes in different differentiating stages, and immune cells (e.g., T regulatory cells and macrophages) (Hassan et al. 2012). Mature adipocytes (also named fat cells or lipocytes) are capable of storing energy in the form of lipid, while preadipocytes, serving as the precursors, have the ability to differentiate into mature adipocytes.

1.7.1 Adipogenesis is a multiple-stage event

Adipogenesis is a process in which mesenchymal precursors commit to the adipose lineage and develop into mature adipocytes (Fig. 1.1). This process occurs in several stages including committed preadipocyte, mitotic clonal expansion, terminal differentiation and mature adipocyte. Mesenchymal precursors have the ability to differentiate into multiple lineages, i.e., adipocytes, myocytes, chondrocytes, and osteocytes (Covas et al. 2008; Huang et al. 2009; Lin et al. 2010). Upon appropriate stimulation, these precursors commit to differentiate along the adipocyte lineage and become fibroblast committed preadipocytes. After exposure to hormonal stimulation, the G1-growth-arrested preadipocytes immediately reenter the cell cycle and undergo several rounds of cell division, a prerequisite phase for differentiation often referred as mitotic clonal expansion. During mitotic clonal expansion, the stimulated preadipocytes express cell cycle regulators as well as specific adipogenic transcriptional regulators such as CCAAT-enhancer-binding protein- β and δ (C/EBP β and C/EBP δ). Following this event, the stimulated cells undergo terminal differentiation in which activation of the transcriptional regulator peroxisome proliferator-activated receptor- γ (PPAR γ) and C/EBP α results in expression of adipocyte genes

that involve in fatty acid synthesis, lipid metabolism, as well as adipokine production. At the end of terminal differentiation stage, fibroblast preadipocytes become large spherical lipid-producing adipocyte (Lefterova and Lazar 2009).

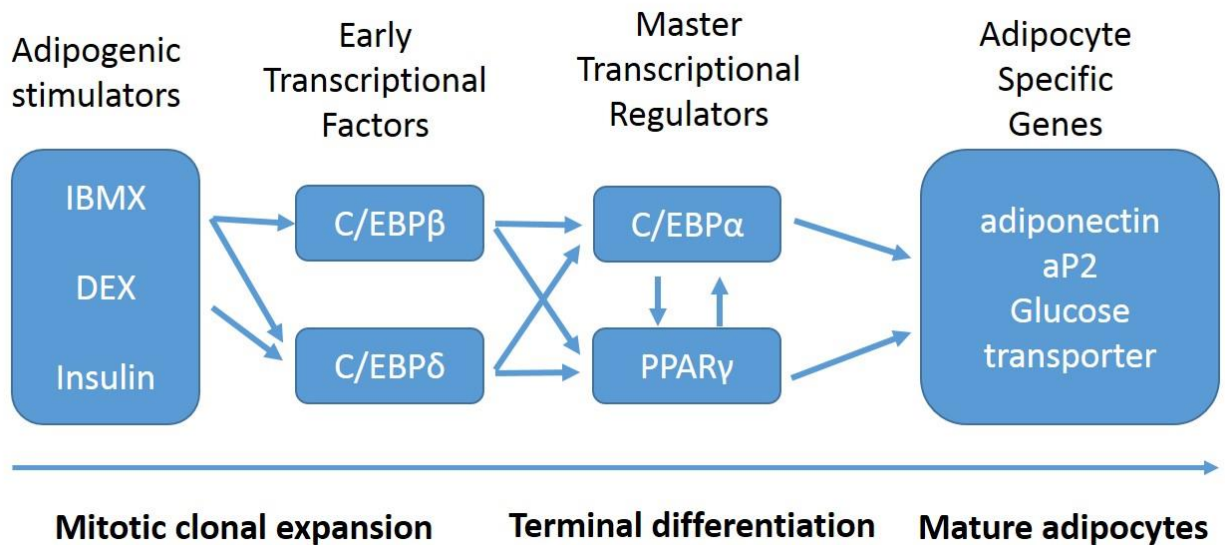


Figure 1.1 Scheme of different stages of adipogenesis in 3T3-L1 cells.

After adding adipogenic stimulators, post-confluent 3T3-L1 preadipocytes re-enter the cell cycle, a stage called mitotic clonal expansion. During this two-three-round proliferation, early transcriptional factors C/EBP β and C/EBP δ are activated, which together initiate the activation of two master transcriptional regulators of adipogenesis, C/EBP α and PPAR γ . C/EBP α and PPAR γ function in the terminal differentiation stage to regulate the expression of a variety of adipocyte-specific genes such as adiponectin, aP2, glucose transporters, leading to the conversion of preadipocytes to mature adipocytes.

1.7.2 *The transcriptional cascade of adipogenesis*

Adipocyte differentiation is a multi-step process involved in a sequential transcriptional-factor-activation cascade regulating cell cycle proteins and adipogenic gene expression (Tang and Lane 2012). Immediately after induction, the activation and phosphorylation of cyclic AMP response element-binding protein (CREB) initiate the expression of C/EBP β (Davis and Zur Nieden 2008; Zhang et al. 2004). During mitotic clone expansion, C/EBP β and C/EBP δ are the first two activated transcriptional factors. The expression of C/EBP β and C/EBP δ can be detected within 4 hours post induction; however, these two transcriptional regulators become functionally active after 16 hours post induction (Tang and Lane 1999). The acquisition of DNA-binding ability by C/EBP β is achieved via sequential phosphorylation (Tang et al. 2005). Later, dual phosphorylated C/EBP β , in combination with C/EBP δ , regulates the expression of C/EBP α and PPAR γ , two master transcriptional regulators of adipogenesis, by binding to C/EBP regulatory elements in their proximal promoters, initiating the terminal differentiation stage (Cao et al. 1991; Wu et al. 1995; Wu et al. 1996; Yeh et al. 1995). C/EBP α and PPAR γ function together as activators regulating a large group of adipocyte genes, such as fatty acid binding protein 4 (FABP4, also known as aP2), insulin receptor substrate (IRS) and GLUT4 (Rosen and MacDougald 2006). PPAR γ is both necessary and sufficient for adipocyte formation (Rosen et al. 1999), whereas C/EBP α is a robust driver of adipogenesis and is required for maintaining the expression of PPAR γ . Though C/EBP α cannot induce adipocyte differentiation in the absence of PPAR γ , it is crucial for controlling insulin action such as insulin-dependent glucose uptake (Rosen et al. 2002; Wu et al. 1999).

1.7.3 Other factors that control adipogenesis

Hormones and extracellular factors directly control adipogenesis upstream of transcriptional regulators. Among these secreted proteins and factors, insulin is a well-studied inducer of adipocyte differentiation. Insulin and insulin-like growth factors (IGF) act through the insulin receptor and the IGF-1 receptor on the cell membrane to initiate the insulin/IGF-1 signaling pathway. Autophosphorylation of tyrosine residues in the insulin/IGF-1 receptor activates its intrinsic tyrosine kinase to recruit and phosphorylate insulin receptor substrate-1/2 (IRS-1/2), which further attracts various adaptor proteins. The insulin signaling pathway for adipogenesis involves two downstream kinase systems, the phosphatidylinositol 3-kinase-protein kinase B/Akt (PI3K/Akt) pathway (Inoue et al. 1998; Saad et al. 1994) and the MAP kinases (Boney et al. 2000). Akt serves as a crucial effector of insulin-induced adipogenesis. The phosphorylation of Akt suppresses the anti-adipogenic Forkhead Box O1 (FOXO1), leading cells to re-enter the cell cycle (Tong et al. 2000; Tong et al. 2005; Yun et al. 2008). PI3K/Akt also modulates the activation of the pro-adipogenic cyclic AMP response element-binding protein (CREB) and GSK3 β , which further promotes C/EBP β expression and phosphorylation (Tang et al. 2005; Zhang et al. 2004). Furthermore, it regulates PPAR γ and sterol responsive element binding protein 1 (SREBP1) through the active mammalian target of rapamycin (mTOR) complex (Yu et al. 2008).

The role of MAP kinase system in adipogenesis is not clear, and contradictory roles of ERK 1/2 have been reported. Phosphorylation on Thr188 of C/EBP β first occurs by MAP/ERK1/2 within two hours after induction. Later, glycogen synthase kinase 3 β (GSK3 β) comes in and phosphorylates the second site on Thr179 or Ser184 about 12 to 14 h after induction, allowing

its eventual transactivation of C/EBP α and PPAR γ (Tang et al. 2005; Tang and Lane 1999). Conversely, sustained ERK 1 activation during the terminal differentiation phase leads to decreased PPAR γ activity (Bost et al. 2005). These conflicting results indicate that the function of MAP/ERK in adipogenesis is time restricted, which is necessary during early stages of differentiation but inhibitory in the terminal stage.

1.7.4 Mouse 3T3-L1 preadipocyte Model

Mouse 3T3-L1 preadipocytes are a widely used and well-studied *in vitro* cell model for adipocytes and obesity-related research. This cell line was isolated from 17-19-day-old Swiss mouse embryonic tissue in Green's laboratory and characterized by its indefinite and homogenous cellular population (Green and Kehinde 1974; Green and Meuth 1974; Green and Kehinde 1975). Based on its faithful recapitulation of the adipogenic transcriptional cascade, 3T3-L1 preadipocytes become a complementary tool to animal models for investigating adipocyte differentiation.

3T3-L1 preadipocytes can be induced to differentiate into mature adipocytes by a standard differentiation cocktail, which includes 3-isobutyl-1-methylxanthine (IBMX), dexamethasone (DEX) and insulin. The addition of IBMX and DEX spontaneously activates C/EBP β and C/EBP δ by stimulating cAMP accumulation and activating CREB (Cao et al. 1991; Gonzalez and Montminy 1989; Reusch et al. 2000). The presence of insulin accelerates the differentiation process by activating the PI3K/Akt pathway. In the standard differentiation protocol, post-confluent 3T3-L1 preadipocytes are stimulated with the differentiation medium in the presence of bovine serum on day 0, and the differentiation medium is replaced on day 3 with the basic culture medium containing insulin alone. Cells are maintained in this insulin medium until day 8.

1.8 Research overview

Many environmental pollutants are considered to be obesogens. The adipogenic properties of some environmental pollutants, such as BPA, PCBs, and DDT, have already been demonstrated *in vitro* and *in vivo* (Schug et al. 2011). Epidemiological studies indicate that PAHs and the heavy metal lead are associated with obesity, but no clear and direct evidence is currently available to confirm their adipogenic activity.

Adipocytes play multiple roles in regulating immune functions. Mature adipocytes secrete adipokines to promote inflammation, recruit leukocytes, and modify lymphocyte functions (Loffreda et al. 1998). Differentiating adipocytes produce the antimicrobial peptide cathelicidin to modulate innate immunity (Zhang et al. 2015). Several environmental pollutants exhibit a modulatory role on mature adipocyte function as it relates to adipokine production (Valentino et al. 2013). The effect of environmental pollutants on antimicrobial peptide production in adipocytes has not yet been studied.

The major goal of the present dissertation is to characterize the potential obesogenic effects of 2-NAP and lead, and their ability to induce antimicrobial peptide production, by using the mouse 3T3-L1 preadipocytes model. By exposing 3T3-L1 cells to 2-NAP and lead, we have shown that:

- (a) 2-NAP accelerates 3T3-L1 differentiation in a dose-dependent manner (Chapter 2);
- (b) Lead is capable of upregulating 3T3-L1 adipogenesis. However, the dose effects are non-monotonic (Chapter 3);

(c) The effect of lead at higher doses attenuates the 2-NAP effect on adipogenesis

(Chapter 4);

(d) 2-NAP and lead modulate cathelicidin production (Chapter 5).

Therefore, we demonstrate the adipogenic properties of 2-NAP and lead, and the co-modulatory effects of 2-NAP and lead on adipogenesis.

Environmental pollutants are epidemiologically associated with a variety of adverse health effects, including obesity and dysregulated immune responses. The characterization of the direct modulatory roles and co-effects of environmental pollutants during adipocyte differentiation will help to define the environmental causes of the obesity and inflammation pandemic.

2 Chapter 2: The polycyclic Aromatic Hydrocarbon 2-Naphthol Contributes to Adipocyte Differentiation in the Mouse 3T3-L1 Model

2.1 Summary

Polycyclic aromatic hydrocarbons (PAHs) are a family of chemicals generated by the incomplete combustion of coal, oil, and gas. Once in the body, PAHs accumulate in fat tissue, liver, and spleen. The presence of low-molecular-weight PAHs metabolites in the urine is associated with a higher body mass index and with obesity in children 6-11 years old. In particular, 2-naphthol (2-NAP), the major metabolite of the PAH naphthalene, is positively associated with childhood obesity. Thus, we hypothesized that 2-NAP induces the differentiation of pre-adipocytes to adipocytes.

To test our hypothesis, we used an *in vitro* model consisting of mouse 3T3-L1 preadipocytes. This cell line can be induced to differentiate into mature adipocytes using a standard differentiation protocol, which includes exposure of the 3T3-L1 cells to 3-isobutyl-1-methylxanthine (IBMX), dexamethasone (DEX) and insulin for the first three days, followed by insulin alone for six days. In our study, 3T3-L1 cells were exposed to six ten-fold concentrations of 2-NAP (100 pM to 10 μ M) in two experimental protocols. In the first experimental protocol (Insulin+2-NAP D3-8), cells were induced by the standard differentiation medium with IBMX, DEX, and insulin for three days followed by insulin and 2-NAP for six days. In the second experimental protocol (2-NAP D0-8), cells were induced by IBMX, DEX, and 2-NAP for three days followed by 2-NAP alone for six days. Terminal differentiation was evaluated by cell morphology, lipid production, and expression levels of three marker genes of adipogenesis: C/EBP α , PPAR γ , and

aP2. The early transcriptional cascade was evaluated by assessing the gene expression levels of the early transcriptional factor C/EBP β , the insulin signaling molecule IRS2, and the insulin-regulated transcriptional factor SREBP1c.

Results from both experiments show that 2-NAP-treated 3T3-L1 cells differentiated from fibroblast cells into mature lipid-producing spherical adipocytes and accumulated a higher level of lipids in comparison to cells treated with the basic DMEM medium. In the Insulin+2-NAP D3-8 experiment, in presence of insulin, 2-NAP elevated the mRNA level of two major transcriptional regulators of terminal adipocyte differentiation C/EBP α and PPAR γ , and the mature adipocyte-specific gene aP2, in a dose-dependent manner. In the 2-NAP D0-8 experiment, in the absence of insulin, C/EBP α , PPAR γ , and aP2 were also activated in 2-NAP-treated 3T3-L1 cells. In cells treated with higher concentrations, the activation fold of C/EBP α and PPAR γ was as high as in cells treated with the standard differentiation protocol. Results from the transcriptional cascade of adipocyte differentiation revealed that during the early differentiation phase (day 0-3), 2-NAP increased C/EBP β , IRS2, and SREBP1c expression levels similarly to those seen in the 2-NAP D0-8 experiment, compared to those induced by insulin in the standard differentiation protocol.

Together, these results indicated that 2-NAP is capable of inducing adipocyte differentiation of 3T3-L1 cells. 2-NAP contributes to adipocyte differentiation by regulating transcriptional regulators of adipocyte differentiation and molecules involved in insulin signaling pathway. Therefore, 2-NAP plays a potential role in interrupting lipid homeostasis, possibly leading to obesity and associated disorders.

2.2 Introduction

Childhood obesity can be associated with many adverse health outcomes in adulthood (Freedman et al. 2007). The causes of childhood obesity have been widely studied over the past couple decades. One emerging hypothesis is that the exposure of ubiquitous environmental chemicals may effect childhood growth (Newbold 2010). In particular, the exposure of environmental endocrine disrupting chemicals is an important factor for childhood obesity.

A recent study by researchers at the Centers for Disease Control and Prevention, has found that urinary low-molecular-weight PAH metabolites are associated with higher body mass index and obesity in younger children (6-11 years old). Specifically, 2-NAP, the major metabolite of naphthalene, is found to be positively associated with childhood obesity, indicating its potential role in fat cell formation and obesity (Scinicariello and Buser 2014). As an endocrine disruptor, the question of whether 2-NAP is capable to induce adipocyte formation (also known as adipogenesis) and lipid homeostasis has not been answered.

Therefore, in this study, we aimed to investigate the effect of 2-NAP on adipocyte differentiation and lipid homeostasis *in vitro*. Mouse 3T3-L1 cells were initiated with differentiation cocktail for 72 hours, then incubated with six ten-fold concentrations of 2-NAP (100 pM to 10 μ M). The terminal adipocyte differentiation was evaluated by lipid accumulation using Oil Red O staining, and by evaluating the expression of CCAAT-enhancer-binding protein- α and β (C/EBP α and C/EBP β), peroxisome proliferator-activated receptor- γ (PPAR γ), and fatty acid binding protein 4 (FABP4, also known as aP2). The molecules involved in and regulated by the insulin signaling pathway were also analyzed by determining the gene expression levels of the

Insulin receptor substrate proteins (IRS) 2 and sterol responsive element binding protein (SREBP) 1c.

2.3 Materials and methods

2.3.1 Materials

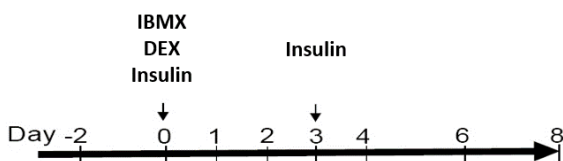
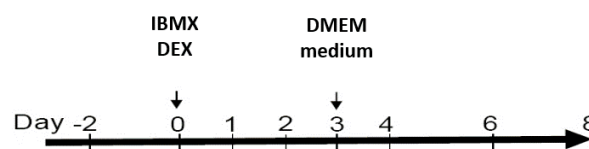
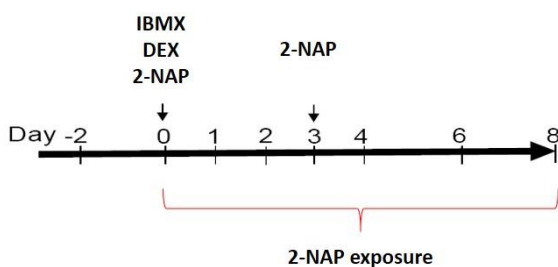
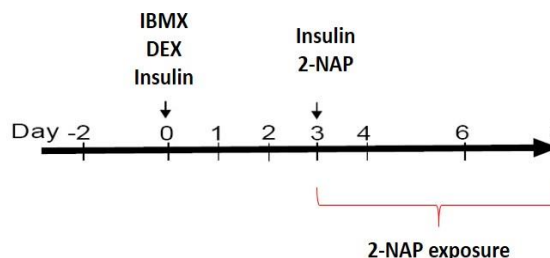
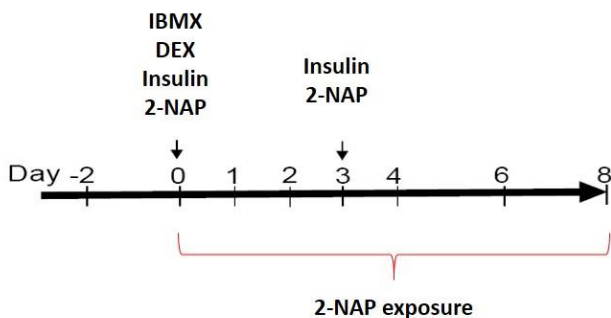
Mouse embryo fibroblast 3T3-L1 cells (ATCC CL-173, lot 59796011) and bovine calf serum (ATCC, 30-2030) were obtained from ATCC. Dulbecco's modified Eagle's medium (DMEM) (Cellgro 10-013CV), 100X penicillin-streptomycin solution (Cellgro 30-002-CI) were purchased from Mediatech, Inc. Human insulin solution (I9278), dexamethasone (D2915), 3-Isobutyl-1-methylxanthine (I5879), formalin solution (HT501128), Oil Red O (O0625) were obtained from Sigma-Aldrich Co. LLC. 2-Naphthol was purchased from Acros Organics.

2.3.2 Experimental design

Confluent 3T3-L1 preadipocytes can be induced to differentiate synchronously by using a standard differentiation protocol with the most commonly used differentiation cocktail. This cocktail contains 0.5 mM 3-isobutyl-1-methylxanthine (IBMX), 0.25 μ M dexamethasone (DEX), and 1 μ g/mL insulin (Zebisch et al. 2012). After the first several hours, insulin alone is required to continue the differentiation process (Caprio et al. 2007). This standard differentiation protocol, as shown in Figure 2.1, was used as the positive control in our study. 3T3-L1 preadipocytes were seeded (day -2) and cultured in the basic medium until 100% confluent. Post-confluent preadipocytes were induced with the differentiation medium containing IBMX, DEX, and insulin for three days (day 0 to day 3), during which 3T3-L1 cells underwent several cell cycles and expressed the two early adipocyte transcriptional regulators C/EBP β and C/EBP δ . On day 3, the

differentiation medium was removed and replaced with the basic culture medium with 1 $\mu\text{g}/\text{mL}$ insulin. During the last six days (day 3 to day 8), the stimulated preadipocytes entered the terminal differentiation phase and gradually became mature adipocytes.

Here in our study, we firstly replaced the insulin in the standard differentiation protocol by 2-NAP (Experiment 2-NAP D0-8), and then exposed the cells to 2-NAP during the entire experiment from day 0 to day 8 in order to compare the role of 2-NAP with that of insulin during 3T3-L1 adipogenesis. In the second experiment (Experiment Insulin+2-NAP D3-8) we stimulated cells with the standard differentiation protocol, then added 2-NAP to the cells on day 3 and kept it until day 8. This exposure protocol allowed us to evaluate the effect of 2-NAP on the terminal differentiation phase of adipogenesis. We also designed the third experiment as comparison to Experiment Insulin+2-NAP D3-8. In the third experiment (Experiment insulin+2-NAP D0-8), post-confluent cells were induced with the standard differentiation protocol. 2-NAP was added on day 0 and kept in the cell culture for the entire experiment (Fig.2.1).

A. Positive control protocol**B. IBMX+DEX control protocol****C. 2-NAP exposure protocols***1) Experiment 2-NAP D0-8**2) Experiment Insulin+2-NAP D3-8**3) Experiment Insulin+2-NAP D0-8***Figure 2.1 Protocols for adipogenic differentiation and 2-naphthol exposure in 3T3-L1 cells.**

Confluent cells were differentiated (designated as day 0, indicated by the first black arrow) by replacing the basic DMEM medium with the desired differentiation media for three days, followed by addition of the chemical containing media for six days. The concentrations of each component used were 0.5 mM for IBMX, 0.25 μ M for DEX, and 1 μ g/mL for insulin. Differentiation media containing IBMX and DEX with or without insulin were used for the positive control and IBMX+DEX control, respectively. In the 2-NAP experiments, the differentiation medium containing IBMX, DEX, and 2-NAP was used for Experiment 2-NAP D0-8 differentiation, whereas the differentiation medium containing IBMX, DEX, and insulin with or without 2-NAP was used for insulin+2-NAP experiments. On Day 3 (indicated by the second black arrow), differentiation media were changed to DMEM medium with 1 μ g/mL insulin for the positive control; the basic DMEM medium for the IBMX+DEX control; DMEM medium with 2-NAP for Experiment 2-NAP D0-8; or DMEM medium with 1 μ g/mL insulin and 2-NAP for Insulin+2-NAP experiments, respectively, until the end of the experiments (day 3 to day 8). 2-NAP exposure period in each experiment was indicated by a red curly bracket.

2.3.3 Cell culture and differentiation

3T3-L1 cells were cultured in the DMEM medium supplemented with 10% bovine calf serum (BCS), 100 I.U. penicillin and 100 µg/mL streptomycin. Cells were grown in 75 cm² culture flasks in a humidified atmosphere with 5% CO₂ at 37 °C and subcultured when they became 80% confluent. Cells were seeded at a density of 6x10⁴ cells/well in Costar 6-well plates with the basic DMEM medium. In the cell viability test, cells were seeded at 5000 cells/well in 96-well plates. After reaching confluency (Day 0), cell differentiation was induced by replacing the basic DMEM medium with differentiation media for three days (day 0 to day 2) followed by chemical-containing medium for six days. The concentrations of each component in the standard differentiation cocktail were 0.5 mM for IBMX, 0.25 µM for DEX, and 1 µg/mL for insulin. Differentiation media containing IBMX and DEX with or without insulin were used for the positive control and the IBMX+DEX control, respectively. In the 2-NAP experiments, the differentiation medium containing IBMX, DEX, and 2-NAP was used for Experiment 2-NAP D0-8 differentiation, whereas the differentiation medium containing IBMX, DEX, and insulin with or without 2-NAP was used for Insulin+2-NAP experiments. On Day 3, differentiation media were changed to DMEM medium with 1 µg/mL insulin for the positive control; the basic DMEM medium for the IBMX+DEX control; DMEM medium with 2-NAP for Experiment 2-NAP D0-8; or DMEM medium with 1 µg/mL insulin and 2-NAP for the Insulin+2-NAP experiments, respectively, until the end of experiments (day 3 to day 8). Six ten-fold concentrations of 2-NAP, 100 pM, 1 nM, 10 nM, 100 nM, 1 µM and 10 µM, were used in the first two experiments, while 1 nM, 100 nM, and 10 µM were used for Experiment Insulin+2-NAP D0-8. 3T3-L1 cells maintained with the basic DMEM medium were used as negative control.

2.3.4 Oil Red O staining

On the termination day, adipocytes were stained with Oil Red O solution. Briefly, the culture medium was gently and slowly removed from each well, and cells were washed twice with 1X phosphate buffered saline (PBS). Cells were then fixed with 10% formalin solution at 4 °C overnight or longer. After formalin fixation, cells were washed with DI water twice and incubated with 1.5 mL 60% isopropanol for 5 min at room temperature. After removal of isopropanol, cells were completely dried at room temperature, then incubate with 1 mL Oil Red O working solution for 30 min. Subsequently, cells were washed with DI water for three times, dried and analyzed under the microscope. The Oil Red O working solution is stable for only 2 hours, so it was prepared freshly before use. Oil Red O stock was made by dissolving 300 mg Oil Red O powder in 100 mL isopropanol (this stock is stable for one year). The working solution was prepared as follow: Oil Red O stock was filtered by Whatman filter papers and diluted with DI water at 3:2 ratio. After 10 min incubation, Oil Red O working solution was filtered with 0.22 μ m syringe filter.

Triglyceride droplets stained with Oil Red O were photographed under the microscope at 10X and 20X magnification. Lipid accumulation was quantified by measuring the absorbance at 490 nm using EnSpire multilabel plate reader (PerkinElmer) with well area scan mode (Program setting parameters in Table 2.1). The absorbance was expressed as means \pm standard error of 80 spots scanned for each sample.

Table 2.1 Parameter settings for EnSpire multilabel plate reader.

| | | | |
|------------------------|--|-------------|----------|
| Culture plate supplier | Coring Life Sciences: Costar® 6 Well Clear TC-Treated Multiple Well Plates, Bulk Packed, Sterile (Product #3506) | | |
| Plate Dimensions | Wells | Column (mm) | Row (mm) |
| | A1 | 24.76 | 23.16 |
| | A3 | 102.99 | 23.16 |
| | B1 | 24.76 | 62.28 |
| | B3 | 102.99 | 62.28 |
| Scan setting | Number of horizontal points (X) | | 10 |
| | Number of vertical points (Y) | | 10 |
| | Distance between points (mm) | | 1.56 |
| | Scan mode | | Round |
| | Wavelength | | 490 |
| | Measurement height (mm) | | 7.5 |
| | Number of flashes | | 100 |

2.3.5 XTT assays

Cell viability was tested on the termination day of experiments by XTT assays. The XTT assay measures the mitochondrial dehydrogenase activity in viable cells. The tetrazolium ring of XTT salt can be reduced by mitochondrial dehydrogenase of living cells, resulting in a water-soluble orange formazan derivative. In brief, cells were seeded in 96-well plates and cultured according to the experimental protocol mentioned above. On the termination day, the culture medium was replaced by 100 μ L freshly prepared XTT working solution. After 4-hour incubation at 37 °C, the absorbance of orange formazan was measured at 450 nm and 690 nm with a Bio-Tek microplate spectrophotometer. The results were presented as proliferation percentage of the negative control and expressed as means \pm standard error of triplicate samples.

2.3.6 Quantitative real-time reverse transcription-polymerase chain reaction (Real-Time PCR)

Total RNA was extracted from cells using QIAGEN RNeasy Plus Mini Kit (Qiagen Inc., Valencia, CA). 5 μ L, 7.5 μ L and 10 μ L of total RNA extracted on Day 8, Day 5, and Day 2 respectively

was reverse transcribed into cDNA using High-Capacity cDNA reverse transcription kit (Applied Biosystems). The reaction mixture contained 1x reverse transcriptase buffer, 4 mM dNTP (deoxynucleotide triphosphate), 5x Random primers, 1 U RNase inhibitors, and 2.5 U of MultiScribe Reverse Transcriptase. The RT-PCR was performed with the following cycle parameters: 25°C for 10 min, 37°C for 120 min, and 85°C for 5 min. Synthesized cDNA was diluted with RNase-free water. Then, quantitative real-time PCR amplification was performed with appropriate sets of primers using Taqman gene expression assays in a total volume of 20 μ L containing aliquoted cDNA samples. The gene expression assays were carried out with the following cycle parameters: 55°C for 2min; 94°C for 10 min; 40 cycles of 94°C for 15 sec and 60°C for 60 sec. The primers and probes were obtained from Applied Biosystems: C/EBP α (Mm00514283_s1), C/EBP β (Mm00843434_s1), PPAR γ (Mm01184322_m1), α 2 (Mm00445878_m1), Irs2 (Mm03038438_m1), Srebf1c (Mm00550338_m1), and housekeeping gene GAPDH (Cat: 4352339E) as endogenous control to correct the variation of RNA and cDNA loading. Data were analyzed using the Δ CT method. Target gene expression was normalized to GAPDH for Δ CT value, then calibrated to the control sample in each experiment to give the $\Delta\Delta$ C $_T$ value. Data were calculated based on three replicates in the same experiment and presented as the means of relative quantification. Error bars represented the Lower and Upper 95% Confidence Interval. Each set within the experiment was run in triplicate, and each experiment was performed with an additional run to confirm the repeatability.

Table 2.2 Primer/probe information for Real-Time RT-qPCR.

| Gene | Assay ID | Transcripts | Assay design note |
|----------------|-----------------|--------------------|---|
| C/EBP β | Mm00843434_s1 | 1 RefSeqs | primers and probes map within a single exon (will detect genomic DNA) |
| C/EBP α | Mm00514283_s1 | 1 RefSeqs | primers and probes map within a single exon (will detect genomic DNA) |
| PPAR γ | Mm01184322_m1 | 2 RefSeqs | probe spans an exon junction |
| Fabp4/aP2 | Mm00445878_m1 | 1 RefSeqs | probe spans an exon junction |
| Irs2 | Mm03038438_m1 | 1 RefSeqs | probe spans an exon junction |
| Srebf1 | Mm00550338_m1 | 1 RefSeqs | probe spans an exon junction |
| Camp | Mm00438285_m1 | 1 RefSeqs | probe spans an exon junction |

2.3.7 Statistical analysis

Statistical analyses among multi-group data were carried out using ANOVA followed by Post Hoc Tukey's difference test. $P < 0.05$ was considered significant. Each experiment was repeated at least twice, and each set within the experiments were run in triplicates.

2.4 Results

2.4.1 Effect of 2-NAP on cell viability

Regardless of insulin, of all the different concentrations of 2-NAP tested in the experiments described above, none showed effects on cell proliferation as compared to the positive control (Fig.2.2 A-C). In the presence of insulin, even though the average proliferation percentages of 2-NAP treated cells in Experiment Insulin+2-NAP D0-8 were slightly higher than those in Experiment Insulin+2-NAP D3-8, the longer exposure of 2-NAP did not show significant additional promotion of cell proliferation (Fig.2.2 C).

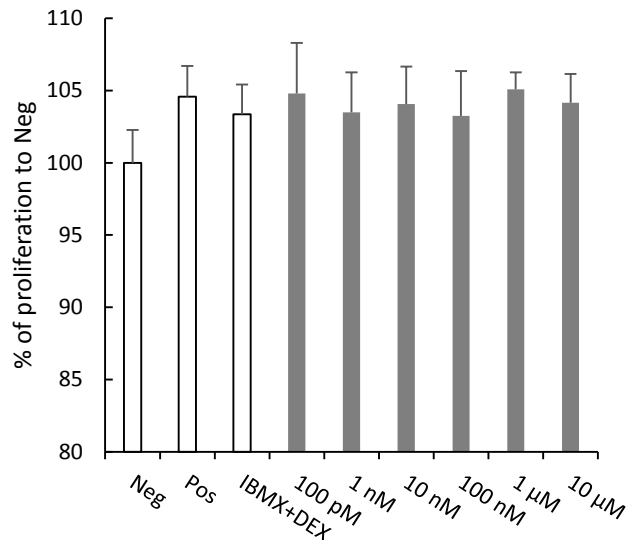
2.4.2 Effect of 2-NAP on cell morphology and lipid accumulation

The first hallmark of adipogenesis is the change in cell shape from fibroblast preadipocytes into spherical, large and lipid producing adipocytes. Figure 2.3 A shows the morphology change and lipid production in three controls. After staining with Oil Red O, the positive control and IBMX+DEX control cells increased their size and accumulated cytosolic triglycerides, indicating the presence of mature adipocytes (Fig.2.3 A lower panel). Stained lipid droplets as well as spherical cell shapes were observed in all doses of 2-NAP treated cells in both microscopic pictures and plate pictures, indicating successful cell differentiation (Fig.2.3 B-D).

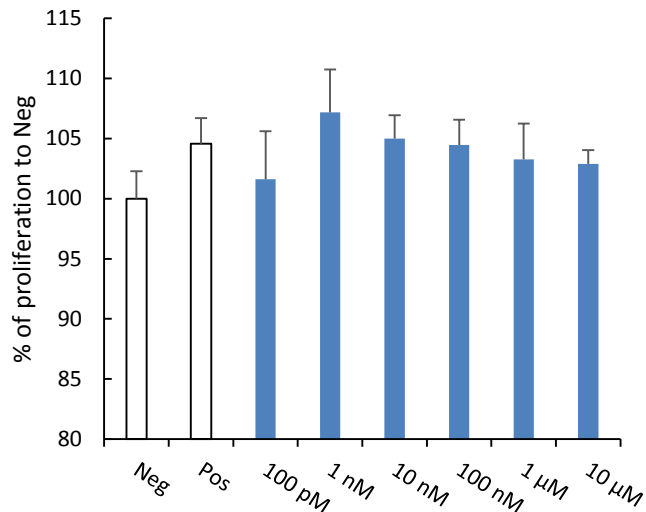
To quantify lipid accumulation, we developed the whole well scan method by using an EnSpire multilabel plate reader (PerkinElmer), which detected Oil Red O staining absorbance for 80 spots in each culture well. In the absence of insulin, although the absorbance of all 2-NAP treated cells in experiment 2-NAP D0-8 was lower than that of the positive control, it was significantly higher than that of the negative control ($P<0.01$), indicating the presence of lipid-producing mature adipocytes (Fig.2.4 A).

In the Experiment Insulin+2-NAP D3-8, a higher absorbance in 2-NAP treated cell was observed compared with the positive control. In particular, cells treated with 100 nM, 1 μ M and 10 μ M of 2-NAP showed a significantly higher content of lipid droplets, and this difference was statistically significant ($P<0.01$) (Fig.2.4 A). Compared to Experiment Insulin+2-NAP D3-8, longer exposure of 2-NAP at the onset of stimulation (Experiment Insulin+2-NAP D0-8) did not further upregulate the lipid accumulation as expected, but showed a lesser extent of upregulation (Fig.2.4 B).

A. Experiment 2-NAP D0-8



B. Experiment Insulin+2-NAP D3-8



C. Experiment Insulin+2-NAP D3-8 and Insulin+2-NAP D0-8

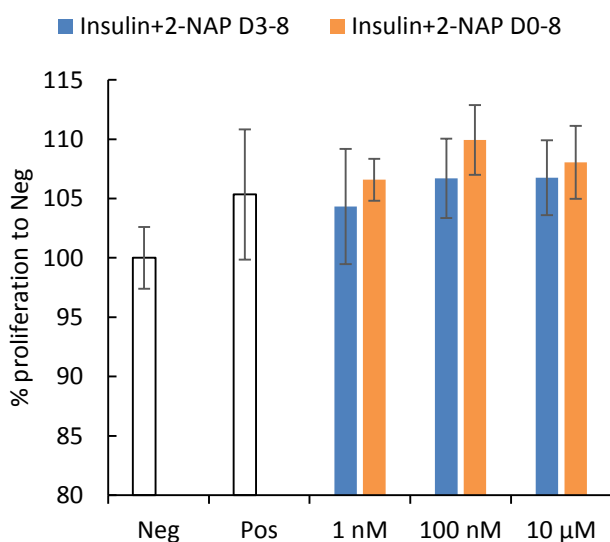


Figure 2.2 Effects of 2-NAP on 3T3-L1 cell viability.

Cell viability was determined using the XTT assay on the termination day of each experiment. Post-confluent 3T3-L1 cells were induced to differentiation as designed. On the termination day (day 8), culture medium was carefully removed and replaced with phenol red-free RPMI-1640 containing XTT solution for 4 hour. The absorbance was measured at 450 nm and 690 nm. The results were presented as proliferation percentage of the negative control and expressed as means \pm standard error of triplicate samples. Statistical analyses among multi-group data were carried out using ANOVA followed by Post Hoc test. $P < 0.05$ was considered significant. (Neg: negative control; Pos: positive control; IBMX+DEX: IBMX+DEX control)

Microscopic view


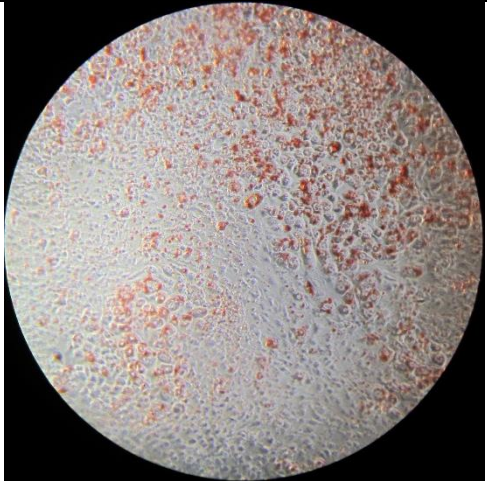
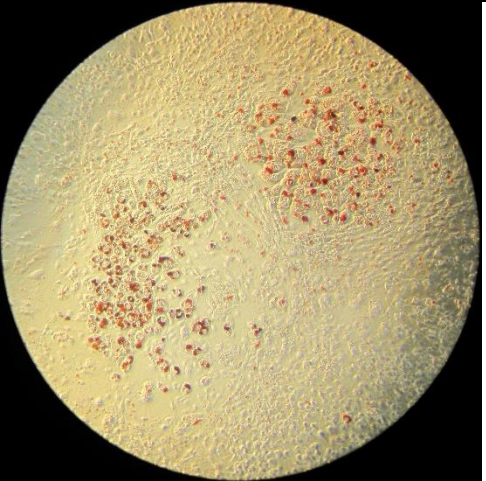



| | | Neg | Pos | IBMX+DEX |
|--------------------------|-----|--|---|--|
| A. Experimental controls | 10X |  |  |  |
| | 20X |  |  |  |

Figure 2.3 continued

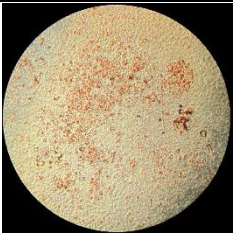



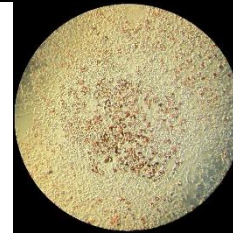
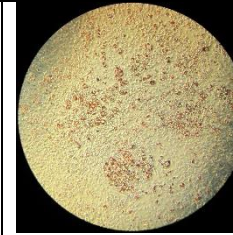

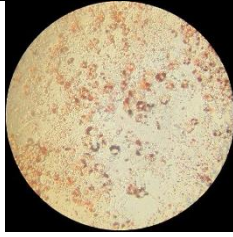



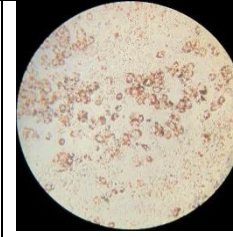

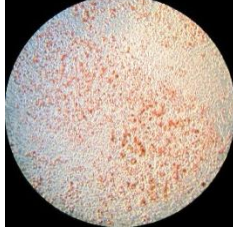
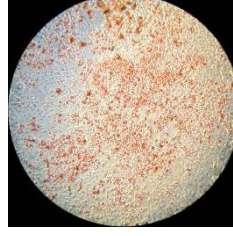
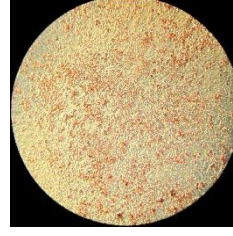
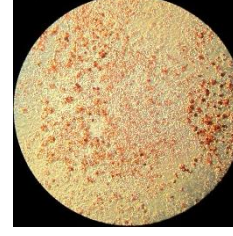





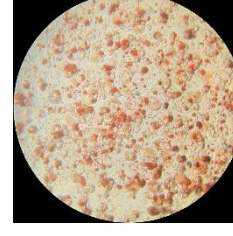
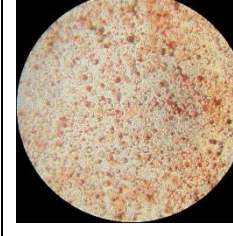
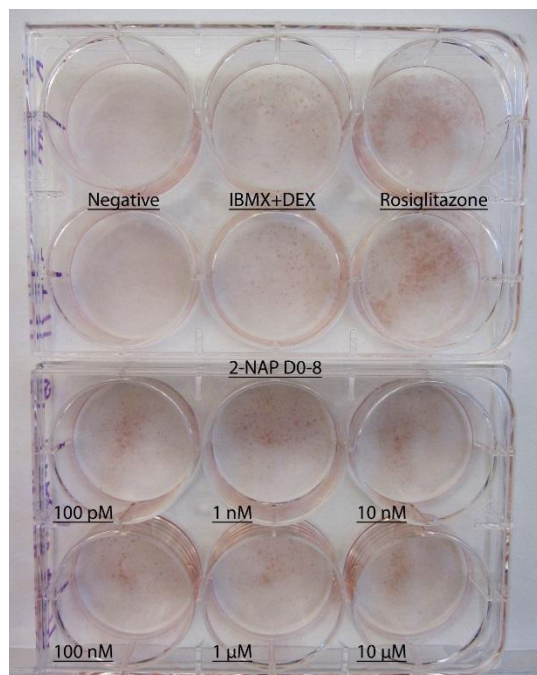
| 2-NAP | | 100 pM | 1 nM | 10 nM | 100 nM | 1 μM | 10 μM |
|---|-----|---|---|--|---|---|---|
| B. Experiment 2-NAP D0-8 | 10X |  |  |  |  |  |  |
| | 20X |  |  |  |  |  |  |
| C. Experiment Insulin+2-NAP D3-8 | 10X |  |  |  |  |  |  |
| | 20X |  |  |  |  |  |  |

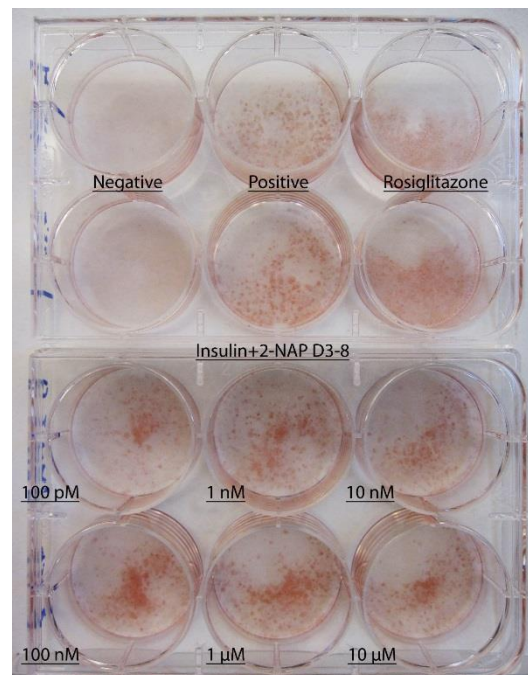
Figure 2.3 continued

Plate view

B. Experiment 2-NAP D0-8



C. Experiment Insulin+2-NAP D3-8



D. Experiment Insulin+2-NAP D0-8

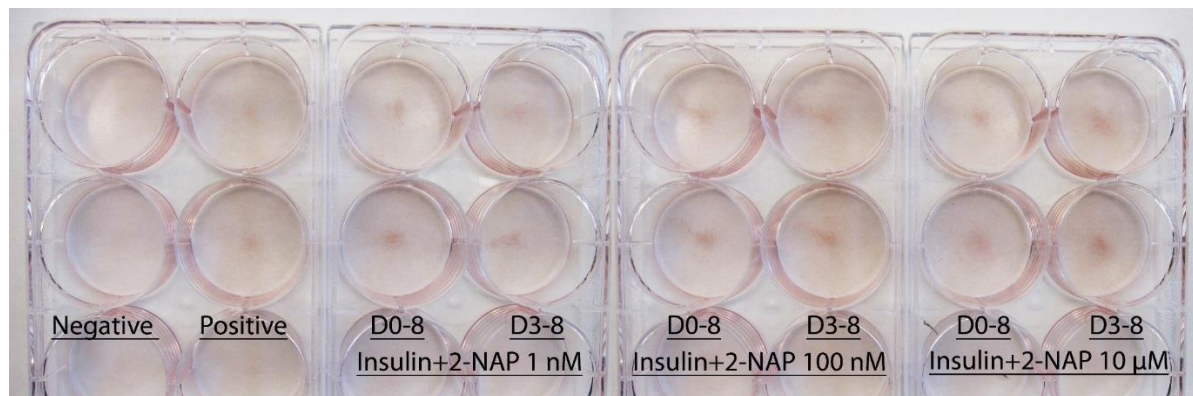
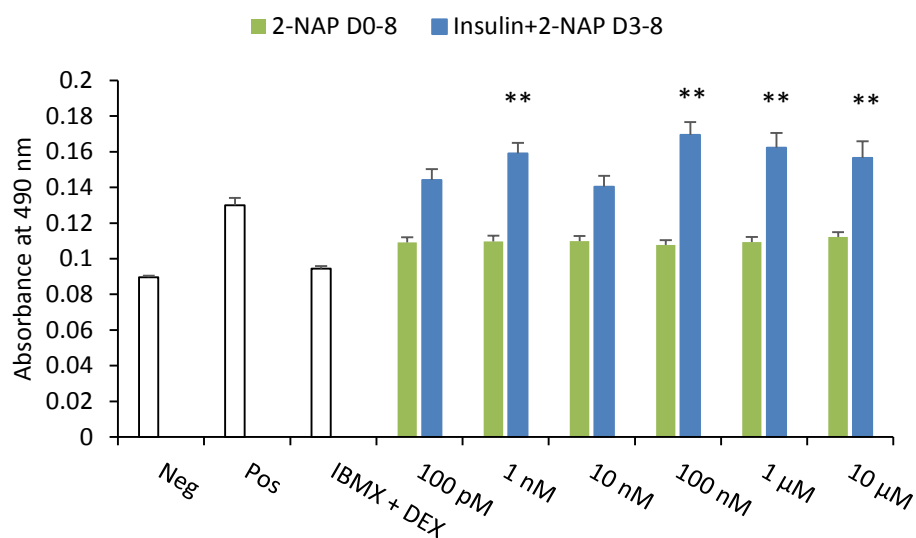


Figure 2.3 Cell morphology change and lipid accumulation in 2-NAP treated 3T3-L1 cells.

At the termination day, cells were fixed with 10% formalin solution at 4 °C overnight, then stained with Oil Red-O solution. 2 μM of Rosiglitazone, a known inducer of 3T3-L1 adipogenesis, was used to test feasibility of the system. Triglyceride droplets stained with Oil Red O were photographed under microscope at 10X and 20X magnification (microscopic view) or directly (plate view). **A.** Experimental controls; **B.** Experiment 2-NAP D0-8; **C.** Experiment Insulin+2-NAP D3-8; **D.** Experiment Insulin+2-NAP D0-8. (Neg: negative control; Pos: positive control; IBMX+DEX: IBMX+DEX control)

A. Experiment 2-NAP D0-8 and Experiment Insulin+2-NAP D3-8



B. Experiment Insulin+2-NAP D3-8 and Experiment Insulin+2-NAP D0-8

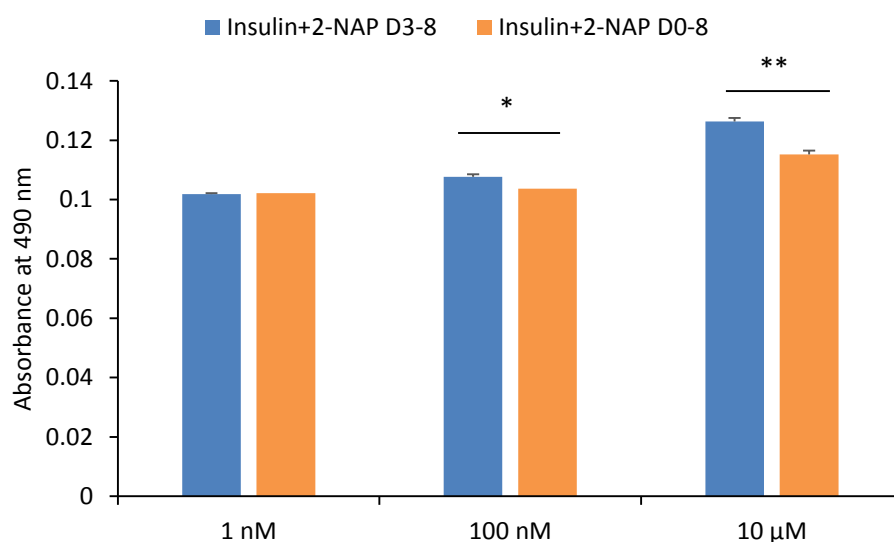


Figure 2.4 Quantification of lipid accumulation in 2-NAP treated 3T3-L1 cells.

Cytosolic triglyceride droplets stained with Oil Red O were measured by an EnSpire multilabel plate reader (PerkinElmer) using well area scan mode for the absorbance at 490 nm. The absorbance was expressed as means \pm standard error. Statistical analyses among multi-group data were carried out using ANOVA followed by Post Hoc test. * donates as $P < 0.05$, ** donates as $P < 0.01$. (Neg: negative control; Pos: positive control; IBMX+DEX: IBMX+DEX control)

2.4.3 Effect of 2-NAP on adipogenic gene expression

Adipogenesis is a multi-step process. During terminal adipocytes differentiation, a series of transcriptional regulators are either activated or suppressed. The first two transcriptional factors that are stimulated by the differentiation cocktail *in vitro* are CCAAT-enhancer-binding protein β and δ (C/EBP β , C/EBP δ) (Ramji and Foka 2002). Both C/EBP β and C/EBP δ can induce the expression of CCAAT-enhancer-binding protein- α (C/EBP α) and peroxisome proliferator-activated receptor- γ (PPAR γ), the two key transcriptional regulators of adipocyte differentiation (Tang et al. 2005). C/EBP α and PPAR γ can directly initiate expression of many adipogenic genes, including leptin, adiponectin, and fatty acid binding protein 4 (FABP4, also as aP2). Therefore, C/EBP α and PPAR γ are commonly used as markers of adipocyte differentiation.

To evaluate terminal adipocyte differentiation on day 8, we focused on the expression of the two master transcriptional regulators in terminal adipocyte differentiation, C/EBP α and PPAR γ , and one of the adipogenic marker genes, aP2. As illustrated in Figure 2.5, in experiment 2-NAP D0-8, even in the absence of insulin, 1 nM, 1 μ M and 10 μ M of 2-NAP were able to activate C/EBP α expression ($P < 0.05$, Fig.2.5 A). In particular, more than two fold increase in upregulation of C/EBP α expression was seen in cells treated with 10 μ M of 2-NAP, compared with the positive control. 2-NAP was also able to induce PPAR γ expression (Fig.2.5 B). Compared to the negative control, the upregulation of PPAR γ expression in 100 pM, 100 nM to 10 μ M 2-NAP treated cells was significantly higher ($P < 0.05$). In particular, 3T3-L1 cells exposed to 10 μ M of 2-NAP showed higher expression of PPAR γ than the positive control, suggesting that the induction of PPAR γ by 10 μ M of 2-NAP was comparable to that of insulin in the standard differentiation protocol. The expression of aP2 in the 2-NAP D0-8 experiment, though lower than the positive control, was

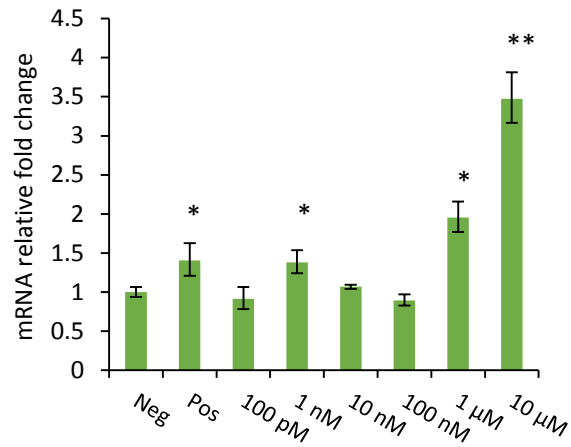
significantly elevated by all doses of 2-NAP ($P < 0.05$, Fig.2.5 C), indicating the maturation of adipocytes.

In the presence of insulin, the addition of 2-NAP from day 3 to day 8 (Experiment Insulin+2-NAP D3-8) showed an additive effect on terminal adipocyte differentiation. Higher concentrations of 2-NAP (1 μM and 10 μM) strongly stimulated the expression of C/EBP α ($P < 0.01$, Fig.2.6 (I) A). The mRNA level of PPAR γ in 2-NAP treated cells increased in a dose-dependent manner, and was significantly higher than the positive control even at 100 pM ($P \leq 0.01$, Fig.2.6 (I) B). In cells treated with 10 μM of 2-NAP, PPAR γ expression was three and two fold higher than the negative control and positive control, respectively. Expression of the mature adipocyte-specific gene aP2 was also upregulated by 2-NAP in a dose-dependent manner, however, only higher concentrations (from 10 nM to 10 μM) of 2-NAP were significantly higher than the positive control ($P < 0.05$, Fig.2.6 (I)C).

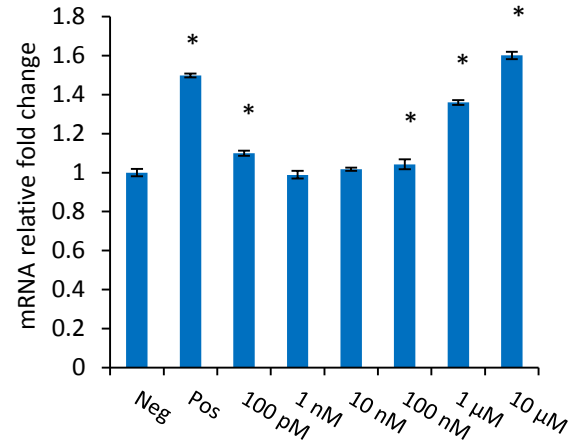
Figure 2.6 (II) shows the comparison of the expression levels of the three marker genes in Experiment Insulin+2-NAP D0-8 and D3-8. Similar to gene expression levels in Experiment Insulin+2-NAP D3-8, in Experiment Insulin+2-NAP D0-8 2-NAP upregulated C/EBP α and PPAR γ expression in a dose-dependent manner, and significantly elevated the aP2 level ($P < 0.01$, Fig.2.6 (II)A-B). In contrast, exposure of cells to 2-NAP from the differentiation onset (day 0 to day 8) did not show higher extent of upregulation on C/EBP α and PPAR γ . 2-NAP at 100 nM in Experiment Insulin+2-NAP D0-8 showed lower C/EBP α and PPAR γ expression compared with cells treated with the same concentration of 2-NAP in Experiment Insulin+2-NAP D3-8 ($P < 0.01$). Even though cells exposed to 1 nM 2-NAP from day 0 to day 8 showed higher expression of aP2, the other higher concentrations showed no significant additional effect (Fig.2.6 (II) C). Therefore, in the

following experiments, we only focused on Experiment Insulin+2-NAP D3-8 to explore the role of 2-NAP during adipogenesis in the presence of insulin.

A. C/EBP α mRNA expression



B. PPAR γ mRNA expression



C. aP2 mRNA expression

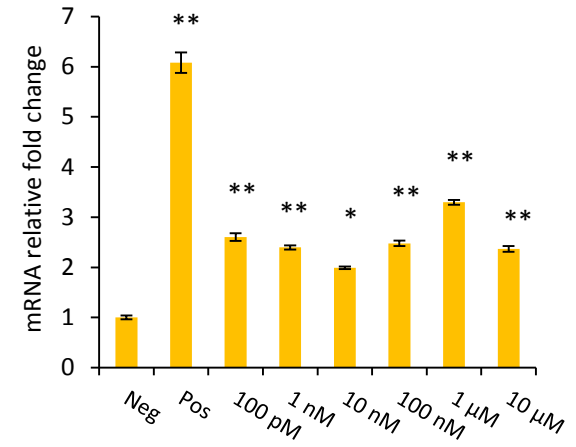
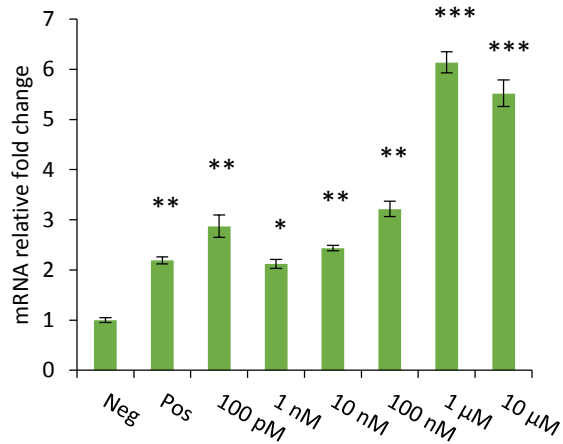


Figure 2.5 Effects of 2-naphthol (Experiment 2-NAP D0-8) on adipogenic gene expression at day 8 of 3T3-L1 differentiation.

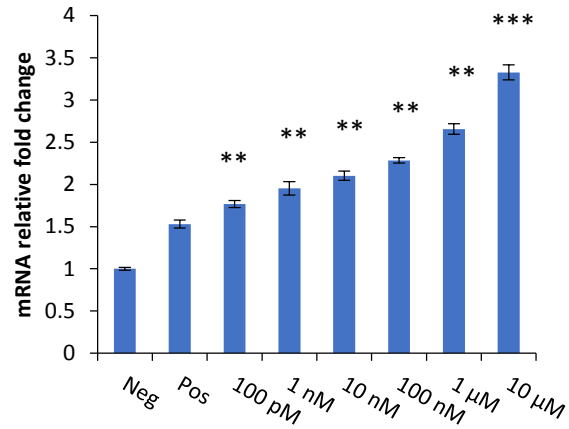
Major transcriptional regulators in terminal adipocyte differentiation: C/EBP α (A) and PPAR γ (B); mature adipocyte-specific protein: aP2 (C). Post-confluent 3T3-L1 cells were induced to differentiate into adipocytes with 0.5 mM IBMX, 0.25 μ M DEX and 2-NAP for three days followed by incubation with 2-NAP alone for six days. Cells treated with the same concentration of IBMX and DEX, and 1 μ g/mL insulin for 3 days followed by 1 μ g/mL insulin were used as the positive control (Pos), whereas cells maintained with DMEM medium were used as the negative control (Neg). Gene expression was evaluated by qRT-PCR, normalized to GAPDH expression and expressed as the relative fold change to the negative control. Data were calculated based on three replicates in the same experiment and presented as the means of relative quantification. Error bars represented the Lower and Upper 95%CI. Each set within the experiment was run in triplicate, and each experiment was performed with an additional run to confirm the repeatability. Statistical analyses among multi-group data were carried out using ANOVA followed by Tukey's difference test. * denotes $p < 0.05$; ** denotes $p = 0.01$.

I. Experiment Insulin+2-NAP D3-8

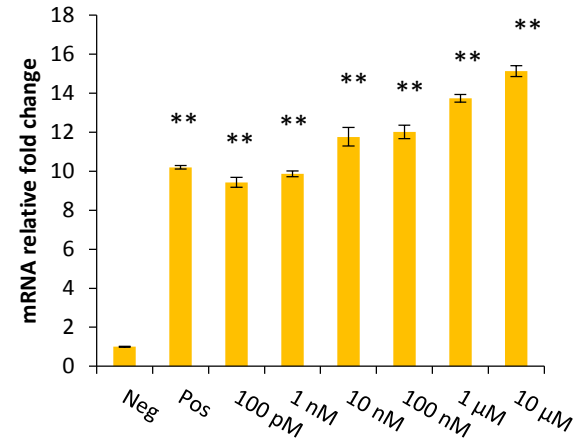
A. C/EBP α mRNA expression



B. PPAR γ mRNA expression

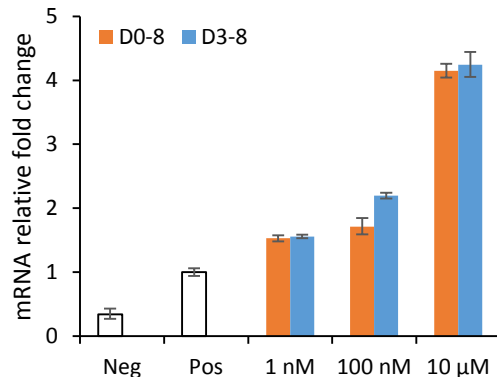


C. aP2 mRNA expression

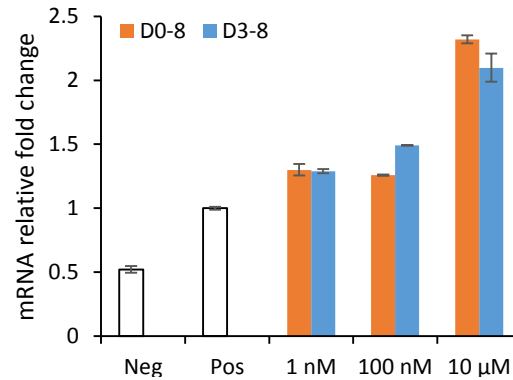


II. Experiment Insulin+2-NAP D3-8 and Experiment Insulin+2-NAP D0-8

A. C/EBP α mRNA expression



B. PPAR γ mRNA expression



C. aP2 mRNA expression

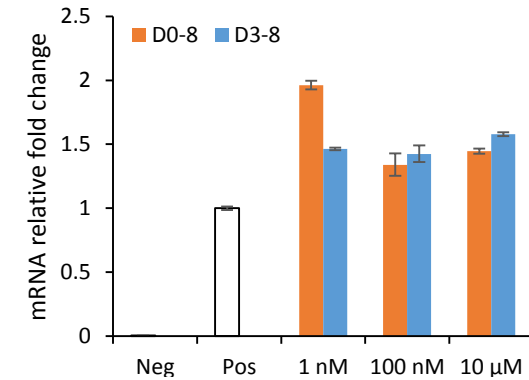


Figure 2.6 Effects of 2-naphthol in the presence of insulin (Insulin+2-NAP) on adipogenic gene expression at day 8 of 3T3-L1 differentiation.

Major transcriptional regulators in terminal adipocyte differentiation: C/EBP α (A) and PPAR γ (B); mature adipocyte-specific protein: aP2 (C). Post-confluent 3T3-L1 cells were induced by the standard differentiation protocol, and 2-NAP was exposed to the cells either from day 0 (Experiment Insulin+2-NAP D0-8) (III) or day 3 (Experiment Insulin+2-NAP D3-8) (I) to day 8. Cells treated with the standard differentiation protocol were used

as the positive control (Pos), whereas cells maintained with the basic DMEM medium were used as the negative control (Neg). Gene expression was evaluated by qRT-PCR, normalized to GAPDH expression and expressed as the relative fold change to the negative control. Data were calculated based on three replicates in the same experiment and presented as the means of relative quantification. Error bars represented the Lower and Upper 95%CI. Each set within the experiment was run in triplicate, and each experiment was performed with an additional run to confirm the repeatability. Statistical analyses among multi-group data were carried out using ANOVA followed by Tukey's difference test. * denotes $p < 0.05$; ** denotes $p = 0.01$ and *** denotes $p < 0.01$.

2.4.4 Effect of 2-NAP on signaling and transcriptional cascade of adipogenesis

Based on previous results, we concluded that 2-NAP accelerates adipocyte differentiation in 3T3-L1 cells at the terminal differentiation phase. To further explore the effect of 2-NAP during adipogenesis, we aimed to investigate the signaling and transcriptional cascade of adipogenesis at day 2 and day 5 post induction of differentiation, as well as on the termination day (day 8) in Experiment 2-NAP D0-8 and Experiment Insulin+2-NAP D3-8. The relative expressions of the early adipogenesis regulator, C/EBP β , IRS2 and SREBP1c, which are involved in insulin signaling pathway during adipogenesis, were evaluated, in addition to C/EBP α , PPAR γ and aP2 expression at day 5 and day 8.

Within the first three days, only cells in Experiment 2-NAP D0-8 were exposed to 2-NAP, whereas cells in Experiment Insulin+2-NAP D3-8 were exposed to the same differentiation medium as in the positive control. On day 2, in the absence of insulin, 2-NAP treated cells (Experiment 2-NAP D0-8) activated IRS2 and SREBP1c gene expressions (Fig.2.7 A-B). IRS2 mRNA levels were comparable to that induced by insulin in the positive control, which was about five fold of the negative control. SREBP1c mRNA levels were significantly increased in a dose-dependent manner with 2-NAP treatment compared with the positive control ($P < 0.05$). Similar levels of C/EBP β mRNA expression (Fig.2.7 C) were observed among 2-NAP treated cells and the positive control, indicating that 2-NAP may contribute to C/EBP β expression during the initiation phase of adipogenesis, in a similar fashion as insulin. 100 nM and 10 μ M 2-NAP significantly upregulated the expression of C/EBP α by 60 and 45 fold compared to the negative control, and three and two fold compared to the positive control, respectively. PPAR γ expression was

moderately affected by 2-NAP (Fig.2.7 D and E). The expression of aP2 in 2-NAP treated cells was comparable to the positive control (Fig.2.7 F).

On day 5, in Experiment 2-NAP D0-8 and Experiment Insulin+2-NAP D3-8, levels of both IRS2 and SREBP1c expression were downregulated to levels comparable to the negative control. No significant difference was detected between 2-NAP treated cells and the positive control (Fig. 2.8 A and B, blue diamond). Moreover, C/EBP β expressions were extensively suppressed on day 5 in both 2-NAP treated cells and the positive control, compared to the negative control (Fig.2.8 C). This result is consistent with the C/EBP β expression pattern observed during adipocyte differentiation in the 3T3-L1 model, where C/EBP β is activated immediately after stimulation, maintained at the maximal expression level for about 48 hours, and then declined to the level of undifferentiated cells (Tang and Lane 1999). In both experiments, all C/EBP α expressions in the positive control and 2-NAP treated cells decreased from more than 20 fold to three to five fold of the negative control, compared with the expression on day 2 (Fig.2.8 D). Cell treated with insulin and 2-NAP (Experiment Insulin+2-NAP D3-8) showed slightly higher C/EBP α expression level than cells treated with 2-NAP in the absence of insulin (Experiment 2-NAP D0-8). With the standard differentiation protocol, the expression of aP2 was activated on day 2, and reached the maximum on day 5 (Fig.2.7F and 2.8F, positive control). In both experiments, 2-NAP treated cells showed the same aP2 expression pattern (Fig.2.7F and 2.8F). In the absence of insulin (Experiment 2-NAP D0-8), 2-NAP was able to activate aP2 expression to a level similar to that of the positive control on day 2; however, on day 5, the upregulated levels of aP2 in 2-NAP treated cells were significantly lower than in the positive control. Conversely, in Experiment insulin+2-

NAP D3-8, the expression level of aP2 in 2-NAP treated cells was comparable to the level observed in the positive control (Fig.2.7F).

On day 8, in the absence of insulin (Experiment 2-NAP D0-8), 2-NAP was capable of upregulating aP2 expression to a similar level of the positive control (Fig.2.8 F). In presence of insulin, (Experiment Insulin+2-NAP D3-8), 2-NAP upregulated the expression levels of C/EBP α , PPAR γ and aP2 (Fig.2.8 D-F) to levels significantly higher than those of the positive control. Taken together, 2-NAP significantly upregulated C/EBP α and PPAR γ expression during the entire terminal differentiation phase, and finally increased the expression of aP2 in the presence or absence of insulin.

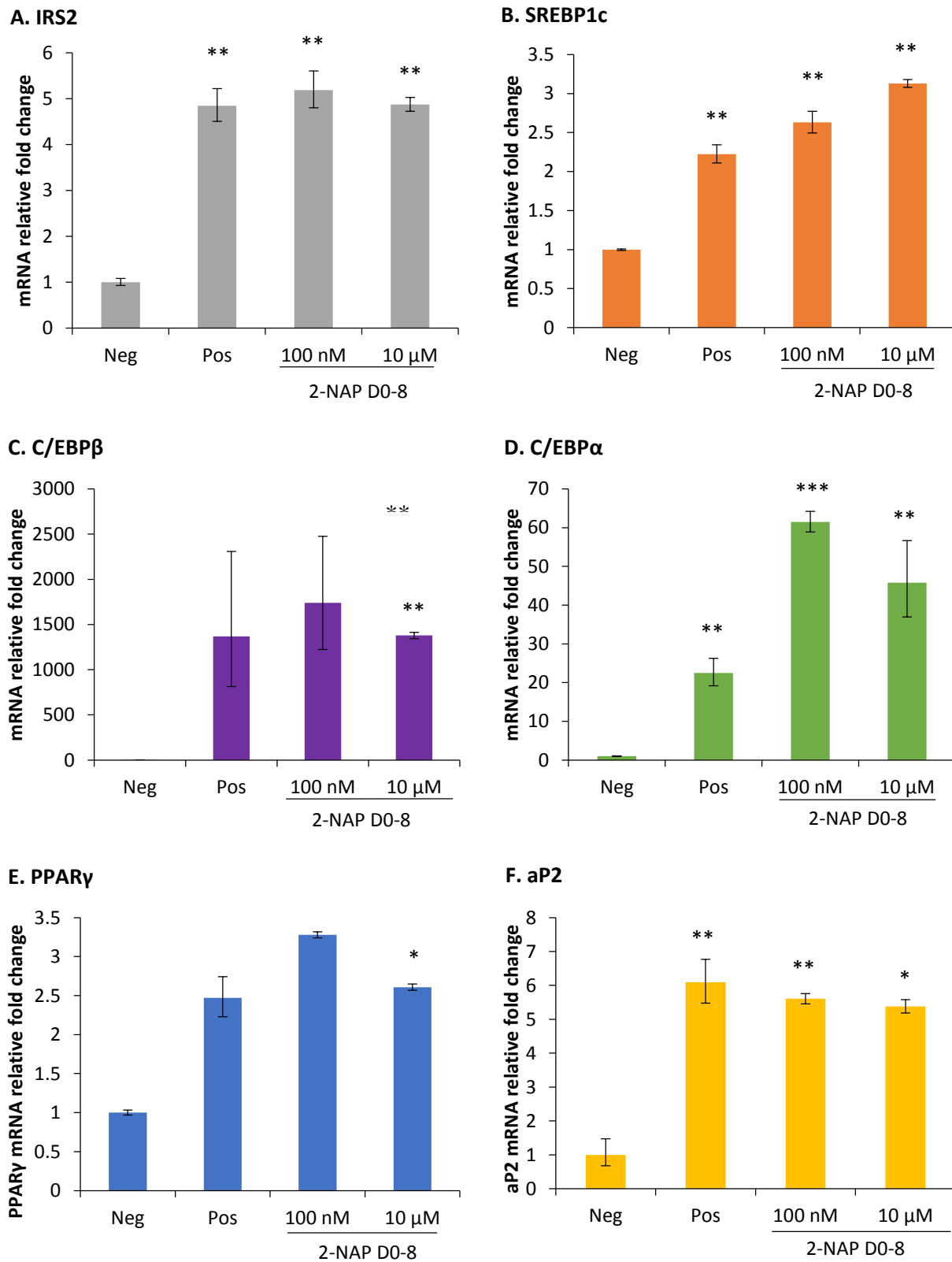


Figure 2.7 Effects of 2-naphthol on IRS2, SREBP1c, and adipogenic gene expression at day 2 of 3T3-L1 differentiation.

Downstream adaptor of insulin receptors: IRS2 (**A**); insulin-regulated lipogenic transcriptional factor: SREBP1c (**B**); early transcriptional factor in initiation phase of adipocyte differentiation: C/EBP β (**C**); major transcriptional regulators in terminal adipocyte differentiation: C/EBP α (**D**) and PPAR γ (**E**); mature adipocyte-specific protein: aP2 (**F**). Post-confluent 3T3-L1 cells were induced to differentiate into adipocytes as designed. Gene expression was evaluated by qRT-PCR, normalized to GAPDH expression and expressed as the relative fold change to the negative control. Data were calculated based on three replicates in the same experiment and presented as the means of relative quantification. Error bars represented the Lower and Upper 95%CI. Each set within the experiment was run in triplicate, and each experiment was performed with an additional run to confirm the repeatability. Statistical analyses among multi-group data were carried out using ANOVA followed by Tukey's difference test. * denotes $p < 0.05$; ** denotes $p = 0.01$ and *** denotes $p < 0.01$.

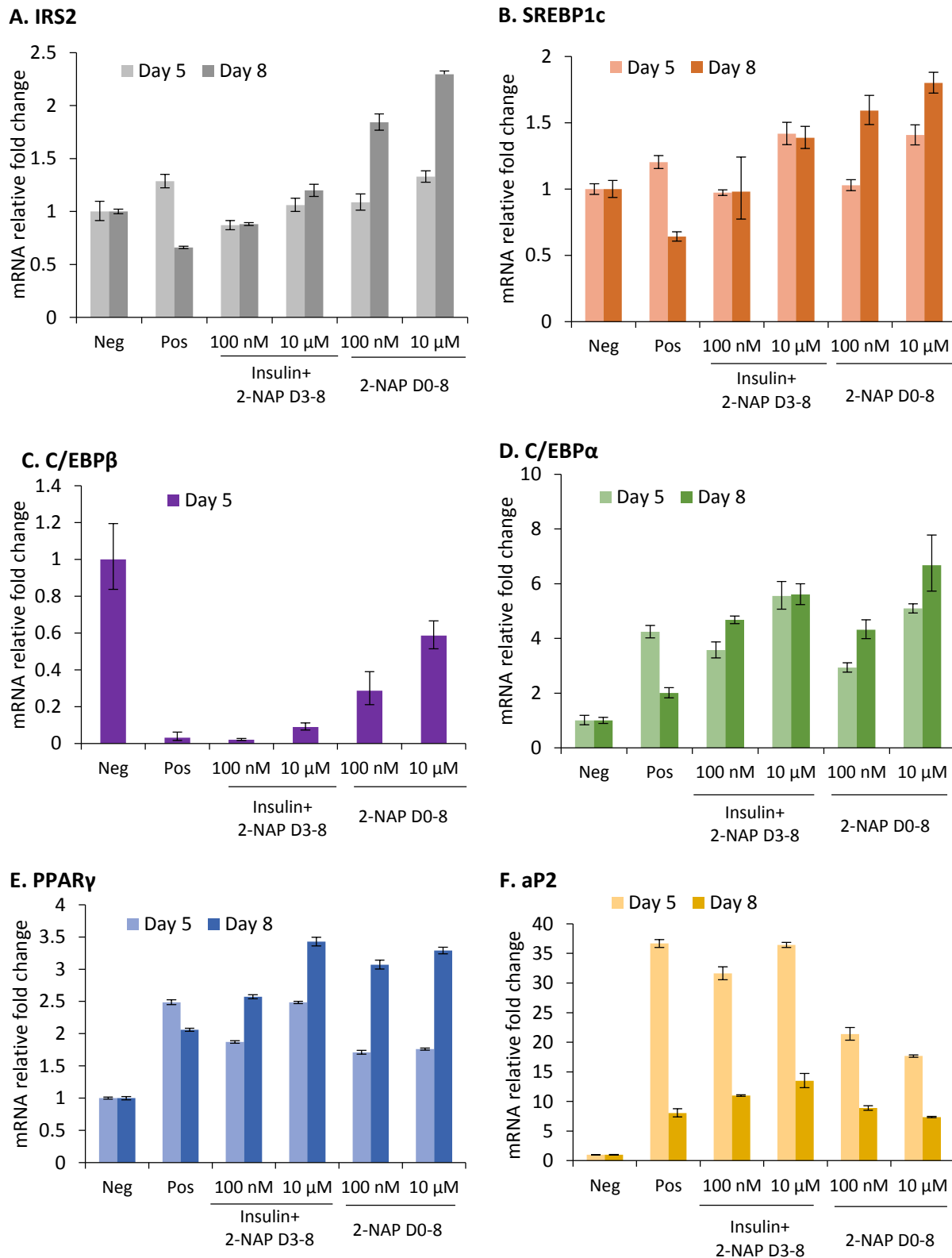


Figure 2.8 Effects of 2-naphthol in the presence or absence of insulin on adipogenic gene expression at day 5 and day 8 of 3T3-L1 differentiation.

Downstream adaptor of insulin receptor: insulin receptor substrate 2 (IRS2) (**A**); insulin-regulated lipogenic transcriptional factor: sterol responsive element binding protein 1c (SREBP1c) (**B**); early transcriptional regulator, C/EBP β (**C**); major transcriptional regulators in terminal adipocyte differentiation: C/EBP α (**D**) and peroxisome proliferator-activated receptor- γ (PPAR γ) (**E**); mature adipocyte-specific protein: fatty acid binding protein 4 (aP2) (**F**). Post-confluent 3T3-L1 cells were induced to differentiate into adipocytes as designed. Gene expression was evaluated by qRT-PCR, normalized to GAPDH expression and expressed as relative fold change to negative control. Data were calculated based on 3 replicates in the same experiment and presented as the means of relative quantification. Error bars represented the Lower and Upper 95%CI. Each set within the experiment was run in triplicate, and each experiment was performed with an additional run to confirm the repeatability. Statistical analyses among multi-group data were carried out using ANOVA followed by Tukey's difference test. * denotes $p < 0.05$.

2.5 Discussion

PAHs are a large family of environmental chemical pollutants present in the air, and 2-NAP is one of the biomarkers of PAH exposure in humans. Results from a recent study show that the concentration of 2-NAP in the urine is positively linked to increased body mass index and obesity in children (Scinicariello and Buser 2014). Despite such epidemiological association, the direct relationship between 2-NAP exposure and adipocyte differentiation has not yet been determined using laboratory models. Mouse 3T3-L1 preadipocytes are a commonly used and a well-studied *in vitro* cell model for adipocytes and obesity-related research. The combination of IBMX, DEX, and insulin for 2-3 days followed by insulin alone has been established as the standard mean to trigger the differentiation of confluent 3T3-L1 cells (Green and Kehinde 1975; Rubin et al. 1978). Based on this standard differentiation protocol, 3T3-L1 cells have been widely used in analyzing the impact of chemicals and the molecular mechanisms of action in adipocytes. A variety of chemicals has been studied for their roles in regulating adipogenesis via this model, including hormones like 17 β -estradiol (Jeong and Yoon 2011), endocrine disruptors like BPA (Masuno et al. 2005) and tolylfluanid (Neel et al. 2013), and heavy metals such as cadmium (Lee et al. 2012). In the present study, we designed two sets of experiments to address the following questions: i) whether 2-NAP itself can accelerate 3T3-L1 differentiation initiated by the combination of IBMX and DEX; ii) whether 2-NAP in combination with insulin can further accelerate 3T3-L1 differentiation. Therefore, according to the time course and the components of the standard differentiation protocol, we exposed the chemical to the cells either at the onset of differentiation (day 0) or after the induction (day 3) with or without insulin.

In this study, we developed an alternative method of quantifying lipid accumulation in differentiated 3T3-L1 cells within the culture plates, instead of comparing the intensity of isopropanol-extracted Oil Red O staining from lipid-producing adipocytes. In our experimental system, lipid-producing 3T3-L1 cells were grown as scattered clusters over the Costar 6-well culture plates (Fig.2.3). Moreover, this brand of culture plates is reported to have the lowest differentiation ratio compared to other culture plate brands (Mehra et al. 2007). Because of the scattered distribution and the low differentiation rate, the amount of Oil Red O staining extracted from lipid-producing cells will be greatly affected by the dye that remains on the outside of cells and plastic plates. Therefore, the common method using the dye extraction to quantify lipid accumulation is not suitable and accurate in our system. The whole well scan method allows us to divide each culture well into 80 scan spots and precisely quantify the red absorbance on non-homogenized cell grown surface. In addition, this method also minimizes the variables of the average absorbance of each well that are created by empty spots where cells are detached from the plates and washed away during the staining process.

In the first set of experiments (Experiment 2-NAP D0-8), 3T3-L1 differentiation was initiated by the combination of IBMX and DEX, and insulin in the standard differentiation protocol was replaced by 2-NAP. After 9 days treatment, regardless of the concentration, 2-NAP-treated 3T3-L1 cells successfully differentiated from fibroblasts into mature adipocytes. In addition, 2-NAP increased lipid droplet production in 3T3-L1 cells induced by IBMX and DEX (Fig.2.3 B). The quantification results confirmed the significance of 2-NAP-induced upregulation of lipid accumulation (Fig.2.4 A). Compared to the positive control, 2-NAP even at the highest concentration did not induce a comparable amount of lipid in 3T3-L1 cells. This result is confirmed

by aP2 expression at mRNA level. aP2 is specifically expressed in mature adipocytes and functions as a mediator of lipid transportation and metabolism (Gorbenko et al. 2006). On day 5 and day 8 aP2 was markedly less expressed in 2-NAP-treated cells than the positive control (Fig.2.5 C and Fig.2.8 F). These results demonstrate that, in comparison to insulin, 2-NAP exerts a reduced effect on lipid accumulation in adipocytes. The expression of transcriptional regulators of adipogenesis and key molecules involved in insulin pathway was another important marker to evaluate. In this study, the two master transcriptional regulators of adipogenesis C/EBP α and PPAR γ were elevated in a dose-dependent manner by 2-NAP during adipogenesis. Particularly, 2-NAP at higher concentrations significantly increased expression of C/EBP α and PPAR γ levels at their 48-hour peak time as well as during the terminal differentiation phase (Fig.2.5 A-B and Fig.2.7 D-E). Compared to the positive control, similar expression levels of C/EBP β and IRS2, as well as upregulated expression of SREBP1c induced by 2-NAP in the combination of IBMX and DEX, suggested that 2-NAP is able to elevate early factors in the signal cascade of adipogenesis despite the absence of insulin.

In the second set of experiments (Experiment Insulin+2-NAP D3-8), 3T3-L1 differentiation was induced by the standard differentiation protocol, and 2-NAP treatment was started on day 3 in order to evaluate its effect on the terminal differentiation phase. As expected, 2-NAP increased lipid accumulation in 3T3-L1 cells induced by the standard differentiation protocol (Fig.2.4 A), and elevated gene expression levels of C/EBP α and PPAR γ in a dose-dependent manner (Fig.2.6 I). In particular, as low as 100 pM of 2-NAP was capable of upregulating PPAR γ expression on the termination day. On the other hand, in Experiment Insulin+2-NAP D0-8, where 2-NAP was added on day 0 together with IBMX, DEX and insulin, both lipid accumulation and

marker gene expression results did not show any additive effect on termination day, indicating that 2-NAP in the presence of insulin exerts its modulating role on adipogenesis during the terminal differentiation phase (Fig.2.4 B and Fig.2.6 II).

Many epidemiological and laboratorial studies *in vitro* and *in vivo* have identified intriguing links between environmental endocrine disrupting chemicals (EDC) and obesity. A variety of EDCs have been screened for their hormone receptor-binding affinity and adipogenic potential. Structurally similar to endogenous hormones, 2-NAP has the ability to bind estrogen receptors (Schultz and Sinks 2002) and thyroid hormone receptors (Sun et al. 2008). Thus, 2-NAP is characterized as a potential EDCs. This study is the first to report the adipogenic property of 2-NAP. Here, we show that, regardless of insulin, 2-NAP at higher concentrations promotes the expression of C/EBP α and PPAR γ during terminal differentiation. In addition, 2-NAP is capable of activating and upregulating expression of IRS2 and SREBP1c, the two molecules involved in and regulated by the insulin signaling pathway (Fig.2.7 A-B and Fig.2.8 A-B). This finding suggests that 2-NAP may induce 3T3-L1 differentiation via the PPAR γ pathway and may modulate the action of insulin pathway during adipogenesis. Of course, the possibility of using other pathways and multiple pathways at one time cannot be excluded. Further work will be needed to fully elucidate the utilization of signaling pathways under variant conditions.

In conclusion, 2-NAP is capable of inducing adipocyte differentiation of 3T3-L1 cells by regulating molecules involved in the insulin signaling pathway, and transcriptional regulators of adipogenesis. Therefore, 2-NAP plays a potential role in interrupting lipid homeostasis, possibly leading to obesity and associated disorders.

3 Chapter 3: The effect of lead on 3T3-L1 adipocyte differentiation is non-monotonic

3.1 Summary

Currently available data on the association between lead exposure and obesity are inconclusive. A recent epidemiological study shows that a blood lead concentration higher than 1.10 $\mu\text{g/dL}$ is associated with a lower body mass index and obesity in both children and adolescents. Moreover, another study indicates that mice exposed to 109 ppm of lead via drinking water exhibit decreased body weight when compared to their counterparts subjected to lower levels of lead exposure, but are significantly bigger than the controls. Therefore, we hypothesized that lead at lower concentrations induces adipogenesis, whereas at higher concentrations lead suppress this induction effect.

3T3-L1 cells were induced by the standard differentiation cocktail containing IBMX, DEX, and insulin for the first three days (day 0-2), followed by DMEM medium containing only insulin for six days (day 3-8). Three one-hundred-fold concentrations of lead (1 nM to 10 μM) were exposed to the cells in three experimental protocols. In the first experimental protocol (Insulin+Pb D3-8), cells were induced by the standard differentiation medium with IBMX, DEX, and insulin for three days, followed by insulin and lead for six days. In the second experimental protocol (Insulin+Pb D0-8), cells were induced by IBMX, DEX, and insulin together with lead for three days, followed by insulin and lead for six days. In the third experimental protocol (Pb D0-8), cells were induced by IBMX, DEX, and lead for three days, followed by lead alone for six days. The terminal differentiation was evaluated by cell morphology and lipid production. The transcriptional cascade of adipogenesis was assessed by quantifying the expression of the early

transcriptional factor C/EBP β , two major transcriptional regulators of terminal adipocyte differentiation C/EBP α and PPAR γ , and the mature adipocyte-specific gene aP2.

Results from all three experiments show that all lead-treated cells differentiated from fibroblast cells into mature lipid-producing spherical adipocytes, indicating the induction of adipogenesis. Lead at 10 μ M, however, showed the least induction on lipid accumulation when compared with lower concentrations. Analysis of the transcriptional cascade of adipogenesis revealed that in the presence of insulin, in the Insulin+Pb D0-8 experiment, lead increased the expression of C/EBP β , C/EBP α , PPAR γ , and aP2 after 48 hours during the early differentiation phase. In both Insulin+Pb experiments, C/EBP α remained upregulated on day 5 and day 8 in lead treated cells. Moreover, 10 μ M of lead significantly suppressed the expression of PPAR γ and aP2 from day 5 to day 8 in both Insulin+Pb experiments. On the other hand, in the absence of insulin (experiment Pb D0-8), the upregulation of C/EBP α , PPAR γ , and aP2 was observed from day 5 in lead-treated cells. In 10 μ M lead treated cells, aP2 was significantly upregulated after 48 hours, and the expression of C/EBP α , PPAR γ , and aP2 was significantly higher than that in cells treated with lower concentrations of lead. On day 8, however, gene expression induced by 10 μ M of lead drastically declined.

In conclusion, lead induces adipocyte differentiation by modulating the C/EBP α pathway. Lead promotes adipogenesis by upregulating C/EBP α and aP2 expressions during the early phase; however, during the terminal differentiation phase, a high concentration of lead attenuates the induction of adipogenesis by suppressing PPAR γ and aP2 expression. Therefore, although lead plays a potential role in inducing obesity, higher concentrations of lead may result in minimal obesity-related effects.

3.2 Introduction

Results from studies on the association between lead exposure and obesity are inconclusive. A recent epidemiological study, using multiple logistic and multivariate linear regression to analyze the blood lead level with the body mass index (BMI) from NHANES 1999-2006, shows that higher lead concentration in blood is associated with lower BMI and obesity among all the participants, including children and adolescents (Scinicariello et al. 2013). A longitudinal study conducted with Boston children reported a statistically significant increased association with BMI and dentin lead level, but no association with bone lead level (Kim et al. 1995). Several cross-sectional studies with children and adults found no association between BMI and blood lead level, while other studies reported an inverse dose-response relationship among specific populations, including children and adult women. The Donald group using the mouse model and the Hamir group using the dog model found out that lead exposure is associated with lower body weight (Donald et al. 1988; Hamir et al. 1981), whereas in Leasure's mouse study, mice exposed to higher levels of lead exhibited decreased body weight when compared to lower lead exposure counterparts, but significantly increased than the controls (Leasure et al. 2008). Therefore, the effect of lead exposure on obesity needs to be clarified.

In this study, we aimed to investigate the effect of lead on adipocyte differentiation and lipid homeostasis *in vitro* to test our hypothesis that lower concentrations of lead upregulate adipogenesis, but higher concentrations do not. Mouse 3T3-L1 cells were initiated with the differentiation cocktail, then incubated with three one-hundred-fold concentrations of lead (1 nM, 100 nM, 10 μ M). Terminal adipocyte differentiation was evaluated by lipid accumulation,

gene expression of transcriptional regulators and mature adipocyte markers, as well as molecules involved in the insulin signaling pathway.

3.3 Materials and methods

3.3.1 Materials

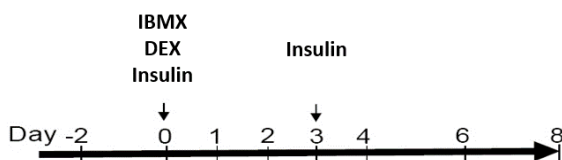
Mouse embryo fibroblast 3T3-L1 cells (ATCC CL-173, lot 59796011) and bovine calf serum (ATCC, 30-2030) were obtained from ATCC. Dulbecco's modified Eagle's medium (DMEM) (Cellgro 10-013CV) and 100X penicillin-streptomycin solution (Cellgro 30-002-CI) were purchased from Mediatech, Inc. Human insulin solution (I9278), dexamethasone (D2915), 3-Isobutyl-1-methylxanthine (I5879), formalin solution (HT501128), and Oil Red O (O0625) were obtained from Sigma-Aldrich Co. LLC. Lead acetate solution (SL9000-250) was purchased from Fisher Scientific Co. In this study, lead acetate was used as the source for all lead exposure experiments.

3.3.2 Experimental design

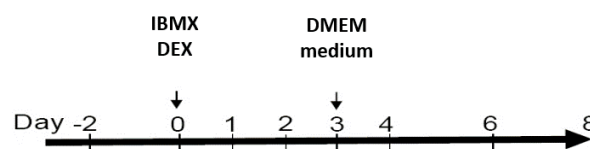
To test whether lead influences adipogenesis, we exposed 3T3-L1 preadipocytes to lead by three different protocols (Fig.3.1). Cells treated with the standard differentiation protocol were used as the positive control, whereas cells maintained with the basic DMEM medium were used as the negative control. In the first experiment (Insulin+Pb D3-8), lead was added to cell cultures on day 3, in order to evaluate its effect on the terminal differentiation phase of adipogenesis. In the second experiment (Insulin+Pb D0-8), lead was exposed to the cells at the onset of differentiation (on day 0). In the third experiment (Pb D0-8), lead substituted insulin in the standard protocol and was kept in the culture medium from day 0 to day 8. Cell viability, cell morphology change, and lipid production were investigated; and the expression of marker genes

of adipogenesis, C/EBP α , PPAR γ , and aP2 was evaluated on termination day. To assess the transcriptional cascade during early and terminal differentiation phases, the expression of C/EBP β , IRS2, and SREBP1c was quantified at different time points during adipogenesis.

A. Positive control protocol

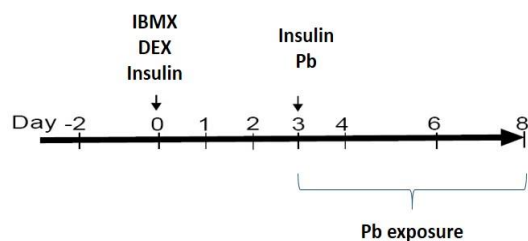


B. IBMX+DEX control protocol

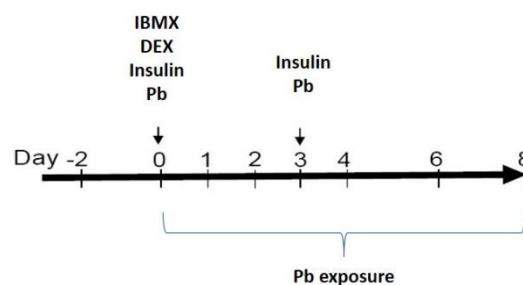


C. Lead exposure protocols

1) Experiment Insulin+Pb D3-8



2) Experiment Insulin+Pb D0-8



3) Experiment Pb D0-8

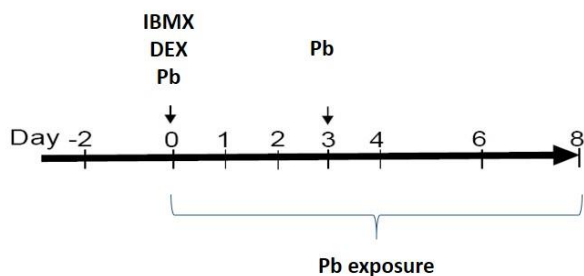


Figure 3.1 Protocols for adipogenic differentiation and lead exposure in 3T3-L1 cells.

Cells were differentiated one day after confluence (designated as day 0, indicated by the first black arrow) by replacing the DMEM medium with the differentiation medium for 3 days. The concentrations of each component in the differentiation medium were 0.5 mM for IBMX, 0.25 μ M for dexamethasone (DEX) and 1 μ g/mL for insulin. On Day 3 (indicated by the second black arrow), the differentiation media were changed to DMEM medium with 1 μ g/mL insulin. Three one-hundred-fold concentrations of lead (1 nM to 10 μ M) were exposed to the cells in three experimental protocols. Experiment 1: Insulin+Pb D3-8, cells were induced by the standard differentiation medium with IBMX, DEX, and insulin for three days followed by insulin and lead for six days. Experiment 2: Insulin+Pb D0-8, cells were induced by IBMX, DEX, and insulin together with lead for three days followed by insulin and lead for six days. Experiment 3: Pb D0-8, cells were induced by IBMX, DEX, and lead for three days followed by lead alone for six days. The lead exposure period in each experiment is indicated by the blue curly bracket.

3.3.3 Cell culture and differentiation

3T3-L1 cells were cultured in the DMEM medium supplied with 10% bovine calf serum (BCS), 100 I.U. penicillin and 100 µg/mL streptomycin. Cells were grown in 75 cm² culture flask in a humidified atmosphere with 5% CO₂ at 37 °C, and subcultured when they became 80% confluent.

Cells were seeded at a density of 6x10⁴ cells/well in Costar 6-well plates with the basic DMEM medium. In the cell viability test, cells were seeded at 5000 cells/well in 96-well plates. 48 hours later (Day 0), cell differentiation was induced by replacing the basic DMEM medium with differentiation media for three days (day 0 to day 2), followed by the chemical-containing medium for six days. The concentrations of each component in the standard differentiation cocktail were 0.5 mM for IBMX, 0.25 µM for DEX, and 1 µg/mL for insulin. Differentiation media containing IBMX and DEX with or without insulin were used for the positive control and the IBMX+DEX control, respectively. In lead experiments, the differentiation medium containing IBMX, DEX, and lead was used for Experiment Pb D0-8 differentiation, whereas the differentiation medium containing IBMX, DEX, and insulin with or without lead was used for the Insulin+Pb experiments. On Day 3, differentiation media were changed to DMEM medium with 1 µg/mL insulin for the positive control; the basic DMEM medium for the IBMX+DEX control; DMEM medium with lead for Experiment Pb D0-8; or DMEM medium with 1 µg/mL insulin and lead for Insulin+Pb experiments, respectively, until the end of experiments (day 3 to day 8). Three one-hundred-fold concentrations of lead, 1 nM, 100 nM, and 10 µM, were used in these experiments. 3T3-L1 cells maintained with the basic DMEM medium were used as the negative control.

3.3.4 Oil Red O staining

On the termination day, adipocytes were stained with Oil Red O solution. Briefly, the culture medium was gently and slowly removed from each well, and cells were washed twice with 1X phosphate buffered saline (PBS). Cells were then fixed with 10% formalin solution at 4 °C overnight or longer. After formalin fixation, cells were washed with DI water twice and incubated with 1.5 mL 60% isopropanol for 5 min at room temperature. After removal of isopropanol, cells were dried completely at room temperature, then incubate with 1 mL Oil Red O working solution for 30 min. Subsequently, cells were washed with DI water for three times, dried and analyzed under the microscope. The Oil Red O working solution is stable for only 2 hours, so it was prepared freshly before use. Oil Red O stock was made by dissolving 300 mg Oil Red O powder in 100 mL isopropanol (this stock is stable for one year). The working solution was prepared as follow: Oil Red O stock was filtered by Whatman filter papers and diluted with DI water at a 3:2 ratio. After 10 min incubation, the Oil Red O working solution was filtered with a 0.22 µm syringe filter.

Triglyceride droplets stained with Oil Red O were quantified by measuring the absorbance at 490 nm using an EnSpire multilabel plate reader (PerkinElmer) with well area scan mode (Program setting parameters in Table 2.2). The absorbance was expressed as means ± standard error of 80 spots scanned for each sample.

3.3.5 XTT assays

Cell viability was tested on the termination day of experiments by XTT assays. The XTT assay measures the mitochondrial dehydrogenase activity in viable cells. The tetrazolium ring of XTT salt can be reduced by mitochondrial dehydrogenase of living cells, resulting in a water-

soluble orange formazan derivative. In brief, cells were seeded in 96-well plates and cultured according to the experimental protocol mentioned above. On termination day, the culture medium was replaced by 100 μ L freshly prepared XTT working solution. After 4-hour incubation at 37 °C, the absorbance of orange formazan was measured at 450 nm and 690 nm with a Bio-Tek microplate spectrophotometer. The results were presented as proliferation percentage of the negative control and expressed as means \pm standard error of triplicate samples.

3.3.6 Quantitative real-time reverse transcription-polymerase chain reaction (Real-Time PCR)

Total RNA was extracted from cells using the QIAGEN RNeasy Plus Mini Kit (Qiagen Inc., Valencia, CA). 5 μ L, 7.5 μ L and 10 μ L of total RNA extracted on Day 8, Day 5, and Day 2 respectively was reverse transcribed into cDNA using a High-Capacity cDNA reverse transcription kit (Applied Biosystems). The reaction mixture contained 1x reverse transcriptase buffer, 4 mM dNTP (deoxynucleotide triphosphate), 5x Random primers, 1 U RNase inhibitors, and 2.5 U of MultiScribe Reverse Transcriptase. The RT-PCR was performed with the following cycle parameters: 25°C for 10 min, 37°C for 120 min, and 85°C for 5 min. Synthesized cDNA was diluted with RNase-free water. Then, quantitative real-time PCR amplification was performed with appropriate sets of primers using Taqman gene expression assays in a total volume of 20 μ L containing aliquot cDNA samples. The gene expression assays were carried out with the following cycle parameters: 55°C for 2min; 94°C for 10 min; 40 cycles of 94°C for 15 sec and 60°C for 60 sec. The primers and probes were obtained from Applied Biosystems: C/EBP α (Mm00514283_s1), C/EBP β (Mm00843434_s1), PPAR γ (Mm01184322_m1), aP2 (Mm00445878_m1), Irs2 (Mm03038438_m1), Srebf1c (Mm00550338_m1), and the

housekeeping gene GAPDH (Cat: 4352339E) as endogenous control to correct the variation of RNA and cDNA loading. Data were analyzed using the Δ CT method. Target gene expression was normalized to GAPDH for Δ CT value, then calibrated to the control sample in each experiment to give the $\Delta\Delta$ CT value. Data were calculated based on three replicates in the same experiment and presented as the means of relative quantification. Error bars represented the Lower and Upper 95% Confidence Interval. Each set within the experiment was run in triplicate, and each experiment was performed with an additional run to confirm the repeatability.

3.3.7 Statistical analysis

Statistical analyzes among multi-group data were carried out using ANOVA followed by Tukey's difference test. $P < 0.05$ was considered significant. Each experiment was repeated at least twice, and each set within the experiments were run in triplicates.

3.4 Results

3.4.1 The induction of lead on lipid accumulation

When cells were exposed to lead in presence of insulin during the 9-day differentiation, lipid production was upregulated in cells treated with lead from day 3 to day 8 (Experiment Insulin+Pb D3-8), but a lesser extent of upregulation was observed in cells treated with the highest concentration of lead at 10 μ M (Fig.3.2, top left plate). Quantification of lipid accumulation by whole well scan at 490 nm further proved that the absorbance averages from cells treated with all concentrations of lead were significantly higher than the one from the positive control (Fig.3.3, $P < 0.01$). In comparing the dose effects of lead treatment on lipid production, the results revealed that cells treated with 10 μ M of lead showed significantly lower

induction on lipid production (1.25 fold of the positive control) than that with 1 nM of lead (1.5 fold and 1.4 fold, respectively) ($P \leq 0.01$); whereas no difference was observed between 1 nM and 100 nM, and 100 nM and 10 μ M of lead treated cells.

Similar results of increased lipid production were observed in Experiment Insulin+Pb D0-8. The highest concentration of lead at 10 μ M showed an apparent decrease of induced lipid production, compared to the lower concentrations of lead which drastically upregulated lipid production, compared to the positive control (Fig.3.2, top right plate). Quantification of lipid production demonstrated that there is no significant difference between the cells treated with 10 μ M of lead and the positive control, whereas 1 nM and 100 nM of lead increased lipid production to 1.5 fold of the positive control (Fig.3.3, $P < 0.01$). Compared to Experiment Insulin+Pb D3-8, early exposure from the onset of adipocyte differentiation (day 0) did not show additional effects on lipid homeostasis.

In the absence of insulin, cells (IBMX+DEX control) exhibited less adipogenesis with fewer and smaller mature adipocytes (Fig.2.2 A) and lesser lipid accumulation when compared to the positive control (Fig.2.3, and Fig.3.2, bottom left plate middle wells). In Experiment Pb D0-8, when insulin was absent from the cell culture, lead was still capable of increasing lipid production up to a level similar to that of the positive control. Results from quantification of lipid accumulation confirmed that no difference in absorbance existed between lead-treated cells and the positive control (Fig.3.3). Even when cells treated with 10 μ M of lead exhibited fewer lipid droplets than cells treated with 1 nM and 100 nM of lead, the difference was still not significant.

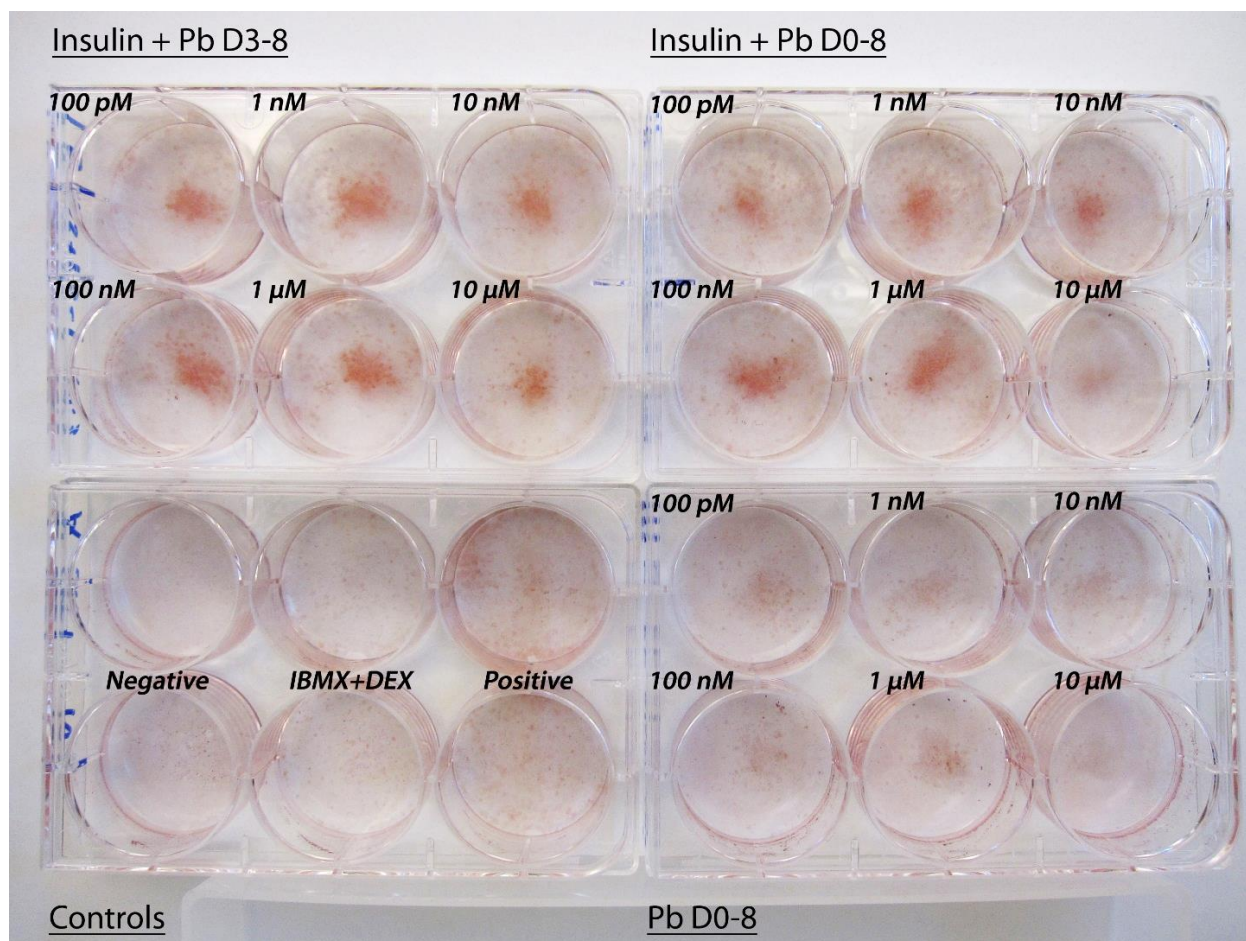


Figure 3.2 Effects of lead on cell morphology change and lipid accumulation.

At termination day, cells were fixed with 10% formalin solution at 4 °C overnight and then stained with Oil Red-O solution. Triglyceride droplets stained with Oil Red-O were photographed. (Upper left plate: Experiment Insulin+Pb D3-8; Upper right plate: Experiment Insulin+Pb D0-8; Bottom left plate: negative, IBMX+DEX, and positive control; Bottom right plate: Experiment Pb D0-8)

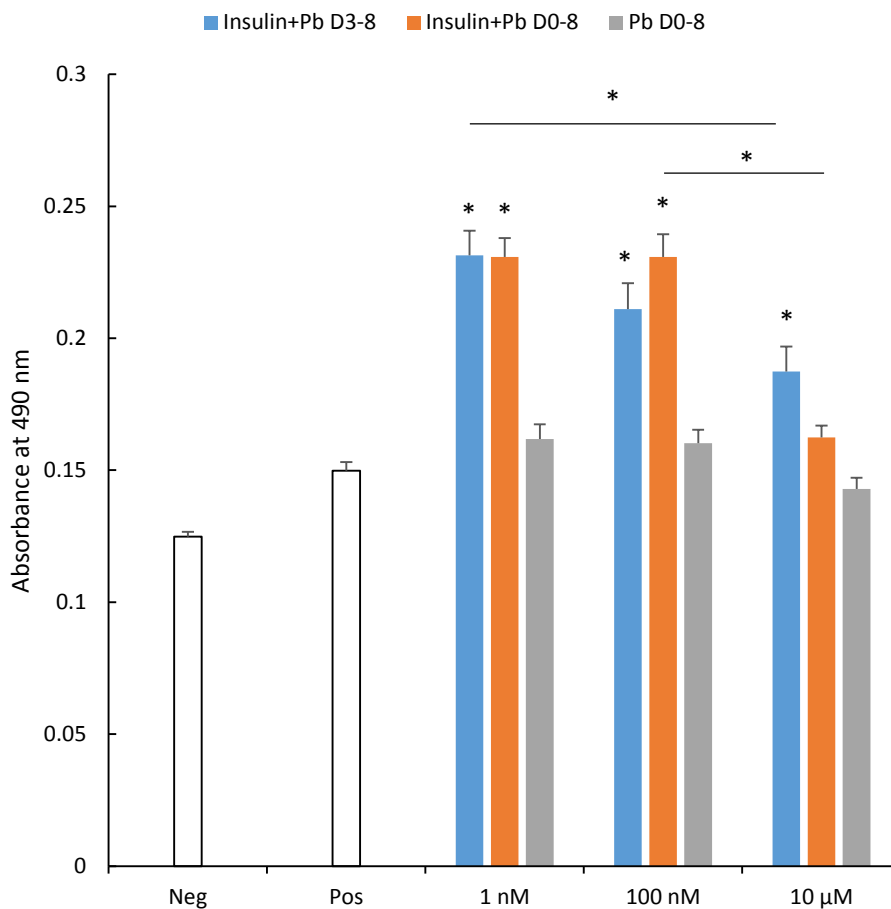


Figure 3.3 Quantification of lipid accumulation in lead treated 3T3-L1 cells.

Cytosolic triglyceride droplets stained with Oil Red-O were measured by an EnSpire multilabel plate reader (PerkinElmer) using the well area scan mode for the absorbance at 490 nm. The absorbance was expressed as means + SEM. Statistical analyses among multi-group data were carried out using ANOVA followed by Tukey's difference test. * denotes $p < 0.01$. (Neg: negative control; Pos: positive control)

3.4.2 Negative regulation of lead on cell proliferation

As shown in Figure 3.4, the positive control showed a significantly higher proliferation rate compared to the negative control ($P < 0.01$). The IBMX+DEX control, where no insulin was present during the whole experimental period, showed a lower proliferation rate (73%) than the positive control ($P < 0.05$) but higher than the negative control (40%). This result was consistent with the finding that insulin promotes cell proliferation via the PI3K pathway (Jung et al. 2000). In addition, the re-entry into the cell cycles, which is referred to as mitotic clonal expansion, has been demonstrated to be crucial for initiating adipogenesis (Tang et al. 2003). Moreover, for 3T3-L1 preadipocytes, the combination of IBMX and DEX is enough to initiate full adipocyte differentiation in 96 hours (Pantoja et al. 2008). Taken together, these findings indicate that, in the IBMX+DEX+insulin differentiation cocktail, insulin may play a role in accelerating cell proliferation during mitotic clonal expansion and the differentiation process of 3T3-L1 preadipocytes.

In the presence of insulin, in Experiment Insulin+Pb D3-8, only lead at the highest concentration of 10 μM showed a suppressive role on cell proliferation (62%), compared with the positive control ($P < 0.01$) (Fig.3.4). In Experiment Insulin+Pb D0-8, similar to Experiment D3-8, only lead at 10 μM showed a significantly suppressive role on cell proliferation (82%) ($P < 0.05$). Regardless of the exposure length, lead at the two lower concentrations showed no different influence on cell growth, whereas a decreasing trend of cell proliferation was observed at 10 μM in both Experiment Insulin+Pb D3-8 and D0-8.

In Experiment Pb D0-8, because of the absence of insulin, all lead -treated cells exhibited lower cell proliferation compared to the positive control ($P < 0.01$). However, when compared to

the IBMX+DEX control, only lead at 10 μ M suppressed cell proliferation ($P<0.01$). Regardless of insulin presence, when comparing Experiment Pb D0-8 with Experiment Insulin+Pb D0-8, the same response pattern was observed: lower concentrations of lead had no effect, but the higher concentration had a suppressive effect on cell proliferation.

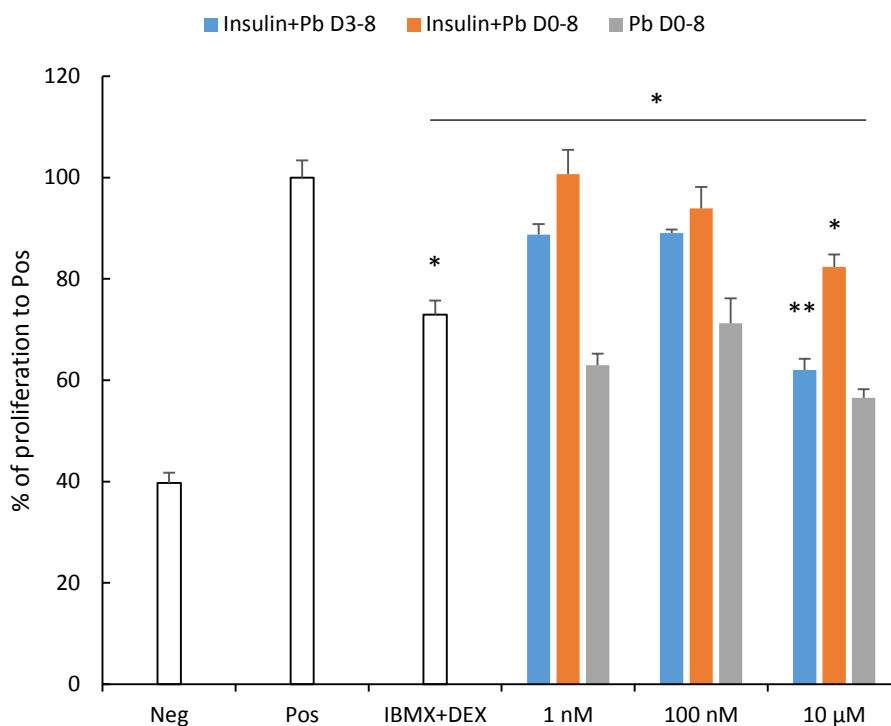


Figure 3.4 Effects of lead on 3T3-L1 cell viability.

Cell viability was determined using the XTT assay on termination day (day 8) of each experiment. Post-confluent 3T3-L1 cells were induced to differentiation as designed. On termination day, culture medium was carefully removed and replaced with phenol red-free RPMI-1640 containing XTT solution for 4 hour. The absorbance was measured at 450 nm and 690 nm. The results were presented as proliferation percentage of the positive control and expressed as means + SEM of triplicate samples. Statistical analyses among multi-group data were carried out using ANOVA followed by Tukey's difference test. * denotes as $P < 0.05$; ** denotes as $P < 0.01$. (Neg: negative control; Pos: positive control; IBMX+DEX: IBMX+DEX control)

3.4.3 Effect of lead on adipogenic genes

To study the effect of lead on adipogenesis at the gene level, we quantified the expression of three marker genes of terminal adipocyte differentiation at the end of the experiments (day 8). In the presence of insulin, when lead was exposed to the cells from day 3 to day 8 (Experiment Insulin+Pb D3-8) lead treated cells showed higher expression of the transcriptional regulator C/EBP α on day 8 than the positive control; however, this difference was not significant. The more important regulator PPAR γ was slightly suppressed by 10 μ M of lead. The mature adipocyte-specific gene aP2 was significantly upregulated in cells treated with 100 nM of lead ($P < 0.01$), but was significantly suppressed in cells treated with 10 μ M of lead ($P < 0.05$, Fig.3.5 A). Therefore, in Experiment Insulin+Pb D3-8, 10 μ M lead suppressed PPAR γ and aP2 expressions on day 8, even though it was capable of increasing lipid accumulation.

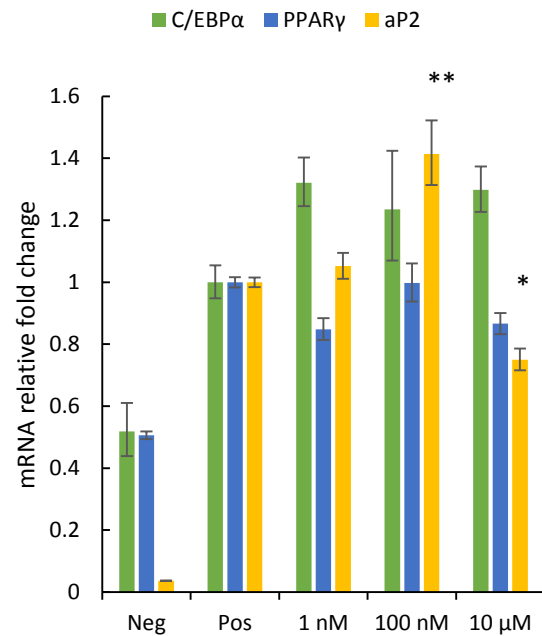
When cells were exposed to lead from day 0 to day 8 in the presence of insulin (Experiment Insulin+Pb D0-8), C/EBP α and aP2 was increased by 1 nM and 100 nM of lead on day 8 (Fig.3.5 B), but only the upregulation of C/EBP α with 1 nM of lead treatment was significant ($P < 0.05$). Lead at lower concentrations did not show any effect on PPAR γ expression on day 8. In contrast, all three marker genes were suppressed by 10 μ M of lead. In particular, C/EBP α and PPAR γ were significantly downregulated ($P < 0.05$), even below the levels of the negative control. When comparing the dose-response difference, the expression levels of the three genes were regulated by lead in an inverse dose-response shape. Significantly decreased gene expression levels were observed between lower concentrations of lead and 10 μ M of lead ($P < 0.01$).

In the absence of insulin, in Experiment Pb D0-8 on day 8, the IBMX+DEX control showed higher levels of C/EBP α , PPAR γ , and aP2 expression than the positive control (Fig.3.5 C, $P < 0.01$).

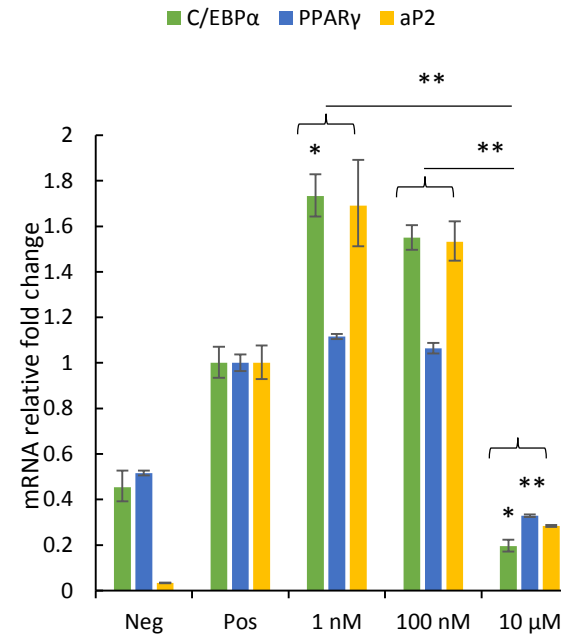
Lead at 1 nM significantly upregulated C/EBP α and aP2 expressions, compared to both the positive control and the IBMX+DEX control ($P<0.01$). Lead at 100 nM also upregulated the expressions of C/EBP α and aP2 compared to the IBMX+DEX control, but was only able to significantly increase C/EBP α expression ($P<0.05$). Lead at 10 μ M showed no significant effect on C/EBP α , even though the expression was a little higher than the IBMX+DEX control; however, PPAR γ and aP2 were significantly suppressed by 10 μ M of lead ($P<0.05$) when compared to the IBMX+DEX control. Notably, PPAR γ was significantly suppressed by all three concentration of lead ($P<0.01$) when compared to the IBMX+DEX control. Compared with Experiment Insulin+Pb D0-8, a similar dose-response pattern was observed in Experiment Pb D0-8: lead affected terminal differentiation marker genes in an inverse dose-response pattern.

Taken together, our results show that on termination day, the presence of lead at lower concentrations upregulated the expression of C/EBP α and aP2, while higher concentration of lead suppressed the expression of PPAR γ and aP2, regardless of insulin presence.

A. Experiment Insulin+Pb D3-8



B. Experiment Insulin+Pb D0-8



C. Experiment Pb D0-8

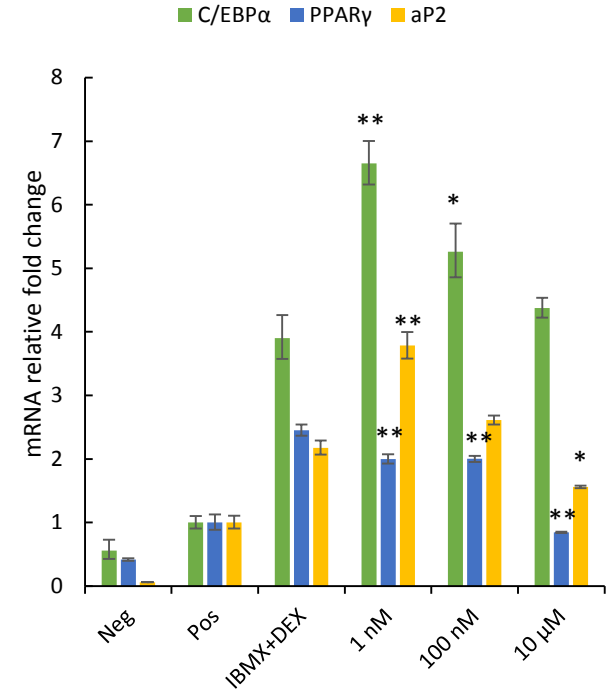


Figure 3.5 Effects of lead on adipogenic gene expression at day 8 of 3T3-L1 differentiation.

Major transcriptional regulators in terminal adipocyte differentiation: C/EBPα and PPARγ; mature adipocyte-specific protein: aP2 were evaluated in each experiment: Experiment Insulin+Pb D3-8 (**A**), Experiment Insulin+Pb D0-8 (**B**), and Experiment Insulin+2-NAP D3-8 (**C**). Cells treated with the standard differentiation protocol were used as the positive control (Pos), and cells induced with IBMX+DEX and followed with the basic DMEM were used as the IBMX+DEX control (IBMX+DEX), whereas cells maintained with the basic DMEM medium were used as the negative control (Neg). Gene expression was evaluated by qRT-PCR, normalized to GAPDH expression and expressed as relative fold change to the positive control. Data were calculated based on 3 replicates in the same experiment and presented as the means of relative quantification. Error bars represented the Lower and Upper 95%CI. Each set within the experiment was run in triplicate, and each experiment was performed with at least one additional run to confirm the repeatability. Statistical analyses among multi-group data were carried out using ANOVA followed by Tukey's difference test. * denotes $p < 0.05$; ** denotes $p < 0.01$.

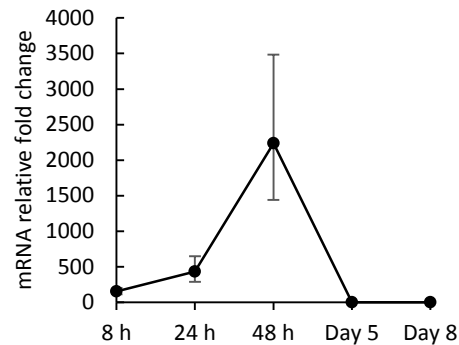
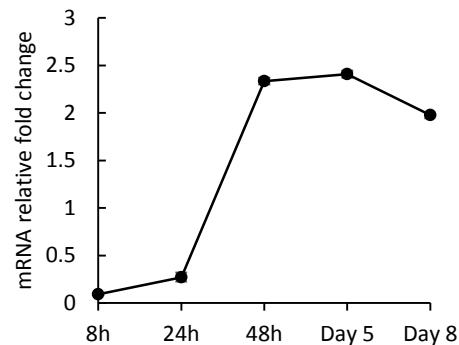
3.4.4 Effect of lead on signaling and transcriptional cascade of adipogenesis

In this study, when 3T3-L1 cells were induced by the standard differentiation protocol, the first important transcriptional factor C/EBP β was activated right after the onset of differentiation, peaked after 48 hours, and shut down on day 5 (Fig.3.6 A). During the early induction phase, the activated C/EBP β initiated the expression of the two terminal transcriptional regulators C/EBP α and PPAR γ around 24 hour-post induction, which maximized at 48 hours post induction, and was then reduced but continuously expressed during the terminal differentiation phase (Fig.3.6 B and C). The mature adipocyte marker aP2, which is regulated by PPAR γ , was activated after 24 hours and peaked on day 5 (Fig.3.6 D).

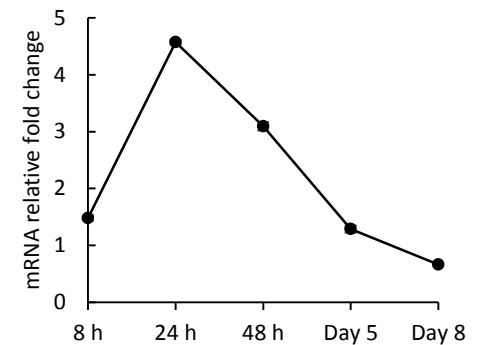
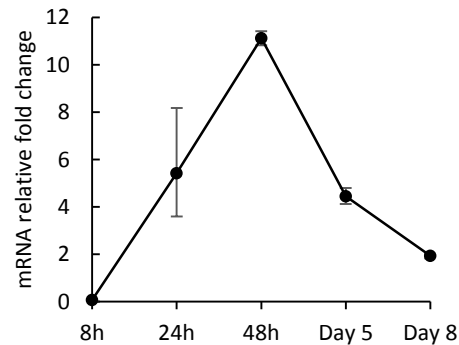
In order to evaluate the effect of lead during adipogenesis, we quantified the mRNA expression of the four marker genes at different time points: C/EBP β at 24 and 48 hours; C/EBP α , PPAR γ , and aP2 at 48 hours, on day 5 and day 8. The time points were chosen based on the peak time of each gene. In experiment Insulin+Pb D3-8, lead was exposed to the cells on day 3, therefore we only quantified the expression of C/EBP α , PPAR γ , and aP2 on day 5 and day 8. On day 5 lead at all three concentrations significantly suppressed the expression of C/EBP α , PPAR γ , and aP2 ($P < 0.01$). On day 8, concentrations of 1 nM and 100 nM lead were able to upregulate the expression of C/EBP α and aP2 (Fig.3.7 A).

In experiment Insulin+Pb D0-8, lead was present in cell culture during the entire experiment period. As shown in Figure 3.7 B, at 48 hours, lead significantly upregulated the expression of C/EBP β , C/EBP α and aP2, especially at concentrations of 1 nM and 10 μ M ($P < 0.01$). In the meantime, lead did not affect the expression of PPAR γ at all concentrations of lead tested in this experiment. On day 5, the presence of lead at 1 nM still maintained the capability to

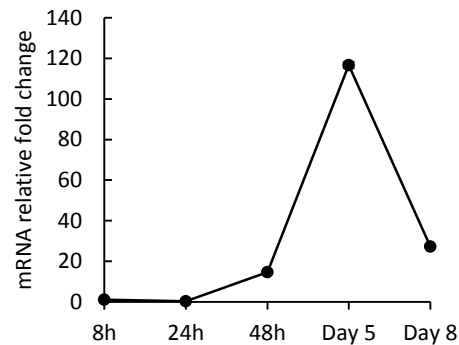
upregulate C/EBP α and aP2 expression, even though upregulation was only significant for aP2 expression ($P < 0.01$). On the other hand, lead at 100 nM and 10 μ M suppressed the expression of C/EBP α and aP2 in a dose-dependent manner, and 10 μ M of lead significantly downregulated aP2 expression on day 5 ($P < 0.01$). As it relates to PPAR γ , all three concentrations of lead showed a suppressive role ($P < 0.01$). In particular, 10 μ M of lead downregulated the expression of PPAR γ to a level similar to the negative control. On day 8, the expressions of C/EBP α , PPAR γ , and aP2 were higher than the positive control at lower concentrations, though only the increasing fold of C/EBP α was statistically significant ($P < 0.05$). The expressions of all three genes remained suppressed in cells treated with 10 μ M of lead. Notably, expression of C/EBP α and PPAR γ fell at levels even lower than the negative control.

A. C/EBP β C. PPAR γ 

E. IRS2

B. C/EBP α 

D. aP2



F. SREBP1c

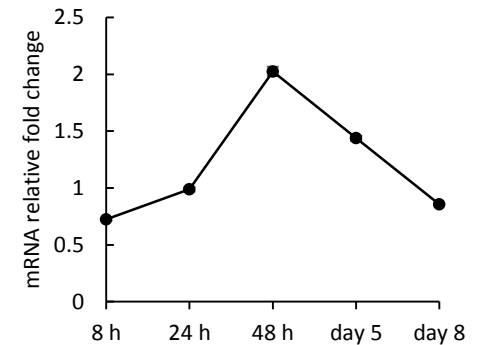


Figure 3.6 Expression of marker genes of adipogenesis during differentiation of 3T3-L1 preadipocytes induced by the standard differentiation protocol.

Major transcriptional regulators: C/EBP β (**A**), C/EBP α (**B**) and PPAR γ (**C**); mature adipocyte-specific protein: aP2 (**D**); insulin receptor substrate: IRS2 (**E**); and transcriptional factor regulated by insulin: SREBP1c (**F**) were evaluated. Gene expression was evaluated by qRT-PCR, normalized to GAPDH expression and expressed as relative fold change to the negative control. Data were calculated based on 3 replicates in the same experiment and presented as the means of relative quantification. Error bars represented the Lower and Upper 95%CI. Each set within the experiment was run in triplicate, and each experiment was performed with at least one additional run to confirm repeatability.

A. Experiment Insulin+Pb D3-8

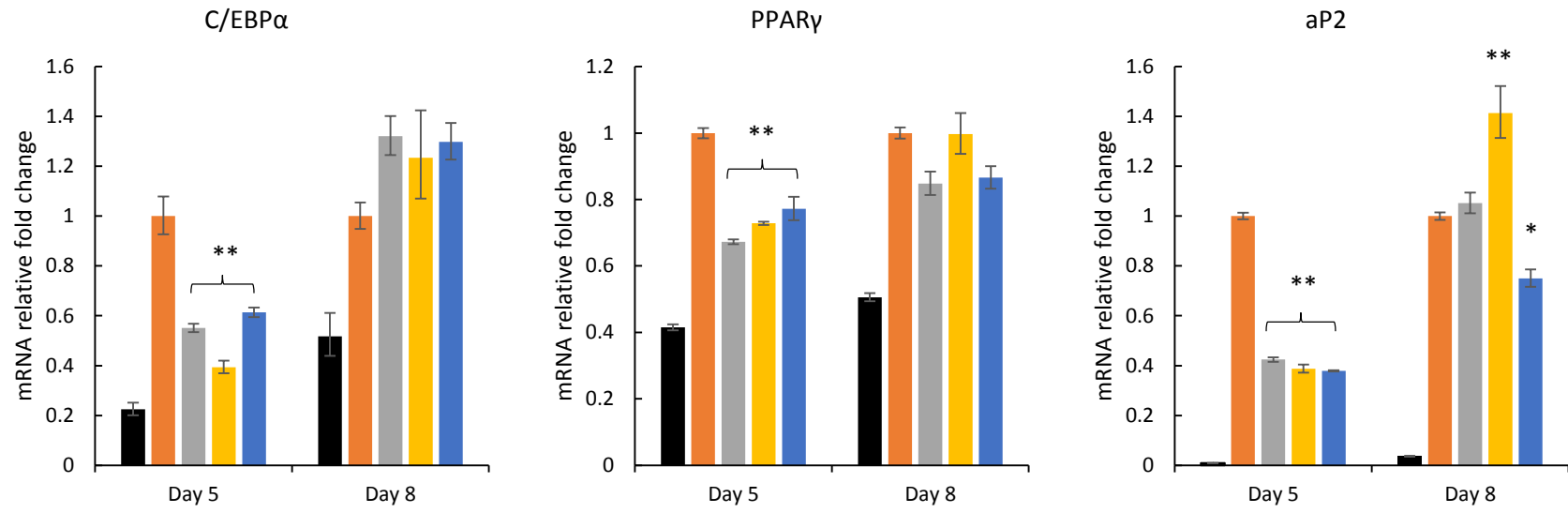


Figure 3.7 continued

B. Experiment Insulin+Pb D0-8

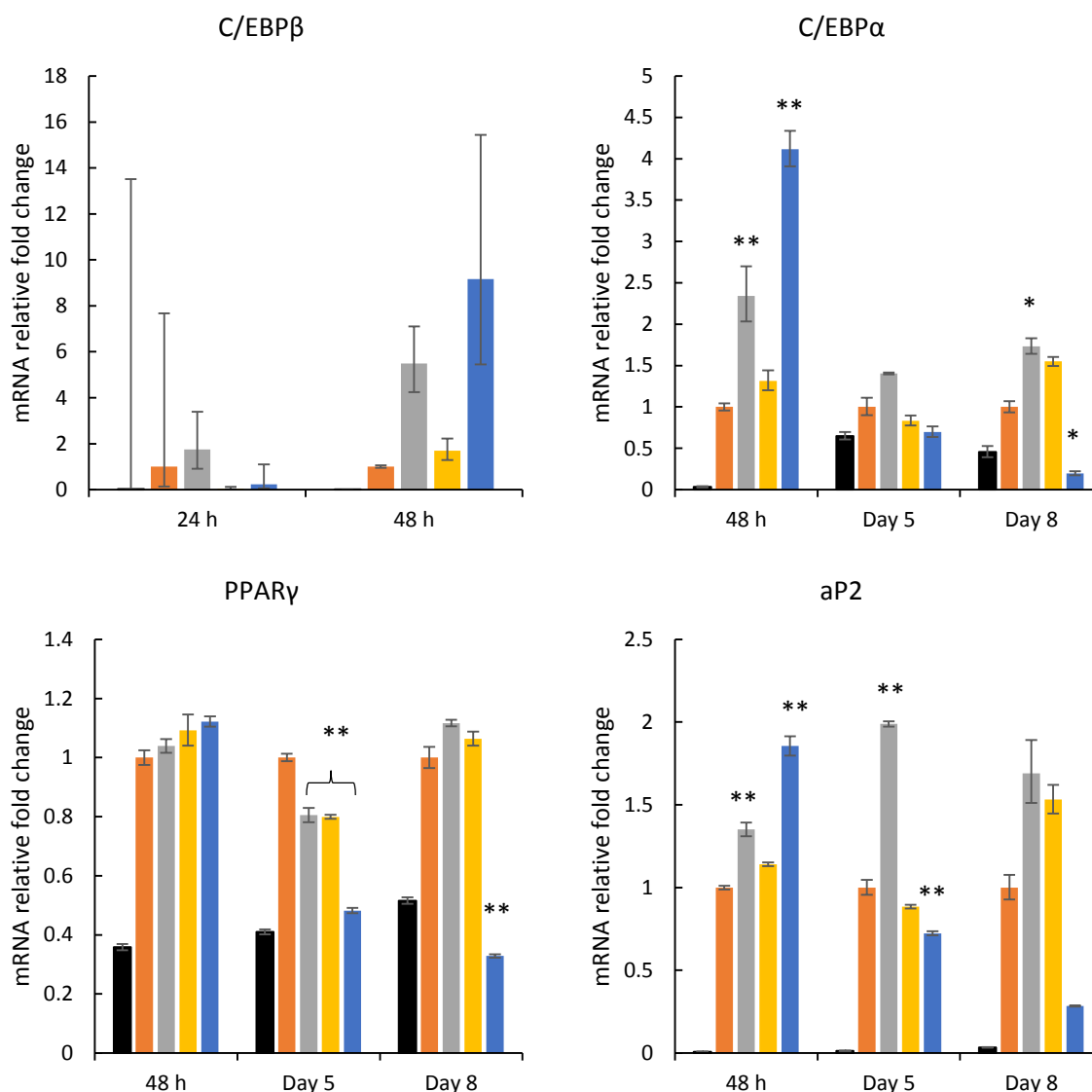


Figure 3.7 Effects of lead on marker gene expression during differentiation of 3T3-L1 preadipocytes in the presence of insulin.

Major transcriptional regulators: C/EBPβ, C/EBPα and PPARγ; mature adipocyte-specific protein: aP2 were evaluated in experiment Insulin+Pb D3-8 (A) and Insulin+Pb D0-8 (B). Gene expression was evaluated by qRT-PCR, normalized to GAPDH expression and expressed as relative fold change to the positive control. Data were calculated based on 3 replicates in the same experiment and presented as the means of relative quantification. Error bars represented the Lower and Upper 95%CI. Each set within the experiment was run in triplicate, and each experiment was performed with at least one additional run to confirm the repeatability. Statistical analyses among multi-group data were carried out using ANOVA followed by Tukey's difference test. * denotes p < 0.05; ** denotes p < 0.01. (Negative: black; Positive: orange; lead 1 nM: grey; 100 nM: yellow; 10 μM: blue)

In experiment Pb D0-8, insulin was absent during the entire experiment. Instead, lead was present in the cell culture from day 0 to day 8. In absence of insulin, during the early differentiation phase, adipogenic gene expressions induced by IBMX+DEX was lower than that induced by the standard protocol, especially for C/EBPs (Fig.3.8). At 24 and 48 hours, the presence of lead suppressed the expression of C/EBP β induced by IBMX+DEX. At 48 hours, the expression of C/EBP α in lower concentrations of lead-treated cells was suppressed, and this suppression was significant in cells treated with 100 nM of lead ($P<0.05$). The expression level of C/EBP α in 10 μ M lead-treated cells was elevated to a level comparable to that exhibited by the positive control. At 48 hours, PPAR γ and aP2 were significantly suppressed by 1 nM and 100 nM of lead ($P<0.01$), but were upregulated by 10 μ M of lead. In particular, aP2 was upregulated more than 2.5 fold when compared to the IBMX+DEX control and the positive control ($P<0.01$). On day 5, C/EBP α was downregulated by lower concentrations of lead ($P<0.05$), but was robustly upregulated by 10 μ M of lead ($P<0.01$), compared to the IBMX+DEX control. PPAR γ was suppressed by 1 nM and 100 nM of lead ($P<0.05$), but was brought to a level similar to the IBMX+DEX control in 10 μ M lead-treated cells. Similar to PPAR γ , the expression of aP2 was significantly downregulated by 1nM and 100 nM of lead ($P<0.01$), but strongly increased by 10 μ M of lead ($P<0.01$). Both at 48 hours and on day 5, 10 μ M of lead showed the highest induction on gene expression when compared with the two lower concentrations. On day 8, C/EBP α and aP2 were upregulated by lower concentrations of lead, but aP2 was strongly suppressed by 10 μ M of lead. PPAR γ was significantly suppressed by all three concentration of lead ($P<0.01$).

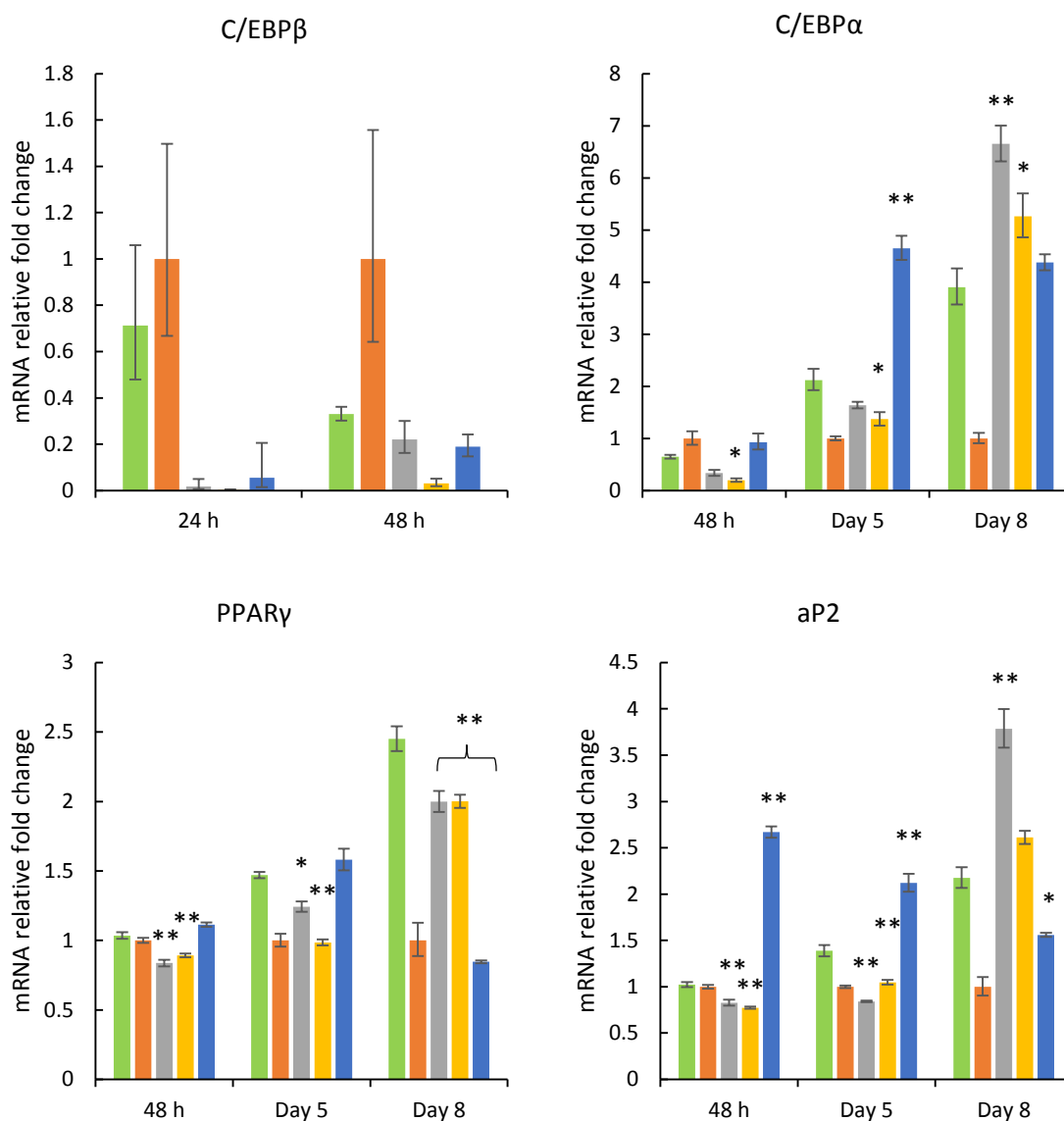


Figure 3.8 Effects of lead on marker gene expression during differentiation of 3T3-L1 preadipocytes in the absence of insulin.

Major transcriptional regulators: C/EBP β , C/EBP α and PPAR γ ; mature adipocyte-specific protein: aP2 were evaluated in experiment Pb D0-8. Gene expression was evaluated by qRT-PCR, normalized to GAPDH expression and expressed as relative fold change to the positive control. Data were calculated based on 3 replicates in the same experiment and presented as the means of relative quantification. Error bars represented the Lower and Upper 95%CI. Each set within the experiment was run in triplicate, and each experiment was performed with at least one additional run to confirm the repeatability. Statistical analyses among multi-group data were carried out using ANOVA followed by Tukey's difference test. * denotes $p < 0.05$; ** denotes $p < 0.01$. (IBMX+DEX: green; Positive: orange; lead 1 nM: grey; 100 nM: yellow; 10 μ M: blue)

The action of insulin is also important during 3T3-L1 adipogenesis. In the 3T3-L1 model, our results show that the insulin receptor substrate IRS2 started to be upregulated within 8 hours post-induction, and maximized at 24 hours to then gradually decline (Fig.3.6 E). Conversely, insulin-regulated transcriptional factor SREBP1c was activated after 24 hours, peaked around 48 hour, then declined to the level of undifferentiated preadipocytes (Fig.3.6 F). Based on the timeline patterns, the effect of lead on the expressions of insulin related molecules IRS2 and SREBP1c was evaluated in each experiment: IRS2 at 24 hour and 48 hour and SREBP1c at 24 hour, 48 hour, and on day 5.

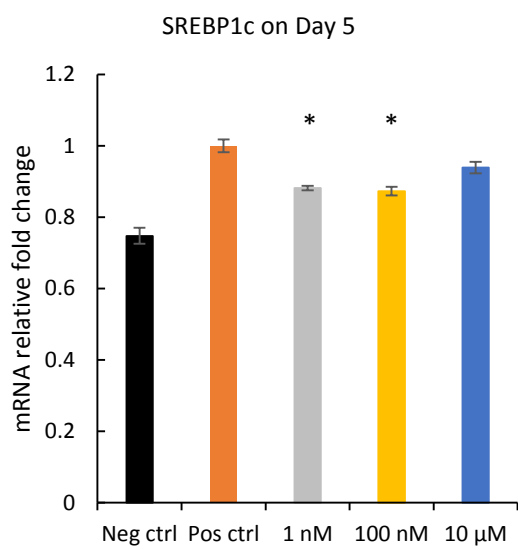
In Experiment Insulin+Pb D3-8, lead was exposed to the cells on day 3; therefore, only the expression of SREBP1c on day 5 was evaluated. In all three concentrations of lead treatment, the expression of SREBP1c was suppressed when compared to the positive control, but was higher than the negative control (Fig.3.9 A). Lead at 1 nM and 100 nM significantly suppressed the SREBP1c expression ($P < 0.05$).

In Experiment Insulin+Pb D0-8, IRS2 expression was suppressed at 8 hours and 24 hours post-induction in lead-treated cells when compared to the positive control, especially for 100 nM and 10 μ M of lead ($P < 0.05$). Lead at 1 nM exhibited the least suppressive activity on IRS2 at both time points. At the onset of activation, lead at all concentrations suppressed SREBP1c expression ($P < 0.01$). At its peak time (48 hours), 1 nM of lead still suppressed its expression ($P < 0.05$), but 100 nM and 10 μ M of lead showed a slight increase in SREBP1c expression. On day 5, however, all three concentrations of lead drastically suppressed SREBP1c expression ($P < 0.01$, Fig.3.9 B).

In Experiment Pb D0-8 (Fig.3.9 C), the absence of insulin resulted in a delayed response of IRS2 gene activation at 8 hour post-induction, where IRS2 expression in cells treated with

IBMX+DEX was similar to the negative control. Lead at 1 nM successfully activated IRS2 expression to a similar level of the positive control, while the other 2 doses did not show any influence. Similar to what observed in Experiment Insulin+Pb D0-8, all three concentrations of lead significantly suppressed IRS2 expression at 24 hours. Lead also suppressed the expression of SREBP1c at 24 hours, 48 hours, and on day 5 post-induction, compared to the IBMX+DEX control.

A. Experiment Insulin+Pb D3-8



B. Experiment Insulin+Pb D0-8

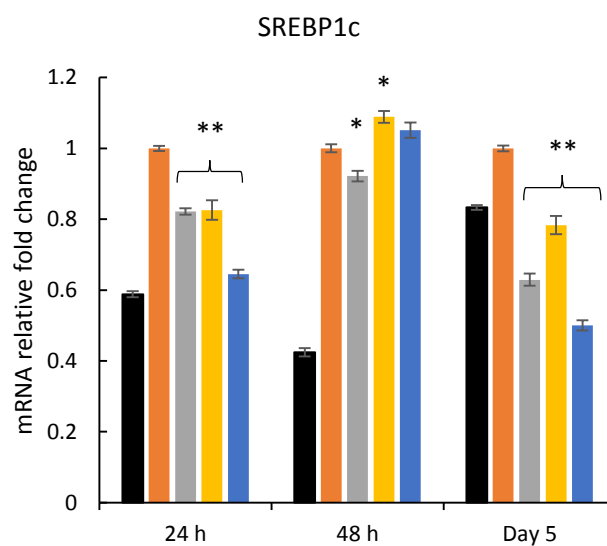
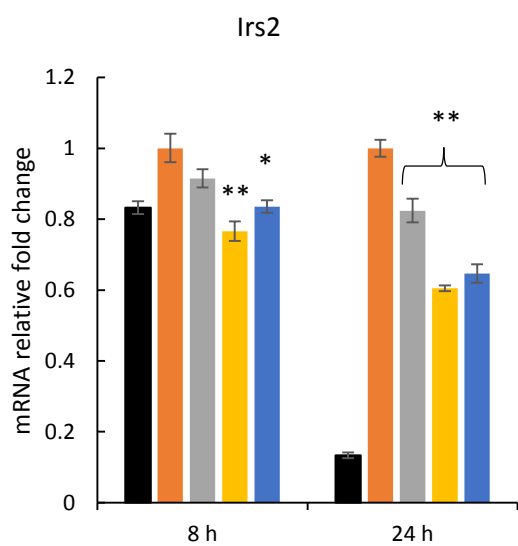


Figure 3.9 continued

C. Experiment Pb D0-8

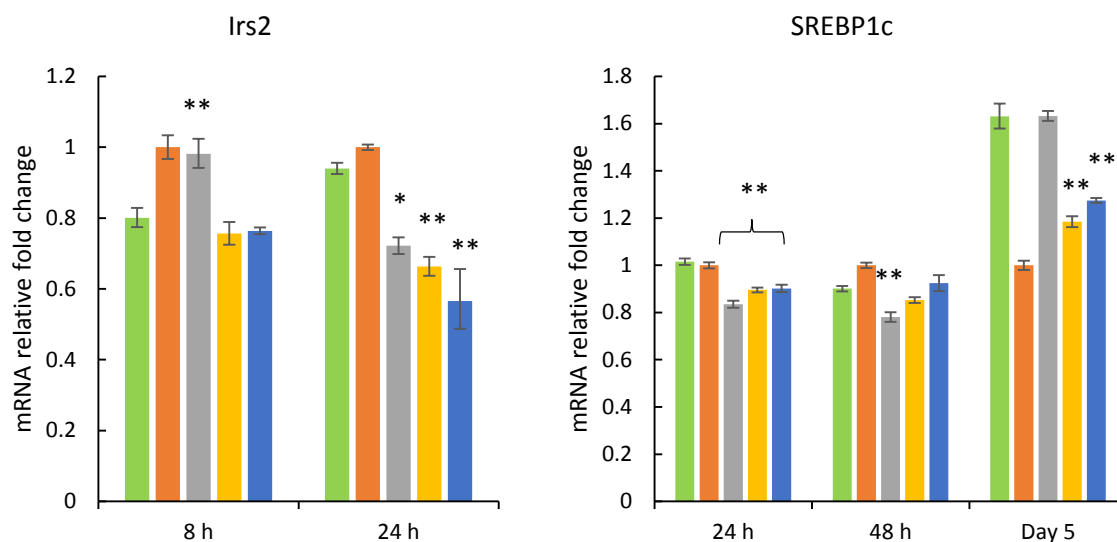


Figure 3.9 Effects of lead on marker gene expression in insulin signaling pathway during differentiation of 3T3-L1 preadipocytes.

IRS2 and SREBP1c were evaluated in all three experiments: Experiment Insulin+Pb D3-8 (A), Experiment Insulin+Pb D0-8 (B), and Pb D0-8 (C). Gene expression was evaluated by qRT-PCR, normalized to GAPDH expression and expressed as relative fold change to the positive control. Data were calculated based on 3 replicates in the same experiment and presented as the means of the relative quantification. Error bars represented the Lower and Upper 95%CI. Each set within the experiment was run in triplicate, and each experiment was performed with at least one additional run to confirm the repeatability. Statistical analyses among multi-group data were carried out using ANOVA followed by Tukey's difference test. * denotes $p < 0.05$; ** denotes $p < 0.01$. (Negative: black; IBMX+DEX: green; Positive: orange; lead 1 nM: grey; 100 nM: yellow; 10 μ M: blue)

3.5 Discussion

Humans have been exposed to the heavy metal lead for a long time. Though the blood lead level is used as the marker for lead exposure, most of the total body burden is in skeletal bone and teeth. Although the relationship between lead exposure and obesity has been analyzed in several studies, both epidemiological and animal studies have reported contradictory results on lead exposure and obesity, including dose-response relationships, making the interpretation of the combined data inconclusive. Here in the current study, we used mouse 3T3-L1 preadipocytes to directly identify the effects of lead on adipocyte differentiation and related dose-response patterns. Our results show that lead upregulates adipogenesis by modulating transcriptional regulators of adipogenesis C/EBPs and increasing lipid accumulation in mature adipocytes; however, the higher concentration of lead exposure results in a decreased level of increased adipogenesis compared with the lower concentration counterparts.

In presence of insulin, both Experiment Insulin+Pb D3-8 and Experiment Insulin+Pb D0-8 show the adipogenic property of lead. Regardless of the exposure time, lead at lower concentrations robustly increased lipid production after 9-day treatment, whereas lead at 10 μ M induced a lesser level of lipid production when compared with the lower concentrations, but still higher than the positive control (Fig.3.3). Consistent with the lipid accumulation results, expression of adipogenic genes on the termination day showed a similar dose-response pattern: lower concentrations of lead with higher gene expression levels. To our surprise, lead at 10 μ M suppressed the expression of PPAR γ and aP2 on day 8 when compared to the positive control, and the suppressive effect of 10 μ M lead was more intense in Experiment Insulin+Pb D0-8 than in Experiment Insulin+Pb D3-8 (Fig.3.4 A-B). The signaling cascade analysis revealed that lead

was capable of significantly upregulating C/EBP α and aP2 expression induced by the standard differentiation cocktail (IBMX, DEX, and insulin) during the early initiation phase of adipogenesis ($P < 0.01$, Fig.3.7 B). In particular, lead at 10 μM had the strongest additive effect on C/EBP α and aP2 expression during the early initiation phase. During the terminal differentiation phase (day 5 and day 8), however, the presence of 10 μM lead exerted a continuously suppressive effect on the marker gene expressions, regardless of the initiation time of lead treatment (Fig.3.7 A-B). The presence of lead also modulated IRS2 and SREBP1c, the former being the key molecule involved in insulin signaling and the latter being regulated by insulin and controlling the production of PPAR γ ligand. Both IRS2 and SREBP1c were suppressed by the presence of lead around their peak times (Fig.3.9 A-B). As a transcriptional regulator of PPAR γ ligand, the suppression of SREBP1c on day 5 might be responsible for the lower expression of PPAR γ mRNA by lead treatment on day 5 and day 8 (Fig.3.5 A-B). In the absence of insulin, cells induced by IBMX+DEX exhibited a slower response of gene activation compared to cells induced by the standard differentiation cocktail (IBMX+DEX+insulin). When compared to the IBMX+DEX control, the presence of lead still contributed to increased adipogenesis in regard to lipid accumulation (Fig.3.3). Similar to Experiment Insulin+Pb, lead at lower concentrations upregulated the expression of C/EBP α and aP2 on day 8; whereas lead at 10 μM significantly suppressed the expression of PPAR γ and aP2 (Fig.3.5 C). The signaling cascade analysis revealed that lead at 10 μM was able to upregulate C/EBP α and aP2 expression at 48 hours, and maintain the elevated gene expressions until day 5; then, on day 8, the suppressive effect of lead at 10 μM on the expressions of all three adipogenic marker genes was observed (Fig.3.8).

In the current study, we demonstrated two results of lead exposure on adipogenesis using the mouse 3T3-L1 preadipocyte model. Firstly, lead has adipogenic properties and is able to directly promote adipocyte differentiation. Our results demonstrate that lead upregulates the expression of C/EBPs, especially C/EBP α , and aP2 during the early differentiation phase, leading to the upregulated level of adipogenesis. A study focusing on lead exposure and bone mass indicated that lead induced inhibition of the Wnt/ β -catenin pathway promotes the shift in mesenchymal differentiation toward an enhanced adipogenesis phenotype (Beier et al. 2013). Wnt has been demonstrated earlier to be an inhibitor of adipocyte differentiation (Ross et al. 2000). Therefore, lead induced adipogenic marker gene expressions may be principally explained by the repression of Wnt signaling.

Secondly, and more importantly, our study revealed that lead exerts non-monotonic dose-dependent responses on adipogenesis. In toxicology, there are two different patterns of dose-response curves: monotonic and non-monotonic. In the monotonic dose-response pattern, along with the increased dose, the effect moves only to one direction, either increasing or decreasing, making a positive or negative slope. In the non-monotonic dose-response pattern, the dose and effect relationship is complex, and the slope of the curve changes at least once, resulting in a 'U' or inverted 'U' shape of curve, or even an undulating curve. In our study, we found out that persisting exposure of lead at higher concentrations during the terminal differentiation phase plays a suppressive role on PPAR γ and aP2, resulting in a lesser fold of increased lipid accumulation. This result is consistent with the conclusions from Leasure et al. (2008) (Beier et al. 2013; Beier et al. 2015) although the experimental design differs in terms of lead exposure time as well as the experimental model. Beier's studies focus on the effect of lead

on bone mass in Long-Evans rats and demonstrate that lifetime exposure of lead in rats results in increased adipocyte profile in bone marrow composition and increased PPAR γ and aP2 expression in the skeleton. These effects appear to be caused by repression of the Wnt/ β -catenin pathway. In their study, Beier et al. also used an *in vitro* model consisting of C3H10t1/2 mouse embryonic mesenchymal cells to validate the finding that pre-treatment of lead during the proliferative phase leads to enhanced adipogenesis in C3H10t1/2 cells. Notably, even though it was not discussed in the C3H10t1/2 experiment, a significant lower level of C/EBP β and δ , PPAR γ proteins was observed in 5 μ M lead-treated cells versus 1 μ M lead-treated cells. Our results, by using three one-hundred-fold concentrations of lead, confirm the non-monotonic dose-dependent response of lead exposure on adipogenesis. Our results may provide a possible explanation for the findings of Scinicariello's epidemiological study as well as Leasure's mice study, in which they observed that higher level of lead exposure are linked to decreased body weight/obesity (Leasure et al. 2008; Scinicariello and Buser 2014).

In conclusion, lead appears to promote adipogenesis by upregulating C/EBP α and aP2 expression, indicating its potential role in inducing obesity. However, high concentrations of lead attenuate the induction of adipogenesis by suppressing PPAR γ and aP2 expressions during the terminal differentiation phase. Therefore, although lead plays a potential role in inducing obesity, higher concentrations of lead may have an opposite effect.

4 Chapter 4: High Concentration of Lead Suppresses Adipocyte Differentiation Induced by 2-Naphthol in the 3T3-L1 Model

4.1 Summary

Polycyclic aromatic hydrocarbons (PAHs) and heavy metals are the most abundant air pollutants. Low-molecular-weight PAHs exert their adverse health effects by mimicking or antagonizing the action of steroid hormones, whereas heavy metals exhibit their toxicity through generation of free radicals or by substituting polyvalent cations. Humans are exposed to these chemicals from the incomplete combustion of oil and gas, tobacco products, vehicle exhaust, and industry waste. A few published studies address the adverse health effects of co-exposure to PAHs and heavy metals as it relates to carcinogenesis and DNA damages. However, the co-effects of these two types of pollutants on adipogenesis and obesity have not been examined yet. In our previous studies, we have found that the PAH metabolite 2-naphthol (2-NAP) is an accelerator of adipocyte differentiation. The heavy metal lead (Pb) is also capable of promoting adipogenesis, but high doses of lead are less effective. Thus, the aim of this study is to evaluate the combined effects of 2-NAP and lead on adipocyte differentiation, using mouse 3T3-L1 preadipocytes.

3T3-L1 cells were induced by the standard differentiation cocktail containing IBMX, DEX, and Insulin for the first three days (day 0-2), followed by the DMEM medium containing insulin alone for six days (day 3-8). 2-NAP and lead, either individually or in combination, were added to the cell culture from day 3 to day 8. The concentration of each chemical used in this experiment was 10 μ M. Terminal differentiation was evaluated by quantifying the expression of three marker

genes of adipogenesis: two major transcriptional regulators of terminal adipocyte differentiation C/EBP α and PPAR γ , and the mature adipocyte-specific gene aP2.

After differentiation induced by the standard differentiation cocktail, 2-NAP at 10 μ M upregulated gene expression of C/EBP α , PPAR γ and aP2, whereas lead at 10 μ M significantly suppressed PPAR γ and aP2 expression. The chemical combination upregulated C/EBP α and PPAR γ . However, upregulation was significant only for PPAR γ . When comparing cells treated with the chemical combination with cells treated with 10 μ M of 2-NAP, a decreased level of mRNA expressions in all three marker genes was observed. In particular, C/EBP α expression was greatly affected by the 2-NAP+lead combination. Compared with cells treated with 10 μ M of lead alone, gene expression levels of PPAR γ and aP2 were significantly enhanced in 2-NAP and lead co-treated cells.

Altogether, these results suggest that lead at a higher concentration plays a suppressive role on 2-NAP induced adipocyte differentiation, indicating the existence of joint effects between the PAH metabolite 2-NAP and the heavy metal lead. Therefore, although exposure to low-molecule-weight PAHs is demonstrated to be associated with higher body mass index and obesity, co-exposure to higher concentrations of lead could counterbalance the effect of PAHs.

4.2 Introduction

Humans and other organisms are exposed to a variety and mixtures of environmental pollutants. In air polluted by tobacco products, industry waste, and car emissions, there is a large amount of PAHs and heavy metals (Bae et al. 2010). Numerous studies have reported the adverse effects of exposure to PAHs (ATSDR 1995) or heavy metals (Tchounwou et al. 2012). The currently

available literature on the toxic effects of co-exposure to these two types of pollutants on human health reveals additive, synergistic, or suppressive effects. However, co-exposure studies of PAH and heavy metals mostly focus on carcinogenesis and DNA damage (Haguenoer et al. 1996; Huang et al. 2013; Vakharia et al. 2001). Little is known about the interactive effects of these two types of pollutants on obesity.

Results from our previous studies (Chapter 2 and 3) highlight the effects of individual 2-NAP and lead exposure on adipogenesis: 2-NAP and low concentrations of lead are capable of accelerating the adipogenesis process in 3T3-L1 cells, whereas lead at high concentration (10 μ M) suppresses adipogenesis. Therefore, we hypothesized that exposure to lead at a high concentration down-modulates the adipogenesis-inducing effects of exposure to 2-NAP.

4.3 Materials and Method

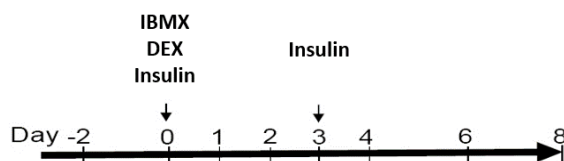
4.3.1 Materials

Mouse embryo fibroblast 3T3-L1 cells (ATCC CL-173, lot 59796011) and bovine calf serum (ATCC, 30-2030) were obtained from ATCC. Dulbecco's modified Eagle's medium (DMEM) (Cellgro 10-013CV) and 100X penicillin-streptomycin solution (Cellgro 30-002-CI) were purchased from Mediatech, Inc. Human insulin solution (I9278), dexamethasone (D2915), 3-Isobutyl-1-methylxanthine (I5879), formalin solution (HT501128), and Oil Red O (O0625) were obtained from Sigma-Aldrich Co. LLC. Lead acetate solution (SL9000-250) was purchased from Fisher Scientific Co, and 2-Naphthol was obtained from Acros Organics. In this study, lead acetate was used as the source for all lead exposure experiments.

4.3.2 *Experimental design*

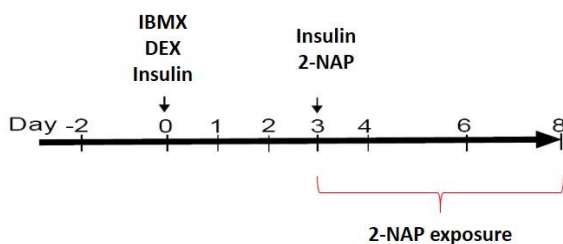
To test whether lead at 10 μ M plays a suppressive role on adipogenesis induced by 2-NAP, we exposed 3T3-L1 cells induced by standard differentiation medium to the mixture of these two chemicals from day 3 to day 8 (Fig.4.1) and evaluated gene expression of the three markers at day 8.

A. Standard differentiation protocol for 3T3-L1 cells (Positive control protocol)

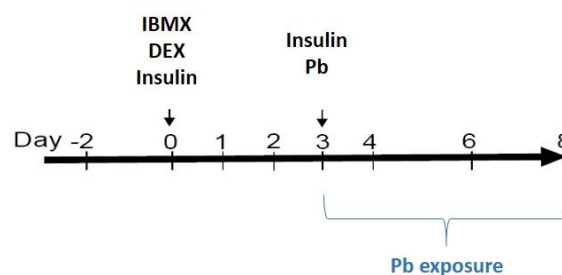


B. chemical exposure protocol

1) 2-NAP:



2) Lead:



3) The chemical combination:

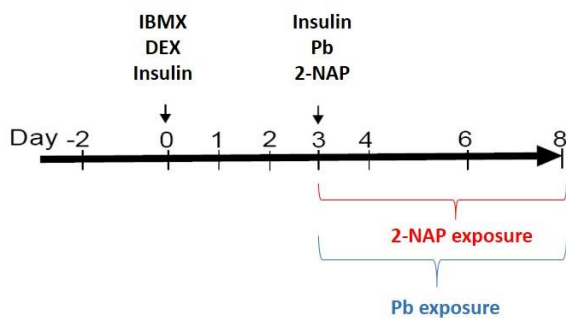


Figure 4.1 Protocols for adipogenic differentiation and chemical exposure in 3T3-L1 cells.

Cells were differentiated after confluence (designated as day 0, indicated by the first black arrow) by replacing the basic DMEM medium with the differentiation medium for three days. The concentrations of each component in the differentiation medium were 0.5 mM for IBMX, 0.25 μ M for dexamethasone (DEX) and 1 μ g/mL for insulin. Cell cultures were exposed to 10 μ M of 2-NAP or lead, or to the combination of 10 μ M 2-NAP and lead from day 3 to day 8 in the presence of 1 μ g/mL insulin. Curly brackets indicated the chemical exposure period.

4.3.3 Cell culture and differentiation

3T3-L1 cells were cultured in the DMEM medium supplemented with 10% bovine calf serum (BCS), 100 I.U. penicillin and 100 µg/mL streptomycin. Cells were grown in 75 cm² culture flasks in a humidified atmosphere with 5% CO₂ at 37 °C and subcultured when they became 80% confluent.

Cells were seeded at a density of 6x10⁴ cells/well in Costar 6-well plates with the basic DMEM medium. After reaching confluency (Day 0), cell differentiation was induced by replacing the basic DMEM medium with the differentiation medium containing 0.5 mM IBMX, 0.25 µM DEX, and 1 µg/mL insulin for three days (day 0 to day 2). On day 3, the differentiation medium was replaced with the DMEM medium containing 1 µg/mL insulin in the presence or absence of 10 µM 2-NAP, 10 µM lead, or the combination of 10 µM 2-NAP and 10 µM lead. 3T3-L1 cells maintained with DMEM medium were used as negative control.

4.3.4 Quantitative real-time reverse transcription-polymerase chain reaction (Real-Time PCR)

Total RNA was extracted from cells using QIAGEN RNeasy Plus Mini Kit (Qiagen Inc., Valencia, CA). Using High-Capacity cDNA reverse transcription kit (Applied Biosystems), 5 µL of the total RNA was reverse-transcribed into cDNA. The reaction mixture contained 1x reverse transcriptase buffer, 4 mM dNTP (deoxynucleotide triphosphate), 5x Random primers, 1 U RNase inhibitors, and 2.5 U of MultiScribe Reverse Transcriptase. The RT-PCR was performed with the following cycle parameters: 25°C for 10 min, 37°C for 120 min, and 85°C for 5 min. Synthesized cDNA was diluted with RNase-free water. Then, quantitative real-time PCR amplification was performed with appropriate sets of primers using Taqman gene expression assays in a total

volume of 20 μ L that contained aliquoted cDNA samples. Gene expression assays were carried out with the following cycle parameters: 55°C for 2min; 94°C for 10 min; 40 cycles of 94°C for 15 sec and 60°C for 60 sec. The following primers and probes were obtained from Applied Biosystems: C/EBP α (Mm00514283_s1); PPAR γ (Mm01184322_m1); aP2 (Mm00445878_m1); and housekeeping gene GAPDH (Cat: 4352339E), as an endogenous control to correct the variation of RNA and cDNA loading. Data were analyzed using the Δ CT method. Target gene expression was normalized to GAPDH for Δ CT value, then calibrated to the control sample in each experiment to give the $\Delta\Delta C_T$ value. Data were calculated based on three replicates in the same experiment and presented as the means of relative quantification. Error bars represented the Lower and Upper 95% Confidence Interval. Each set of the experiment was run in triplicate, and each experiment was performed with an additional run to confirm the repeatability.

4.3.5 Statistical analysis

Statistical analysis among multi-group data were carried out using ANOVA followed by the Tukey's difference test. $P < 0.05$ was considered significant. Each experiment was repeated twice, and each set of the experiments were run in triplicates.

4.4 Results

4.4.1 The co-effect of 2-NAP and lead on marker gene expressions of adipogenesis

As shown in Figure 4.2, consistent with our previous experiments, on the termination day, 2-NAP at 10 μ M drastically upregulated the gene expression of C/EBP α , PPAR γ , and aP2 ($P < 0.01$). In addition, lead at 10 μ M significantly suppressed the expression of PPAR γ and aP2 ($P < 0.01$). The chemical combination was still capable of upregulating C/EBP α and PPAR γ to 1.7 and 1.6 fold

respectively, even though it was only significant for PPAR γ ($P < 0.01$). A significantly decreased level of mRNA expression of all three genes was observed in cells treated with the chemical combination when compared with cells treated with 10 μ M of 2-NAP ($P < 0.01$). C/EBP α expression was greatly affected by 2-NAP and lead combination which, together, were reduced from 5.6 fold in 10 μ M of 2-NAP treated cells to 1.7 fold in chemical combination treated cells. The lead suppressive effect on 2-NAP-induced PPAR γ and aP2 expression was less intense, but the difference was still significant ($P < 0.01$). Compared with cells treated with 10 μ M of lead, gene expression levels of PPAR γ and aP2 were significantly upregulated in 2-NAP and lead co-treated cells ($P < 0.01$). Two fold of increasing PPAR γ expression was observed between the lead-only and the chemical combination treatments, from 0.74 fold to 1.56 fold ($P < 0.01$). Similar to PPAR γ , aP2 expression was also slightly but significantly upregulated ($P < 0.01$). Taken together, these results suggest that 10 μ M of lead significantly suppresses the adipogenesis induced by 10 μ M of 2-NAP, indicating the existence of joint effects between the PAH metabolite 2-NAP and heavy metal lead.

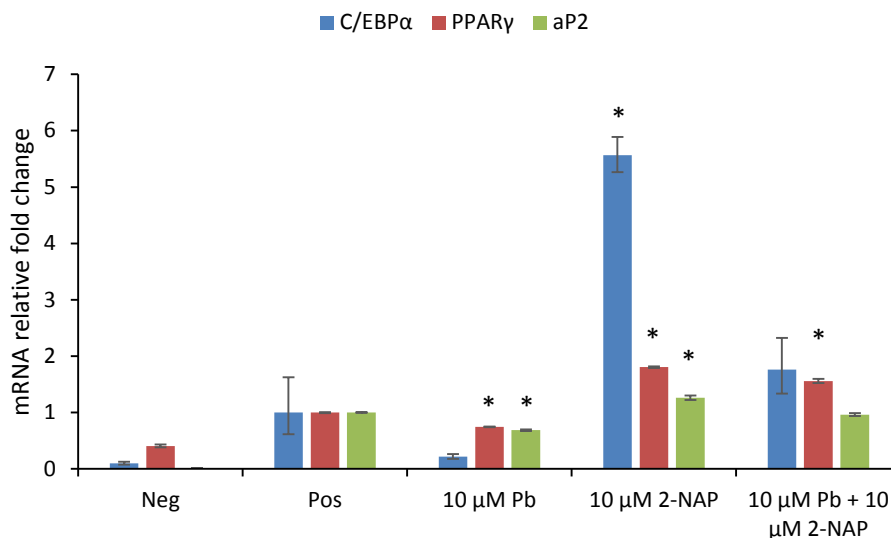


Figure 4.2 Effects of 2-naphthol in the presence of lead on adipogenic gene expression at day 8 of 3T3-L1 differentiation.

Major transcriptional regulators in terminal adipocyte differentiation: C/EBP α and PPAR γ ; mature adipocyte-specific protein: aP2. Post-confluent 3T3-L1 cells were induced to differentiate into adipocytes by the standard differentiation protocol, with 0.5 mM IBMX, 0.25 μ M DEX and 1 μ g/mL insulin for 3 days followed by 1 μ g/mL insulin for six days. Cells were exposed to the individual chemicals or the mixture of 10 μ M 2-NAP and 10 μ M from day 3 to day 8. Cells treated with 0.5 mM IBMX, 0.25 μ M DEX and 1 μ g/mL insulin for 3 days followed by 1 μ g/mL insulin were used as positive control (Pos), whereas cells maintained with DMEM medium were used as negative control (Neg). Gene expression was evaluated by qRT-PCR, normalized to GAPDH expression and expressed as relative fold change to the positive control. Data were calculated based on three replicates in the same experiment and presented as the means of relative quantification. Error bars represented the Lower and Upper 95% confidence interval. Each set of the experiment was run in triplicate, and each experiment was performed with an additional run to confirm the repeatability. Statistical analyses among multi-group data were carried out using ANOVA followed by Tukey's difference test. * denotes $p < 0.01$.

4.5 Discussion

Humans and other organisms are exposed to a variety and mixtures of environmental pollutants. PAHs and heavy metals are the most abundant components of air pollution. Co-exposure to these two may result from smoking or secondary smoking, car emissions from heavy traffics, coal production-related industry waste or occupational exposure (Bae et al. 2010). Co-exposure studies of PAH and heavy metals are very scarce and mostly focus on carcinogenesis and DNA damage. Little is known about the interaction effects between these two types of pollutants on obesity. Therefore, the current study was designed to test the co-effect of 2-NAP and lead on adipogenesis in mouse 3T3-L1 preadipocytes. Our results show evidence that lead at a higher concentration plays a suppressive role on 2-NAP induced adipogenesis, indicating an attenuated acceleration of adipocyte differentiation when co-exposed to high concentrations of 2-NAP and lead.

In general, additive, synergistic, and suppressive effects are the three possible patterns of interactions between two chemicals. The additive and suppressive toxic co-effects have already been reported between PAHs and heavy metals. Haguenoer et al. described the additive effects of PAHs and heavy metals in an animal study, demonstrating that iron oxides can induce lung cancer only when benzo(a)pyrene is co-administered (Haguenoer et al. 1996). Another epidemiological study that focuses on the exposure to traffic-related air pollutants suggests the additive effects of the PAH metabolite 1-hydroxypyrene-glucuronide (1-OHPG) and cadmium on increasing levels of oxidative stress (Huang et al. 2013). Suppressive effects of PAHs and heavy metals have also been reported. The heavy metal arsenic, lead, mercury, and cadmium efficiently decrease the CYP1A1/1A2 bioactivation induced by PAHs in human hepatocyte cultures (Vakharia

et al. 2001). Our previous results (Chapter 2 and Chapter 3) indicate that both 2-NAP and selected lead concentrations are capable of upregulating adipogenesis. However, when tested in combination in the study described in this Chapter (Chapter 4), no additive effects were observed. In contrast, exposure to 10 μ M of lead during the terminal differentiation phase counterbalanced the increased effect of 2-NAP on adipocyte differentiation, leading to a decreased level of promoted adipogenesis induced by the chemical combination.

This joint effect of 2-NAP and lead on adipocyte differentiation might result from different mechanisms of action used by these two chemicals. In the previous chapters, we demonstrated that 2-NAP induces adipogenesis by modulating the expression of the master transcriptional regulator PPAR γ as well as molecules involved in the insulin signaling pathway. 2-NAP at 10 μ M exhibited the greatest impact on marker gene expressions and phenotypic markers of adipogenesis. The effect of 2-NAP on adipogenesis might tightly associate with its endocrine disrupting capability. On the other hand, we also demonstrated that lead plays an upregulating role on adipogenesis, even though the dose-response of lead is non-monotonic. The induction of adipogenesis by lead results from the upregulation of CEBPs during the early differentiation phase; however, lead also plays a suppressive role on PPAR γ and aP2 expression and mitochondrial activities during the terminal differentiation phase. Even though the detailed mechanisms of action of 2-NAP and lead need to be explored, results from the current study provide evidence that 2-NAP and lead may contribute to the overall adipogenesis induced by the chemical combination via independent pathways, and may counterbalance the roles of each other on the expression of adipogenic genes.

In conclusion, lead at a higher concentration plays a suppressive role on 2-NAP-induced adipocyte differentiation, demonstrating a suppressive co-effect of the PAH metabolite 2-NAP and the heavy metal lead on adipogenesis. This result indicates that although exposure to low-molecule-weight PAH associates with higher body mass index and obesity, co-exposure to higher concentrations of lead could counterbalance the effect of PAHs. Therefore, joint effects of different chemical mixtures should be taken into consideration in studies that focus on the adverse effects of environmental pollutants.

5 Chapter 5: The effect of environmental pollutants on anti-microbial peptide production during adipocyte differentiation

5.1 Summary

Adipocytes play important roles in the host innate immune response. At the site of infection, adipocytes secrete cytokines to recruit immune cells such as macrophages and neutrophils. On the other hand, preadipocytes, upon activation of pathogens, start to differentiate into mature adipocytes. In the meantime, these differentiating adipocytes produce anti-microbial peptides (AMPs) which immediately protect the host from pathogens before the recruitment of other immune cells. In our previous study, we demonstrated that environmental pollutants 2-naphthol (2-NAP) and lead (Pb) are capable of moderating preadipocyte differentiation. Therefore, we hypothesized that environmental pollutants might have an impact on the innate immune response by modulating the production of AMPs in differentiating adipocytes.

To test the hypothesis, we used an *in vitro* model of mouse 3T3-L1 preadipocytes. 3T3-L1 cells were induced by the standard differentiation cocktail with IBMX, DEX, and insulin for the first three days (day 0-2), followed by DMEM medium containing only insulin for six days (day 3-8). Cell cultures were exposed to the chemicals from day 3 to day 8. Bisphenol A (BPA) at 100 nM, three one-hundred-fold concentrations of 2-NAP or lead (1 nM to 10 μ M), or the combination of 2-NAP and lead at 10 μ M were tested. The production of one of AMPs cathelicidin (Camp) mRNA was evaluated by quantitative PCR on the termination day.

Compared with preadipocytes, Camp mRNA expression was significantly activated during adipocyte differentiation. BPA, a known obesogen, was able to upregulate Camp expression. 2-NAP elevated the production of Camp mRNA in a dose-dependent manner. In particular, 2-NAP at 10 μ M drastically upregulated the expression of Camp. Lead, on the other hand, slightly induced the expression of Camp mRNA at lower concentrations, whereas 10 μ M of lead suppressed Camp expression. The combination at 10 μ M of both 2-NAP and lead did not result in a co-effect on the expression of Camp. In comparing cells treated with the chemical combination to cells treated with 10 μ M of 2-NAP, a decreased level of Camp mRNA expression was observed. Compared with cells treated with 10 μ M of lead, the gene expression level was significantly enhanced in 2-NAP and lead co-treated cells.

In conclusion, BPA and 2-NAP, as inducers of adipocyte differentiation, enhance the production of Camp in differentiating adipocytes. Similar to the effect on adipogenesis, lead upregulates Camp production at lower concentrations, but suppresses it at higher concentrations. Moreover, lead at a higher concentration plays a suppressive role on 2-NAP-induced Camp production during adipocyte differentiation. Therefore, environmental pollutants that are capable of influencing adipogenesis appear to also modulate production of Camp in differentiating adipocytes, thus potentially playing a role in modulating inflammation status and innate immune responses.

5.2 Introduction

Cathelicidins, one of the most abundant types of AMPs, are a family of evolutionarily conserved peptides with antibacterial, antiviral, and antifungal activities in reptiles, fish, birds

and mammals (Bucki et al. 2010; Doss et al. 2010). Cathelicidins consist of an N-terminal signal sequence, a conserved cathelin-like domain, and a C-terminal antimicrobial domain (Zanetti et al. 1995). While some mammals have multiple forms of cathelicidins (for example bovine cathelicidins: BMAP28, Bac 5, and indolicidin) (Chan et al. 2006), humans and mice each only produce one cathelicidin, named LL-37/hCAP18 and mCRAMP, respectively (Cowland et al. 1995; Gallo et al. 1997; Larrick et al. 1994).

The gene that encodes human cathelicidin LL-37 contains four exons and lies on chromosome 3 (Gudmundsson et al. 1996; Larrick et al. 1996), and the mature peptide consists of 37 amino acids. LL-37 is secreted by epithelial cells and leukocytes, especially lymphocytes and monocytes (Agerberth et al. 2000; Bals et al. 1998). Due to the amphipathic α -helix structure and the positive charge, cathelicidins directly kill bacteria by forming pores on the cell membranes (Lee et al. 2011). Besides the direct antimicrobial ability, cathelicidins function in stimulating wound healing and participate in immune responses. Research on human cathelicidins suggests that LL-37 is strongly expressed in healing epithelium cells in the skin (Heilborn et al. 2003). LL-37 induces re-epithelization by serving as a pro-migratory factor. This action is mediated through the STAT3 pathway in an EGFR-dependent manner, resulting in increased migration of keratinocytes (Tokumaru et al. 2005). The rat cathelicidin has also been demonstrated to participate in healing of stomach ulcers by stimulating the proliferation of gastric epithelial cells (Yang et al. 2006). The action of rat cathelicidin in promoting gastric epithelial cells proliferation depends on the TGF- α activated MEK/ERK signaling pathway. Altogether, the ability to promote cell proliferation, migration, and angiogenesis shows that cathelicidin is an important factor in wound healing.

In addition, cathelicidins have immunomodulatory properties and can function as leukocytes chemoattractants, regulating neutrophil, monocyte, mast cell, and CD4+ T lymphocyte migration to and infiltration into the inflammatory sites through a G protein coupled transmembrane cell receptor named formyl-peptide receptor-like 1 (De Yang et al. 2000). Moreover, cathelicidins can regulate cytokine and chemokine production in several cell types. LL-37 induces the production of IL-8 in epithelial cells resulting in the recruitment of neutrophils and increased inflammations (Tjabringa et al. 2003). The production of other pro-inflammatory mediators, such as IL-1 β , COX-2, and IL-6 by keratinocytes (Braff et al. 2005) and CXCL8 and CCL2 by macrophages (Huang et al. 1997), have also been reported to be modulated by LL-37.

The study of Ling-juan Zhang revealed an important role of differentiating adipocyte on host defense against bacteria infection. Upon skin infection, accompanied with the local expansion of adipocytes, the increasing production of Camp from differentiating adipocytes protects the host before the recruitment of innate immune cells (Zhang et al. 2015).

In previous studies, we demonstrated that 2-NAP and lead, individually and in combination, were capable of modulating the process of adipocyte differentiation. Here, we aimed to identify whether environmental pollutants modulate Camp production while modulating adipocytes differentiation.

5.3 Materials and methods

5.3.1 Materials

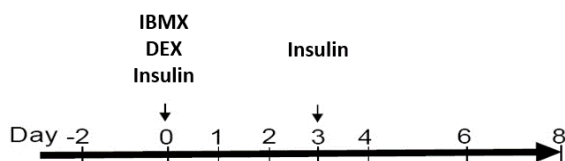
Mouse embryo fibroblast 3T3-L1 cells (ATCC CL-173, lot 59796011) and bovine calf serum (ATCC, 30-2030) were obtained from ATCC. Dulbecco's modified Eagle's medium (DMEM)

(Cellgro 10-013CV) and 100X penicillin- streptomycin solution (Cellgro 30-002-CI) were purchased from Mediatech, Inc. Human insulin solution (I9278), dexamethasone (D2915), 3-Isobutyl-1-methylxanthine (I5879), formalin solution (HT501128), bisphenol A (BPA, 239658), and Oil Red O (O0625) were obtained from Sigma-Aldrich Co. LLC. Lead acetate solution (SL9000-250) was purchased from Fisher Scientific Co, and 2-Naphthol was obtained from Acros Organics. In this study, lead acetate was used as the source for all lead exposure experiments.

5.3.2 Experimental design

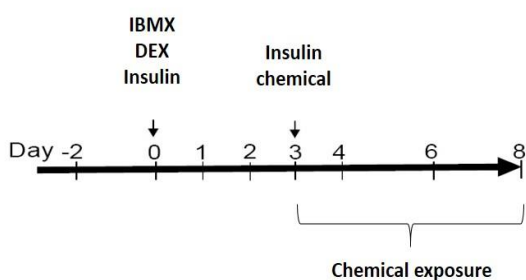
In the current study, 3T3-L1 cells were induced to differentiate by the standard differentiation protocol, and cells were exposed to individual chemicals or the combination of 2-NAP and lead from day 3 to day 8 (Fig.5.1). The mRNA expression of Camp was evaluated on the termination day. BPA was used as a known environmental pollutant that induces 3T3-L1 adipogenesis.

A. Standard differentiation protocol for 3T3-L1 cells (Positive control protocol)



B. Chemical exposure protocol

1) Individual chemical: BPA, 2-NAP and lead



2) The chemical combination: 2-NAP+Pb

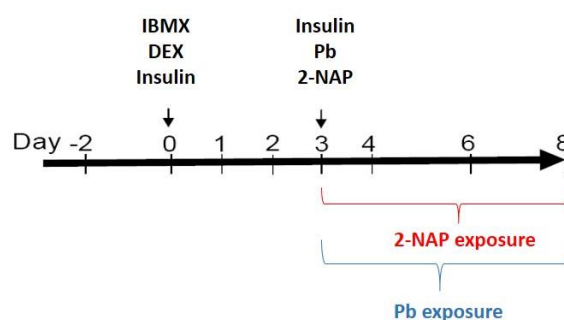


Figure 5.1 Protocols for adipogenic differentiation and chemical exposure in 3T3-L1 cells.

Cells were differentiated after confluence (designated as day 0, indicated by the first black arrow) by replacing the basic DMEM medium with the differentiation medium for three days. The concentrations of each component in the differentiation medium were 0.5 mM for IBMX, 0.25 μ M for dexamethasone (DEX) and 1 μ g/mL for insulin. Individual BPA, 2-NAP, or lead, or the combination of 10 μ M 2-NAP and lead were exposed to the cell culture from day 3 to day 8 in the presence of 1 μ g/mL insulin. Curly brackets indicated the chemical exposure period.

5.3.3 Cell culture and differentiation

3T3-L1 cells were cultured in DMEM medium supplemented with 10% bovine calf serum (BCS), 100 I.U. penicillin and 100 µg/mL streptomycin. Cells were grown in 75 cm² culture flasks in a humidified atmosphere with 5% CO₂ at 37 °C and subcultured when they became 80% confluent.

Cells were seeded at a density of 6x10⁴ cells/well in Costar 6-well plates with the basic DMEM medium. After confluent (Day 0), cell differentiation was induced by replacing the basic DMEM medium with the differentiation medium containing 0.5 mM IBMX, 0.25 µM DEX, and 1 µg/mL insulin for three days (day 0 to day 2). On day 3, the differentiation medium was replaced with the DMEM medium with 1 µg/mL insulin in the presence or absence of BPA, 2-NAP, lead, or 2-NAP and lead mixture. The concentrations of each chemical used in this experiment were, 100 nM for BPA; 1 nM, 100 nM, and 10 µM for 2-NAP; 1 nM, 100 nM, and 10 µM, or the combination of 10 µM 2-NAP and 10 µM lead. 3T3-L1 cells maintained with the DMEM medium were used as negative control.

5.3.4 Quantitative real-time reverse transcription-polymerase chain reaction (Real-Time PCR)

Total RNA was extracted from cells using the QIAGEN RNeasy Plus Mini Kit (Qiagen Inc., Valencia, CA). Using the High-Capacity cDNA reverse transcription kit (Applied Biosystems), 5 µL of total RNA was reverse-transcribed into cDNA. The reaction mixture contained 1x reverse transcriptase buffer, 4 mM dNTP (deoxynucleotide triphosphate), 5x Random primers, 1 U RNase inhibitors, and 2.5 U of MultiScribe Reverse Transcriptase. The RT-PCR was performed with the following cycle parameters: 25°C for 10 min, 37°C for 120 min, and 85°C for 5 min. Synthesized

cDNA was diluted with RNase-free water. Then, quantitative real-time PCR amplification was performed with appropriate sets of primers using Taqman gene expression assays in a total volume of 20 μ L that contained aliquot cDNA samples. Gene expression assays were carried out with the following cycle parameters: 55°C for 2min; 94°C for 10 min; 40 cycles of 94°C for 15 sec and 60°C for 60 sec. The following primers and probes were obtained from Applied Biosystems: C/EBP α (Mm00514283_s1); PPAR γ (Mm01184322_m1); aP2 (Mm00445878_m1); Camp (Assay ID: Mm00438285_m1); and housekeeping gene GAPDH (Cat: 4352339E), as an endogenous control to correct the variation of RNA and cDNA loading. Data were analyzed using the Δ CT method. Target gene expression was normalized to GAPDH for Δ CT value, then calibrated to the control sample in each experiment to give the $\Delta\Delta$ C_T value. Data were calculated based on three replicates in the same experiment and presented as the means of relative quantification. Error bars represented the Lower and Upper 95% Confidence Interval. Each set of the experiment was run in triplicate, and each experiment was performed with an additional run to confirm the repeatability.

5.3.5 Statistical analysis

Statistical analyzes among multi-group data were carried out using ANOVA followed by Tukey's difference test. $P < 0.05$ was considered significant. Each experiment was repeated twice, and each set of the experiments were run in triplicates.

5.4 Results

5.4.1 *The effect of 2-NAP and lead on Camp production*

The adipogenic property of BPA has been well studied in both cell lines and animal models including mouse 3T3-L1 cells. Consistent with others studies, Figure 5.2 shows that 100 nM of BPA was able to significantly elevate the expression of aP2 when compared with the positive control ($P < 0.01$), indicating its additive role on adipogenesis. Moreover, 100 nM of BPA was also able to significantly upregulate Camp production on day 8 ($P < 0.01$).

As shown in Figure 5.3 A, 2-NAP upregulated the mRNA expression of Camp in a dose-dependent manner. Even though at the lower concentrations (1 nM and 100 nM) the effect of 2-NAP on upregulating Camp production was quite weak (1.4 and 1.5 fold of increase, $P < 0.01$), 2-NAP at 10 μ M exhibited a significant impact on Camp production ($P < 0.01$). On the other hand, depending on the concentrations, lead played different roles on Camp production (Fig.5.3 B). At lower concentrations (1 nM and 100 nM), lead significantly upregulated the expression of Camp in an inverse dose-response manner ($P < 0.01$), in which 1 nM of lead was capable of inducing a higher production of Camp than 100 nM of lead. At a higher concentration (10 μ M), lead suppressed the expression of Camp ($P < 0.01$). As it relates to the chemical combination (2-NAP and lead at 10 μ M), the difference in Camp production in 3T3-L1 cells between the positive control and the chemical combination was not significant (Fig.5.3 C). Compared with cells treated with individual chemicals, however, the difference was statistically significant ($P < 0.01$), indicating that the suppressive role of lead at 10 μ M counterweighed the effect of 2-NAP at 10 μ M on inducing Camp production

Taken together, these results suggest that modulation of adipocyte differentiation by 2-NAP and lead may in turn regulate Camp production. Alternatively, the two chemicals may directly modulate Camp production.

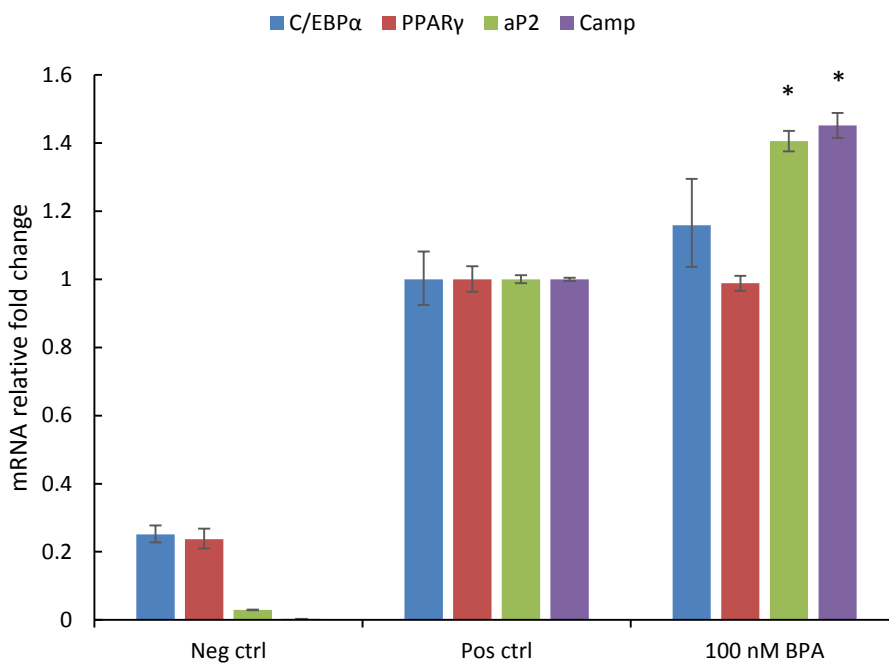
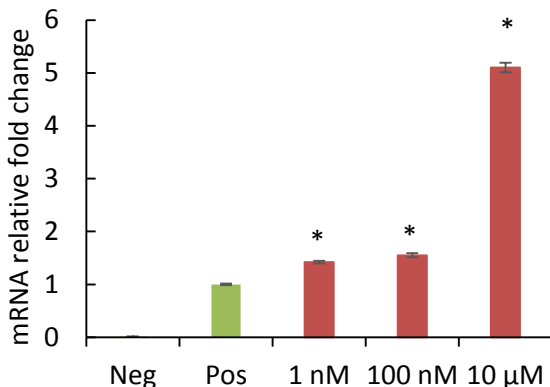


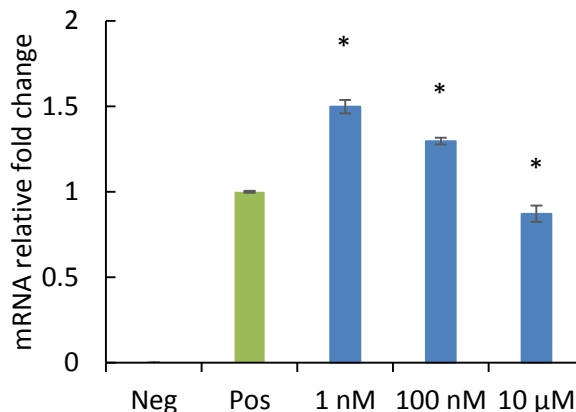
Figure 5.2 Effects of BPA on adipogenic gene and Camp expressions.

Major transcriptional regulators in terminal adipocyte differentiation: C/EBP α and PPAR γ ; mature adipocyte-specific protein: aP2; mouse antimicrobial peptide Cathelicidin: Camp. Post-confluent 3T3-L1 cells were induced to differentiate into adipocytes by the standard differentiation protocol, with 0.5 mM IBMX, 0.25 μ M DEX and 1 μ g/mL insulin for 3 days followed by 100 nM BPA and 1 μ g/mL insulin for six days. Cells treated with 0.5 mM IBMX, 0.25 μ M DEX and 1 μ g/mL insulin for 3 days followed by 1 μ g/mL insulin were used as positive control (Pos), whereas cells maintained with DMEM medium were used as negative control (Neg). Gene expression was evaluated by qRT-PCR, normalized to GAPDH expression and expressed as relative fold change to the positive control. Data were calculated based on three replicates in the same experiment and presented as the means of relative quantification. Error bars represented the Lower and Upper 95% confidence interval. Each set of the experiment was run in triplicate, and each experiment was performed with an additional run to confirm the repeatability. Statistical analyses among multi-group data were carried out using ANOVA followed by Tukey's difference test. * denotes $p < 0.01$.

A. 2-NAP



B. lead



C. 2-NAP+Pb

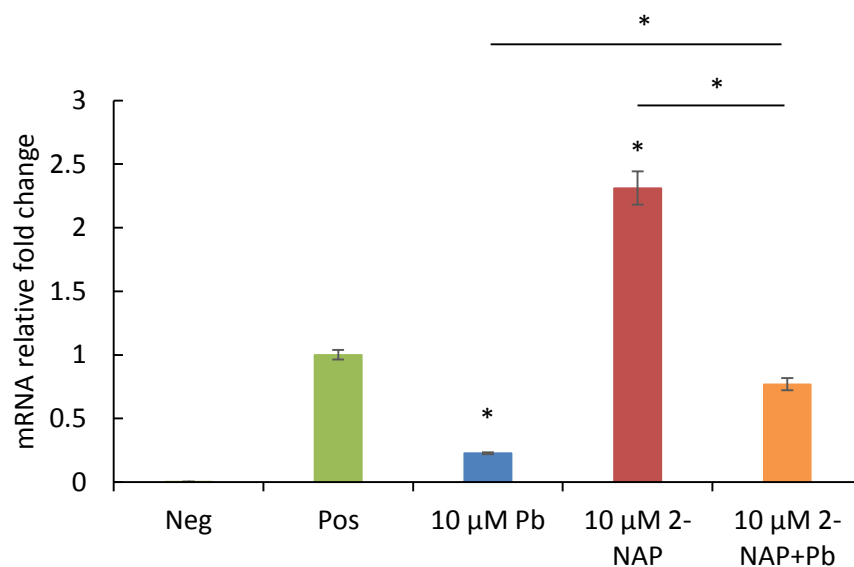


Figure 5.3 Effects of 2-NAP and lead on Camp expression.

Mouse antimicrobial peptide Cathelicidin: Camp. Post-confluent 3T3-L1 cells were induced to differentiate into adipocytes by the standard differentiation protocol, with 0.5 mM IBMX, 0.25 μM DEX and 1 μg/mL insulin for 3 days followed by 1 μg/mL insulin for six days. Individual 2-NAP, lead, or the mixture of 10 μM 2-NAP and 10 μM lead were exposed to the cells from day 3 to day 8. Cells treated with 0.5 mM IBMX, 0.25 μM DEX and 1 μg/mL insulin for 3 days followed by 1 μg/mL insulin were used as positive control (Pos), whereas cells maintained with DMEM medium were used as negative control (Neg). Gene expression was evaluated by qRT-PCR, normalized to GAPDH expression and expressed as relative fold change to the positive control. Data were calculated based on three replicates in the same experiment and presented as the means of relative quantification. Error bars represented the Lower and Upper 95% confidence interval. Each set of the experiment was run in triplicate, and each experiment was performed with an additional run to confirm the repeatability. Statistical analyses among multi-group data were carried out using ANOVA followed by Tukey's difference test. * denotes $p < 0.01$.

5.5 Discussion

AMPs are a group of small-molecular-weight proteins secreted by epithelial cells, keratinocytes, Paneth cells, and immune cells, and have antimicrobial activities that can target a broad spectrum of pathogens. Moreover, AMPs are produced by plants, insects, vertebrates and mammals, and are thus considered an ancient component of innate immunity (Wiesner and Vilcinskas 2010). Adipocytes have been reported to play important roles in regulating the host immune response by producing cytokines and adipokines that recruit immune cells. A recent study has added another vital role of adipocytes in innate immunity: differentiating adipocytes secrete AMPs to kill bacteria directly, thus participating in the first-line of defense against infection (Zhang et al. 2015). Numerous studies have reported the adipogenic effects of a variety of environmental pollutants, as well as their modulating roles on cytokine/adipokine productions; however, none of them have been tested for AMP productions in adipocytes. In the current study, we demonstrated that BPA, 2-NAP and lead, which affect adipocyte differentiation, have the capability of influencing the production of the AMP Camp in differentiating adipocytes, indicating potential immunomodulatory properties of these three environmental pollutants. BPA and 2-NAP are capable of upregulating Camp expression during the terminal differentiation phase, while lead upregulates Camp expression at lower concentrations, but suppresses it at higher concentrations. In addition, the mixture of 2-NAP and lead at higher concentrations counterweighs their individual additive or suppressive effects, consequently showing no net co-effect on Camp production.

Cathelicidins are one of the major groups of mammalian AMPs. These evolutionarily conserved ancient types of AMPs contain an N-terminal signal sequence, a conserved cathelin-

like domain, and a C-terminal antimicrobial domain (Zanetti et al. 1995). Humans and mice only produce one cathelicidin, named LL-37/hCAP18 and CRAMP, respectively (Cowland et al. 1995; Gallo et al. 1997; Larrick et al. 1994). Cathelicidins not only have direct antimicrobial ability, but also show other types of functions in immune modulation (De Yang et al. 2000; Huang et al. 1997), angiogenesis (Koczulla et al. 2003; Li et al. 2000), and wound healing (Heilborn et al. 2003; Yang et al. 2006). This study, for the first time, suggests that selected environmental pollutants (BPA, 2-NAP and lead) modulate the production of antimicrobial peptides in adipocytes. BPA at 100 nM was capable of elevating Camp expression on the termination day. Similar to what observed in our adipogenesis-related studies, both 2-NAP and lead induced specific dose-response patterns of Camp expressions when individually exposed to 3T3-L1 cells: 2-NAP upregulated Camp in a dose-dependent manner, while lead upregulated Camp only at lower concentrations, but suppressed its expression at high concentration. Camp has been shown to serve as a chemoattractor for leucocytes and regulate the expression of pro-inflammatory cytokines and chemokines (Agerberth et al. 2000; De Yang et al. 2000; Niyonsaba et al. 2002; Qian et al. 2015; Scott et al. 2002), suggesting its role in generating a chronic inflammation status. Therefore, the modulated production of Camp by environmental pollutants with adipogenic potentials may contribute to an inflammatory status in adipose tissues, providing a novel link between innate immunity and environmental pollutants.

In conclusion, BPA, 2-NAP, and lead, which interfere with adipogenesis, modify the expression of AMPs during adipocytes differentiation in a fashion similar to that we have observed for the adipogenic genes. These findings will help to design future studies to investigate

the role that environmental pollutants play in the development of inflammation/immune-mediated diseases and overweight/obesity.

6 Chapter 6: Conclusions

Environmental pollution is an increasing global issue. Humans are exposed to environmental pollutants mainly via drinking water, food, air, and, to a lesser extent, via skin contact. Numerous studies have shown epidemiological relationships between exposure to environmental pollutants and a wide range of diseases in humans. In addition, direct adverse health effects of exposure to a variety of environmental pollutants have been shown using *in vitro* and *in vivo* research models.

Exposure to selected environmental pollutants has been linked to obesity, a global pandemic disease that affects both adults and children. For example, Bisphenol A (Masuno et al. 2005) and phthalates (Hao et al. 2012) appear to promote adipogenesis and obesity, whereas cadmium (Lee et al. 2012) seems to inhibit it. Many more pollutants remain to be tested. In this study, we determined the adipogenic properties of two chemicals of unknown obesogenic potential, the PAH 2-naphthol and the heavy metal lead. In addition, we assessed, their effects on antimicrobial peptide production during adipogenesis.

Our results show that both 2-NAP and lead exert adipogenic properties *in vitro*, suggesting their potential role in inducing obesity. Indeed, 2-NAP exerts its effect on 3T3-L1 preadipocyte differentiation in a dose-dependent manner. As low as 100 pM of 2-NAP is capable of upregulating the master transcriptional regulators C/EBP α and PPAR γ . Furthermore, we found that even in the absence of insulin, 2-NAP at concentrations of 100nM and higher is able to successfully accelerate the differentiation process. The finding that 2-NAP increases the expression levels of PPAR γ , IRS2, and SREBP1c indicate that 2-NAP contributes to 3T3-L1

differentiation via modulation of the PPAR γ pathway, and IRS2 and SREBP1c molecules in the insulin pathway. On the other hand, our results show that lead is capable of increasing adipogenesis in the mouse 3T3-L1 model following a non-monotonic curve. Lead upregulates adipogenesis by significantly elevating the expression of C/EBP α and aP2 during the early differentiation phase. This early effect might result from the ability of lead to suppress the Wnt/ β -catenin pathway (Beier et al. 2013). Interestingly, lower concentrations of lead are able to sustain upregulation of C/EBP α and aP2 during terminal differentiation, whereas higher lead concentrations exert a suppressive role on PPAR γ and aP2 expression, resulting in lower increased adipogenesis when compared to the lower concentrations. Further studies will explore the mechanism of action by which 2-NAP and higher concentrations of lead influence terminal differentiation.

PAHs and lead co-exist in polluted air deriving from industry waste, vehicle exhaust, tobacco products, and incomplete combustion of oil and gas. High levels of exposure to PAHs and lead are often occupational, occurring for example among mine and road construction workers, and traffic conductors. Exposure is also common in smoking populations (Bae et al. 2010; Huang et al. 2013; Wang et al. 2015). We have shown that co-exposure to high concentrations of 2-NAP and lead results in a weak net effect on 3T3-L1 adipogenesis compared to 2-NAP exposure alone. The suppressive role of lead at high concentrations during the terminal differentiation phase counterbalances the effect of 2-NAP in inducing adipogenesis. This co-effect suggests that 2-NAP and lead may utilize independent pathways to modulate the key transcriptional regulators PPAR γ and C/EBP α and their downstream adipogenic genes. Furthermore, the no net effect also suggests that though both 2-NAP and lower doses of lead are able to upregulate the expression

of PPAR γ , C/EBP α , and aP2, the combination of 2-NAP and lead at high concentrations do not result in an additive effect.

It is important to note that differentiating adipocytes produce cathelicidins, as recently demonstrated by Zhang et al. (2015). Cathelicidins are antimicrobial peptides that directly target pathogens, and also exert chemoattractant and immunomodulatory functions (De Yang et al. 2000). Results from our study show that environmental obesogens modulate production of cathelicidin during adipocyte differentiation. Similarly, on termination day, 2-NAP upregulates cathelicidin in a dose-dependent manner, whereas lead elevates cathelicidin at lower concentrations but suppresses cathelicidin at high concentrations. The combination of 2-NAP and lead at high concentrations results in no net effect.

Being obese or overweight usually is associated with a low-grade, chronic tissue inflammation status, resulting not only in insulin resistance and type 2 diabetes, but also in other obesity-induced disorders, such as cardiovascular disease and cancer (Lackey and Olefsky 2015). Inflammation in adipose tissue results from infiltration and expansion of macrophages producing inflammatory cytokines that interfere with insulin signaling and a loss of protective cells involved in adipose homeostasis (Kohlgruber and Lynch 2015). These local macrophages are responsible for most of the locally secreted TNF- α and for producing a considerable fraction of IL-6 and inducible nitric oxide synthase. In addition, inflammation in adipose tissue is promoted by the enhanced production of pro-inflammatory adipokines secreted by mature adipocytes (Kwon and Pessin 2013). Therefore, adipocytes play an important role in linking obesity and inflammation as well as immune responses. Here, in our study, we have shown the ability of two environmental pollutants, 2-NAP and lead, to induce adipocyte differentiation and regulate production of the

antimicrobial peptide cathelicidin which, as mentioned above, is known to mediate a wide range of protective immune functions. However, altered cathelicidin expression is also associated with chronic inflammation and chronic inflammatory autoimmune diseases (Choi and Mookherjee 2012). Thus, our findings provide new insight into how environmental pollutants could not only be involved in the development of obesity by participating to increased adipogenesis and related inflammatory responses, but also influence host defense at specific sites of adipocyte presence, as for example beneath the skin where adipocytes form subcutaneous fat. However, it should be noted that, at the present time, it is not clear whether or not 2-NAP and lead are able to accumulate at specific sites.

Interestingly, our studies show not only that different pollutants exert different effects, but also that these effects are dose-dependent in a non-linear fashion. Consequently, different doses of different pollutants in different combinations may result in different modulatory effects on adipogenesis and related inflammatory responses mediated by cathelicidin. As discussed above, our results show that both 2-NAP and lead modulate cathelicidin expression. In addition, when compared to the study by Zhang et al. (2015), our results indicate that 2-NAP and low doses of lead induce cathelicidin production for an extended period of time. Indeed, Zhang et al. demonstrate that production of cathelicidin in differentiating adipocytes is time-restricted. In their study, cathelicidin expression was first detected in differentiating adipocytes on day 1, peaked at day 2 to day 4, declined from day 4, and diminished after day 7 to 10 post-induction. Results from our study show upregulated cathelicidin expression on day 8 in cells treated with 2-NAP and lower doses of lead. Therefore, these two environmental pollutants may extend the time frame expression profile of cathelicidin, possibly resulting in a prolonged inflammatory

response. Thus, our results delineate the general steps of a potential pathway that leads from exposure to 2-NAP and lead to the development of obesity. However, *in vivo* studies in animal models are necessary to further explore this potential pathway.

Many different animal models have been developed or are being developed to study obesity (Lutz and Woods 2012). Therefore, one of the challenges will be to choose the most appropriate one, as such a model should be relevant not only to the development of inflammation and obesity, but also to the route of exposure of environmental pollutants, which might be differently metabolized in individual animal species and strains and may induce different inflammatory pathways. Most traditional small rodent obesity models have been developed on the general premise that a primary causal factor of obesity involves the interaction of the brain with peripheral tissues such as gut, liver, pancreas and adipose tissue. However, the concepts at the basis of the obesity-inflammation interrelationship are relatively recent, resulting in less characterized corresponding models. Despite the current uncertainties related to these models, it will be certainly worthwhile to carry out initial studies using the diet-induced obese (DIO) C57BL/6J male mice model, which represent a pre-diabetic type 2 diabetes and obesity model with elevated blood glucose and impaired glucose tolerance (Wang and Liao 2012), along with the corresponding normal/lean mice.

Another critical implication of this study is to highlight the importance of studying the combination of chemicals/pollutants based on the same exposure route. Combined exposure research, which involves studies from different disciplines such as epidemiology, biology, toxicology, and exposure science, has been conducted and emphasized by the National Institute of Environmental Health Sciences (NIEHS) for more than three decades. Traditional toxicology

focuses on the adverse effects and risk assessments of single chemicals. With the help of epidemiological and biological studies, the relationships and mechanisms of single chemicals in inducing diseases have also been revealed. However, actual exposure consists of a mixture of chemical combinations, especially at low-dose levels, on a daily basis and for the entire human lifespan. Therefore, it's imperative to understand complex exposures and their co-effects on human health and disease development, in order to minimize their impact. Here in our study, we have used a well-characterized *in vitro* model to assess two chemicals for their individual and combined effects on adipogenesis, and highlighted their combined effects.

Our results, by demonstrating at least some of the potential adverse health effects of 2-NAP and lead, may also provide direct evidence that the United States Environmental Protection Agency (US EPA) aims to collect in order to plan further studies that may lead to policy changes aimed to reduce, for example, car emissions and air pollution. Additional studies should be carried out to screen more individual chemicals, more combinations of chemicals from the same or different exposure routes, and combinations of nonchemical stressors and chemical exposures, as well as their effects on different diseases using other biological research models.

In conclusion, our results demonstrate that both 2-NAP and lead up-regulate adipocyte differentiation and modulate antimicrobial peptide production, thus suggesting a potential role for these two environmental pollutants in inducing inflammation and obesity. However, treatment with these two chemicals in combination leads to different results, which are dose-dependent. Thus, the evaluation of exposure to chemicals must take into account exposure to mixtures, and needs to overcome the challenges posed by the many chemicals and the different, variable combinations in which they are present in different environments at different times.

REFERENCES

- Abbondanzi F, Campisi T, Focanti M, Guerra R, Iaconi A. 2005. Assessing degradation capability of aerobic indigenous microflora in pah-contaminated brackish sediments. *Marine environmental research* 59:419-434.
- Abu-Hayyeh S, Sian M, Jones KG, Manuel A, Powell JT. 2001. Cadmium accumulation in aortas of smokers. *Arteriosclerosis, thrombosis, and vascular biology* 21:863-867.
- Agerberth B, Charo J, Werr J, Olsson B, Idali F, Lindbom L, et al. 2000. The human antimicrobial and chemotactic peptides II-37 and alpha-defensins are expressed by specific lymphocyte and monocyte populations. *Blood* 96:3086-3093.
- Ajuwon KM, Spurlock ME. 2005. Adiponectin inhibits lps-induced nf-kappab activation and il-6 production and increases ppargamma2 expression in adipocytes. *Am J Physiol Regul Integr Comp Physiol* 288:R1220-1225.
- Alissa EM, Ferns GA. 2011. Heavy metal poisoning and cardiovascular disease. *Journal of toxicology* 2011:870125.
- Anway MD, Skinner MK. 2008. Epigenetic programming of the germ line: Effects of endocrine disruptors on the development of transgenerational disease. *Reproductive biomedicine online* 16:23-25.
- Agency for Toxic Substances and Disease Registry (ATSDR). 1995. Toxicological profile for polycyclic aromatic hydrocarbons (pahs). Atlanta, GA: U.S. Department of Health and Human Services, Public Health Service.
- Agency for Toxic Substances and Disease Registry (ATSDR). 2007. Toxicological profile for lead. Atlanta, GA: U.S. Department of Health and Human Services, Public Health Service.
- Bae S, Pan XC, Kim SY, Park K, Kim YH, Kim H, et al. 2010. Exposures to particulate matter and polycyclic aromatic hydrocarbons and oxidative stress in schoolchildren. *Environmental health perspectives* 118:579-583.
- Bals R, Wang X, Zasloff M, Wilson JM. 1998. The peptide antibiotic II-37/hcap-18 is expressed in epithelia of the human lung where it has broad antimicrobial activity at the airway surface. *Proceedings of the National Academy of Sciences of the United States of America* 95:9541-9546.
- Beier EE, Maher JR, Sheu TJ, Cory-Slechta DA, Berger AJ, Zuscik MJ, et al. 2013. Heavy metal lead exposure, osteoporotic-like phenotype in an animal model, and depression of wnt signaling. *Environmental health perspectives* 121:97-104.

- Beier EE, Inzana JA, Sheu TJ, Shu L, Puzas JE, Mooney RA. 2015. Effects of combined exposure to lead and high-fat diet on bone quality in juvenile male mice. *Environmental health perspectives*.
- Boehm PD. 2006. Chapter 15 - polycyclic aromatic hydrocarbons (pahs). In: *Environmental forensics: Contaminant specific guide*, (Robert D. Morrison BLM, ed). Amsterdam: Elsevier Academic Press, 313–337.
- Boney CM, Gruppuso PA, Faris RA, Frackelton AR. 2000. The critical role of shc in insulin-like growth factor- α -mediated mitogenesis and differentiation in 3T3-L1 preadipocytes. *Mol Endocrinol* 14:805-813.
- Bost F, Aouadi M, Caron L, Binétruy B. 2005. The role of maps in adipocyte differentiation and obesity. *Biochimie* 87:51-56.
- Braff MH, Hawkins MA, Di Nardo A, Lopez-Garcia B, Howell MD, Wong C, et al. 2005. Structure-function relationships among human cathelicidin peptides: Dissociation of antimicrobial properties from host immunostimulatory activities. *J Immunol* 174:4271-4278.
- Bucki R, Leszczyńska K, Namiot A, Sokołowski W. 2010. Cathelicidin II-37: A multitask antimicrobial peptide. *Arch Immunol Ther Exp (Warsz)* 58:15-25.
- Cao Z, Umek RM, McKnight SL. 1991. Regulated expression of three c/ebp isoforms during adipose conversion of 3T3-L1 cells. *Genes Dev* 5:1538-1552.
- Caprio M, Fève B, Claës A, Viengchareun S, Lombès M, Zennaro M-C. 2007. Pivotal role of the mineralocorticoid receptor in corticosteroid-induced adipogenesis. *The FASEB Journal* 21:2185-2194.
- Centers for Disease Control and Prevention (CDC). 2015. Fourth report on human exposure to environmental chemicals, updated tables, (february, 2015). Atlanta, GA: U.S. Department of Health and Human Services, Centers for Disease Control and Prevention. <http://www.cdc.gov/exposurereport/>.
- Centers for Disease Control and Prevention (CDC). 2002. Childhood lead poisoning associated with tamarind candy and folk remedies--california, 1999-2000. *MMWR Morbidity and mortality weekly report* 51:684-686.
- Chan DI, Prenner EJ, Vogel HJ. 2006. Tryptophan- and arginine-rich antimicrobial peptides: Structures and mechanisms of action. *Biochim Biophys Acta* 1758:1184-1202.
- Chang WK, Wimley WC, Searson PC, Hristova K, Merzlyakov M. 2008. Characterization of antimicrobial peptide activity by electrochemical impedance spectroscopy. *Biochim Biophys Acta* 1778:2430-2436.

- Choi KY, Mookherjee N. 2012. Multiple immune-modulatory functions of cathelicidin host defense peptides. *Front Immunol* 3:149.
- Collins S. 2005. Overview of clinical perspectives and mechanisms of obesity. *Birth Defects Res A Clin Mol Teratol* 73:470-471.
- Couse JF, Dixon D, Yates M, Moore AB, Ma L, Maas R, et al. 2001. Estrogen receptor-alpha knockout mice exhibit resistance to the developmental effects of neonatal diethylstilbestrol exposure on the female reproductive tract. *Developmental biology* 238:224-238.
- Covas DT, Panepucci RA, Fontes AM, Silva WA, Orellana MD, Freitas MC, et al. 2008. Multipotent mesenchymal stromal cells obtained from diverse human tissues share functional properties and gene-expression profile with cd146+ perivascular cells and fibroblasts. *Exp Hematol* 36:642-654.
- Cowland JB, Johnsen AH, Borregaard N. 1995. Hcap-18, a cathelin/pro-bactenecin-like protein of human neutrophil specific granules. *FEBS Lett* 368:173-176.
- Davila DR, Romero DL, Burchiel SW. 1996. Human t cells are highly sensitive to suppression of mitogenesis by polycyclic aromatic hydrocarbons and this effect is differentially reversed by alpha-naphthoflavone. *Toxicol Appl Pharmacol* 139:333-341.
- Davis LA, Zur Nieden NI. 2008. Mesodermal fate decisions of a stem cell: The wnt switch. *Cell Mol Life Sci* 65:2658-2674.
- De Yang, Chen Q, Schmidt AP, Anderson GM, Wang JM, Wooters J, et al. 2000. LI-37, the neutrophil granule- and epithelial cell-derived cathelicidin, utilizes formyl peptide receptor-like 1 (fpr1) as a receptor to chemoattract human peripheral blood neutrophils, monocytes, and t cells. *The Journal of experimental medicine* 192:1069-1074.
- Denissenko MF, Pao A, Tang M, Pfeifer GP. 1996. Preferential formation of benzo[a]pyrene adducts at lung cancer mutational hotspots in p53. *Science* 274:430-432.
- Dhimolea E, Wadia PR, Murray TJ, Settles ML, Treitman JD, Sonnenschein C, et al. 2014. Prenatal exposure to bpa alters the epigenome of the rat mammary gland and increases the propensity to neoplastic development. *PLoS One* 9:e99800.
- Diamanti-Kandarakis E, Bourguignon JP, Giudice LC, Hauser R, Prins GS, Soto AM, et al. 2009. Endocrine-disrupting chemicals: An endocrine society scientific statement. *Endocrine reviews* 30:293-342.
- Donald JM, Bradley M, O'Grady JE, Cutler MG, Moore MR. 1988. Effects of low-level lead exposure on 24 h activity patterns in the mouse. *Toxicology letters* 42:137-147.

- Doss M, White MR, Teclé T, Hartshorn KL. 2010. Human defensins and II-37 in mucosal immunity. *J Leukoc Biol* 87:79-92.
- Elgazar-Carmon V, Rudich A, Hadad N, Levy R. 2008. Neutrophils transiently infiltrate intra-abdominal fat early in the course of high-fat feeding. *J Lipid Res* 49:1894-1903.
- Flora SJ, Saxena G, Gautam P, Kaur P, Gill KD. 2007. Response of lead-induced oxidative stress and alterations in biogenic amines in different rat brain regions to combined administration of dmsa and miadmsa. *Chemico-biological interactions* 170:209-220.
- Freedman DS, Mei Z, Srinivasan SR, Berenson GS, Dietz WH. 2007. Cardiovascular risk factors and excess adiposity among overweight children and adolescents: The bogalusa heart study. *J Pediatr* 150:12-17.e12.
- Gallo RL, Kim KJ, Bernfield M, Kozak CA, Zanetti M, Merluzzi L, et al. 1997. Identification of cramp, a cathelin-related antimicrobial peptide expressed in the embryonic and adult mouse. *J Biol Chem* 272:13088-13093.
- Gan S, Lau EV, Ng HK. 2009. Remediation of soils contaminated with polycyclic aromatic hydrocarbons (pahs). *Journal of hazardous materials* 172:532-549.
- Goldstein GW. 1993. Evidence that lead acts as a calcium substitute in second messenger metabolism. *Neurotoxicology* 14:97-101.
- Gonzalez GA, Montminy MR. 1989. Cyclic amp stimulates somatostatin gene transcription by phosphorylation of creb at serine 133. *Cell* 59:675-680.
- Gorbenko O, Filonenko V, Gout I. 2006. Generation and characterization of monoclonal antibodies against fabp4. *Hybridoma (Larchmt)* 25:86-90.
- Grant RW, Dixit VD. 2015. Adipose tissue as an immunological organ. *Obesity (Silver Spring)* 23:512-518.
- Green H, Kehinde O. 1974. Sublines of mouse 3t3 cells that accumulate lipid. *Cell* 1:113-116.
- Green H, Meuth M. 1974. An established pre-adipose cell line and its differentiation in culture. *Cell* 3:127-133.
- Green H, Kehinde O. 1975. An established preadipose cell line and its differentiation in culture. li. Factors affecting the adipose conversion. *Cell* 5:19-27.
- Gudmundsson GH, Agerberth B, Odeberg J, Bergman T, Olsson B, Salcedo R. 1996. The human gene fall39 and processing of the cathelin precursor to the antibacterial peptide II-37 in granulocytes. *Eur J Biochem* 238:325-332.

- Haguenoer JM, Shirali P, Hannotiaux MH, Nisse-Ramond C. 1996. Interactive effects of polycyclic aromatic hydrocarbons and iron oxides particles. *Epidemiological and fundamental aspects. Cent Eur J Public Health* 4 Suppl:41-45.
- Hamir AN, Sullivan ND, Handson PD, Wilkinson JS, Lavelle RB. 1981. Clinical signs, radiology and tissue lead distribution of dogs administered a mixture of lead chloride, lead bromide and lead sulphate. *Australian veterinary journal* 57:401-406.
- Hancock RE, Scott MG. 2000. The role of antimicrobial peptides in animal defenses. *Proceedings of the National Academy of Sciences of the United States of America* 97:8856-8861.
- Hancock RE, Sahl HG. 2006. Antimicrobial and host-defense peptides as new anti-infective therapeutic strategies. *Nat Biotechnol* 24:1551-1557.
- Hao C, Cheng X, Xia H, Ma X. 2012. The endocrine disruptor mono-(2-ethylhexyl) phthalate promotes adipocyte differentiation and induces obesity in mice. *Biosci Rep* 32:619-629.
- Hassan M, Latif N, Yacoub M. 2012. Adipose tissue: Friend or foe? *Nat Rev Cardiol* 9:689-702.
- Heilborn JD, Nilsson MF, Kratz G, Weber G, Sørensen O, Borregaard N, et al. 2003. The cathelicidin anti-microbial peptide ll-37 is involved in re-epithelialization of human skin wounds and is lacking in chronic ulcer epithelium. *J Invest Dermatol* 120:379-389.
- Hermes-Lima M, Pereira B, Bechara EJ. 1991. Are free radicals involved in lead poisoning? *Xenobiotica; the fate of foreign compounds in biological systems* 21:1085-1090.
- Huang H, Song TJ, Li X, Hu L, He Q, Liu M, et al. 2009. Bmp signaling pathway is required for commitment of c3h10t1/2 pluripotent stem cells to the adipocyte lineage. *Proceedings of the National Academy of Sciences of the United States of America* 106:12670-12675.
- Huang HB, Chen GW, Wang CJ, Lin YY, Liou SH, Lai CH, et al. 2013. Exposure to heavy metals and polycyclic aromatic hydrocarbons and DNA damage in taiwanese traffic conductors. *Cancer Epidemiol Biomarkers Prev* 22:102-108.
- Huang HJ, Ross CR, Blecha F. 1997. Chemoattractant properties of pr-39, a neutrophil antibacterial peptide. *J Leukoc Biol* 61:624-629.
- Inoue G, Cheatham B, Emkey R, Kahn CR. 1998. Dynamics of insulin signaling in 3t3-l1 adipocytes. Differential compartmentalization and trafficking of insulin receptor substrate (irs)-1 and irs-2. *J Biol Chem* 273:11548-11555.
- Janesick A, Blumberg B. 2011. Endocrine disrupting chemicals and the developmental programming of adipogenesis and obesity. *Birth Defects Res C Embryo Today* 93:34-50.
- Jeong S, Yoon M. 2011. 17 β -estradiol inhibition of ppar γ -induced adipogenesis and adipocyte-specific gene expression. *Acta Pharmacol Sin* 32:230-238.

- Jihen el H, Imed M, Fatima H, Abdelhamid K. 2009. Protective effects of selenium (se) and zinc (zn) on cadmium (cd) toxicity in the liver of the rat: Effects on the oxidative stress. *Ecotoxicology and environmental safety* 72:1559-1564.
- Jung F, Haendeler J, Goebel C, Zeiher AM, Dimmeler S. 2000. Growth factor-induced phosphoinositide 3-oh kinase/akt phosphorylation in smooth muscle cells: Induction of cell proliferation and inhibition of cell death. *Cardiovasc Res* 48:148-157.
- Kampa M, Castanas E. 2008. Human health effects of air pollution. *Environmental pollution* 151:362-367.
- Kapitulnik J, Levin W, Morecki R, Dansette PM, Jerina DM, Conney AH. 1977. Hydration of arene and alkene oxides by epoxide hydrase in human liver microsomes. *Clinical pharmacology and therapeutics* 21:158-165.
- Katsouyanni K. 2003. Ambient air pollution and health. *British medical bulletin* 68:143-156.
- Kawanami D, Maemura K, Takeda N, Harada T, Nojiri T, Imai Y, et al. 2004. Direct reciprocal effects of resistin and adiponectin on vascular endothelial cells: A new insight into adipocytokine-endothelial cell interactions. *Biochemical and biophysical research communications* 314:415-419.
- Kiefer F, Cumpelik O, Wiebel FJ. 1988. Metabolism and cytotoxicity of benzo(a)pyrene in the human lung tumour cell line nci-h322. *Xenobiotica; the fate of foreign compounds in biological systems* 18:747-755.
- Kim H, Kang JW, Ku SY, Kim SH, Cho SH, Koong SS, et al. 2005. Effect of 'pc game room' use and polycyclic aromatic hydrocarbon exposure on plasma testosterone concentrations in young male koreans. *Hum Reprod* 20:598-603.
- Kim R, Hu H, Rotnitzky A, Bellinger D, Needleman H. 1995. A longitudinal study of chronic lead exposure and physical growth in boston children. *Environmental health perspectives* 103:952-957.
- Koczulla R, von Degenfeld G, Kupatt C, Krötz F, Zahler S, Gloe T, et al. 2003. An angiogenic role for the human peptide antibiotic ll-37/hcap-18. *J Clin Invest* 111:1665-1672.
- Kohlgruber A, Lynch L. 2015. Adipose tissue inflammation in the pathogenesis of type 2 diabetes. *Curr Diab Rep* 15:92.
- Kopelman PG. 2000. Obesity as a medical problem. *Nature* 404:635-643.
- Kwon H, Pessin JE. 2013. Adipokines mediate inflammation and insulin resistance. *Front Endocrinol (Lausanne)* 4:71.

- Lackey DE, Olefsky JM. 2015. Regulation of metabolism by the innate immune system. *Nature reviews*.
- Laher JM, Rigler MW, Vetter RD, Barrowman JA, Patton JS. 1984. Similar bioavailability and lymphatic transport of benzo(a)pyrene when administered to rats in different amounts of dietary fat. *J Lipid Res* 25:1337-1342.
- Lai Y, Gallo RL. 2009. Amped up immunity: How antimicrobial peptides have multiple roles in immune defense. *Trends Immunol* 30:131-141.
- Larrick JW, Hirata M, Zheng H, Zhong J, Bolin D, Cavallion JM, et al. 1994. A novel granulocyte-derived peptide with lipopolysaccharide-neutralizing activity. *J Immunol* 152:231-240.
- Larrick JW, Lee J, Ma S, Li X, Francke U, Wright SC, et al. 1996. Structural, functional analysis and localization of the human cap18 gene. *FEBS Lett* 398:74-80.
- Law RJ, Kelly C, Baker K, Jones J, McIntosh AD, Moffat CF. 2002. Toxic equivalency factors for pah and their applicability in shellfish pollution monitoring studies. *J Environ Monit* 4:383-388.
- Leasure JL, Giddabasappa A, Chaney S, Johnson JE, Jr., Pothakos K, Lau YS, et al. 2008. Low-level human equivalent gestational lead exposure produces sex-specific motor and coordination abnormalities and late-onset obesity in year-old mice. *Environmental health perspectives* 116:355-361.
- Lee CC, Sun Y, Qian S, Huang HW. 2011. Transmembrane pores formed by human antimicrobial peptide II-37. *Biophys J* 100:1688-1696.
- Lee EJ, Moon JY, Yoo BS. 2012. Cadmium inhibits the differentiation of 3t3-l1 preadipocyte through the c/ebp α and ppar γ pathways. *Drug and chemical toxicology* 35:225-231.
- Lefterova MI, Lazar MA. 2009. New developments in adipogenesis. *Trends Endocrinol Metab* 20:107-114.
- Li C, Yang X, Xu M, Zhang J, Sun N. 2013. Epigenetic marker (line-1 promoter) methylation level was associated with occupational lead exposure. *Clin Toxicol (Phila)* 51:225-229.
- Li J, Post M, Volk R, Gao Y, Li M, Metais C, et al. 2000. Pr39, a peptide regulator of angiogenesis. *Nat Med* 6:49-55.
- Lin CS, Xin ZC, Deng CH, Ning H, Lin G, Lue TF. 2010. Defining adipose tissue-derived stem cells in tissue and in culture. *Histol Histopathol* 25:807-815.
- Loffreda S, Yang SQ, Lin HZ, Karp CL, Brengman ML, Wang DJ, et al. 1998. Leptin regulates proinflammatory immune responses. *FASEB J* 12:57-65.

- Lutz TA, Woods SC. 2012. Overview of animal models of obesity. *Curr Protoc Pharmacol* Chapter 5:Unit5.61.
- Mahaffey KR, Annett JL, Roberts J, Murphy RS. 1982. National estimates of blood lead levels: United states, 1976-1980: Association with selected demographic and socioeconomic factors. *The New England journal of medicine* 307:573-579.
- Maliszewska-Kordybach B. 1999. Sources, concentrations, fate and effects of polycyclic aromatic hydrocarbons (pahs) in the environment. Part a: Pahs in air. *Poish Journal of Environmental Studies* Vol. 8:131-136.
- Manoli E, Samara C. 1999. Occurrence and mass balance of polycyclic aromatic hydrocarbons in the thessaloniki sewage treatment plant. *J Environ Qual* 28:176-187.
- Markowitz M. 2000. Lead poisoning. *Pediatrics in review / American Academy of Pediatrics* 21:327-335.
- Masuno H, Iwanami J, Kidani T, Sakayama K, Honda K. 2005. Bisphenol a accelerates terminal differentiation of 3t3-l1 cells into adipocytes through the phosphatidylinositol 3-kinase pathway. *Toxicol Sci* 84:319-327.
- Mehra A, Macdonald I, Pillay TS. 2007. Variability in 3t3-l1 adipocyte differentiation depending on cell culture dish. *Anal Biochem* 362:281-283.
- Meyer PA, Brown MJ, Falk H. 2008. Global approach to reducing lead exposure and poisoning. *Mutation research* 659:166-175.
- Mokdad AH, Serdula MK, Dietz WH, Bowman BA, Marks JS, Koplan JP. 1999. The spread of the obesity epidemic in the united states, 1991-1998. *JAMA* 282:1519-1522.
- Mokdad AH, Ford ES, Bowman BA, Dietz WH, Vinicor F, Bales VS, et al. 2003. Prevalence of obesity, diabetes, and obesity-related health risk factors, 2001. *JAMA* 289:76-79.
- Monteith DK, Novotny A, Michalopoulos G, Strom SC. 1987. Metabolism of benzo[a]pyrene in primary cultures of human hepatocytes: Dose-response over a four-log range. *Carcinogenesis* 8:983-988.
- Moral R, Wang R, Russo IH, Lamartiniere CA, Pereira J, Russo J. 2008. Effect of prenatal exposure to the endocrine disruptor bisphenol a on mammary gland morphology and gene expression signature. *The Journal of endocrinology* 196:101-112.
- Neel BA, Brady MJ, Sargis RM. 2013. The endocrine disrupting chemical tolylfluaniid alters adipocyte metabolism via glucocorticoid receptor activation. *Mol Endocrinol* 27:394-406.
- Newbold RR. 2010. Impact of environmental endocrine disrupting chemicals on the development of obesity. *Hormones (Athens)* 9:206-217.

- Nisbet IC, LaGoy PK. 1992. Toxic equivalency factors (tefs) for polycyclic aromatic hydrocarbons (pahs). *Regulatory toxicology and pharmacology* : RTP 16:290-300.
- Nishimura S, Manabe I, Nagasaki M, Eto K, Yamashita H, Ohsugi M, et al. 2009. Cd8+ effector t cells contribute to macrophage recruitment and adipose tissue inflammation in obesity. *Nat Med* 15:914-920.
- Niyonsaba F, Iwabuchi K, Someya A, Hirata M, Matsuda H, Ogawa H, et al. 2002. A cathelicidin family of human antibacterial peptide ll-37 induces mast cell chemotaxis. *Immunology* 106:20-26.
- Ogden CL, Carroll MD, Kit BK, Flegal KM. 2014. Prevalence of childhood and adult obesity in the united states, 2011-2012. *JAMA* 311:806-814.
- Ouchi N, Parker JL, Lugus JJ, Walsh K. 2011. Adipokines in inflammation and metabolic disease. *Nat Rev Immunol* 11:85-97.
- Pantoja C, Huff JT, Yamamoto KR. 2008. Glucocorticoid signaling defines a novel commitment state during adipogenesis in vitro. *Mol Biol Cell* 19:4032-4041.
- Philip AT, Gerson B. 1994. Lead poisoning--part i. Incidence, etiology, and toxicokinetics. *Clinics in laboratory medicine* 14:423-444.
- Poloni A, Maurizi G, Ciarlantini M, Medici M, Mattiucci D, Mancini S, et al. 2015. Interaction between human mature adipocytes and lymphocytes induces t-cell proliferation. *Cytotherapy* 17:1292-1301.
- Poschl U. 2005. Atmospheric aerosols: Composition, transformation, climate and health effects. *Angewandte Chemie* 44:7520-7540.
- Prozialeck WC, Edwards JR, Nebert DW, Woods JM, Barchowsky A, Atchison WD. 2008. The vascular system as a target of metal toxicity. *Toxicol Sci* 102:207-218.
- Qian L, Chen W, Sun W, Li M, Zheng R, Qian Q, et al. 2015. Antimicrobial peptide ll-37 along with peptidoglycan drive monocyte polarization toward cd14(high)cd16(+) subset and may play a crucial role in the pathogenesis of psoriasis guttata. *Am J Transl Res* 7:1081-1094.
- Ramesh A, Walker SA, Hood DB, Guillen MD, Schneider K, Weyand EH. 2004. Bioavailability and risk assessment of orally ingested polycyclic aromatic hydrocarbons. *International journal of toxicology* 23:301-333.
- Ramji DP, Foka P. 2002. Ccaat/enhancer-binding proteins: Structure, function and regulation. *Biochem J* 365:561-575.
- Reusch JE, Colton LA, Klemm DJ. 2000. Creb activation induces adipogenesis in 3t3-l1 cells. *Mol Cell Biol* 20:1008-1020.

- Romero DL, Mounho BJ, Lauer FT, Born JL, Burchiel SW. 1997. Depletion of glutathione by benzo(a)pyrene metabolites, ionomycin, thapsigargin, and phorbol myristate in human peripheral blood mononuclear cells. *Toxicol Appl Pharmacol* 144:62-69.
- Rosado CJ, Kondos S, Bull TE, Kuiper MJ, Law RH, Buckle AM, et al. 2008. The macpf/cdc family of pore-forming toxins. *Cell Microbiol* 10:1765-1774.
- Rosen ED, Sarraf P, Troy AE, Bradwin G, Moore K, Milstone DS, et al. 1999. Ppar gamma is required for the differentiation of adipose tissue in vivo and in vitro. *Mol Cell* 4:611-617.
- Rosen ED, Hsu CH, Wang X, Sakai S, Freeman MW, Gonzalez FJ, et al. 2002. C/ebpalpha induces adipogenesis through ppargamma: A unified pathway. *Genes Dev* 16:22-26.
- Rosen ED, MacDougald OA. 2006. Adipocyte differentiation from the inside out. *Nat Rev Mol Cell Biol* 7:885-896.
- Ross SE, Hemati N, Longo KA, Bennett CN, Lucas PC, Erickson RL, et al. 2000. Inhibition of adipogenesis by wnt signaling. *Science* 289:950-953.
- Rubin CS, Hirsch A, Fung C, Rosen OM. 1978. Development of hormone receptors and hormonal responsiveness in vitro. Insulin receptors and insulin sensitivity in the preadipocyte and adipocyte forms of 3t3-l1 cells. *J Biol Chem* 253:7570-7578.
- Saad MJ, Folli F, Araki E, Hashimoto N, Csermely P, Kahn CR. 1994. Regulation of insulin receptor, insulin receptor substrate-1 and phosphatidylinositol 3-kinase in 3t3-f442a adipocytes. Effects of differentiation, insulin, and dexamethasone. *Mol Endocrinol* 8:545-557.
- Sainio EL, Jolanki R, Hakala E, Kanerva L. 2000. Metals and arsenic in eye shadows. *Contact dermatitis* 42:5-10.
- Schug TT, Janesick A, Blumberg B, Heindel JJ. 2011. Endocrine disrupting chemicals and disease susceptibility. *The Journal of steroid biochemistry and molecular biology* 127:204-215.
- Schultz TW, Sinks GD. 2002. Xenoestrogenic gene expression: Structural features of active polycyclic aromatic hydrocarbons. *Environmental toxicology and chemistry / SETAC* 21:783-786.
- Scinicariello F, Buser MC, Mevissen M, Portier CJ. 2013. Blood lead level association with lower body weight in nhanes 1999-2006. *Toxicol Appl Pharmacol* 273:516-523.
- Scinicariello F, Buser MC. 2014. Urinary polycyclic aromatic hydrocarbons and childhood obesity: Nhanes (2001-2006). *Environmental health perspectives* 122:299-303.
- Scott MG, Davidson DJ, Gold MR, Bowdish D, Hancock RE. 2002. The human antimicrobial peptide Il-37 is a multifunctional modulator of innate immune responses. *J Immunol* 169:3883-3891.

- Shimada T. 2006. Xenobiotic-metabolizing enzymes involved in activation and detoxification of carcinogenic polycyclic aromatic hydrocarbons. *Drug metabolism and pharmacokinetics* 21:257-276.
- Shu HP, Nichols AV. 1979. Benzo(a)pyrene uptake by human plasma lipoproteins in vitro. *Cancer Res* 39:1224-1230.
- Sun H, Shen OX, Xu XL, Song L, Wang XR. 2008. Carbaryl, 1-naphthol and 2-naphthol inhibit the beta-1 thyroid hormone receptor-mediated transcription in vitro. *Toxicology* 249:238-242.
- Tabb MM, Blumberg B. 2006. New modes of action for endocrine-disrupting chemicals. *Mol Endocrinol* 20:475-482.
- Tang Q-Q, Grønborg M, Huang H, Kim J-W, Otto TC, Pandey A, et al. 2005. Sequential phosphorylation of ccaat enhancer-binding protein β by mapk and glycogen synthase kinase 3 β is required for adipogenesis. *Proceedings of the National Academy of Sciences of the United States of America* 102:9766-9771.
- Tang QQ, Lane MD. 1999. Activation and centromeric localization of ccaat/enhancer-binding proteins during the mitotic clonal expansion of adipocyte differentiation. *Genes Dev* 13:2231-2241.
- Tang QQ, Otto TC, Lane MD. 2003. Mitotic clonal expansion: A synchronous process required for adipogenesis. *Proceedings of the National Academy of Sciences of the United States of America* 100:44-49.
- Tang QQ, Lane MD. 2012. Adipogenesis: From stem cell to adipocyte. *Annu Rev Biochem* 81:715-736.
- Tchounwou PB, Yedjou CG, Patlolla AK, Sutton DJ. 2012. Heavy metal toxicity and the environment. *Exs* 101:133-164.
- Terasaki M, Shiraishi F, Fukazawa H, Makino M. 2007. Occurrence and estrogenicity of phenolics in paper-recycling process water: Pollutants originating from thermal paper in waste paper. *Environmental toxicology and chemistry / SETAC* 26:2356-2366.
- Tjabringa GS, Aarbiou J, Ninaber DK, Drijfhout JW, Sørensen OE, Borregaard N, et al. 2003. The antimicrobial peptide II-37 activates innate immunity at the airway epithelial surface by transactivation of the epidermal growth factor receptor. *J Immunol* 171:6690-6696.
- Tokumar S, Sayama K, Shirakata Y, Komatsuzawa H, Ouhara K, Hanakawa Y, et al. 2005. Induction of keratinocyte migration via transactivation of the epidermal growth factor receptor by the antimicrobial peptide II-37. *J Immunol* 175:4662-4668.

- Tong Q, Dalgin G, Xu H, Ting C-N, Leiden JM, Hotamisligil GS. 2000. Function of gata transcription factors in preadipocyte-adipocyte transition. *Science* 290:134-138.
- Tong Q, Tsai J, Tan G, Dalgin G, Hotamisligil GS. 2005. Interaction between gata and the c/ebp family of transcription factors is critical in gata-mediated suppression of adipocyte differentiation. *Molecular and Cellular Biology* 25:706-715.
- Vakharia DD, Liu N, Pause R, Fasco M, Bessette E, Zhang QY, et al. 2001. Effect of metals on polycyclic aromatic hydrocarbon induction of cyp1a1 and cyp1a2 in human hepatocyte cultures. *Toxicol Appl Pharmacol* 170:93-103.
- Valentino R, D'Esposito V, Passaretti F, Liotti A, Cabaro S, Longo M, et al. 2013. Bisphenol-a impairs insulin action and up-regulates inflammatory pathways in human subcutaneous adipocytes and 3t3-l1 cells. *PLoS One* 8:e82099.
- Valko M, Morris H, Cronin MT. 2005. Metals, toxicity and oxidative stress. *Current medicinal chemistry* 12:1161-1208.
- Wang CY, Liao JK. 2012. A mouse model of diet-induced obesity and insulin resistance. *Methods Mol Biol* 821:421-433.
- Wang G. 2015. Improved methods for classification, prediction, and design of antimicrobial peptides. *Methods Mol Biol* 1268:43-66.
- Wang T, Feng W, Kuang D, Deng Q, Zhang W, Wang S, et al. 2015. The effects of heavy metals and their interactions with polycyclic aromatic hydrocarbons on the oxidative stress among coke-oven workers. *Environ Res* 140:405-413.
- Weisberg SP, McCann D, Desai M, Rosenbaum M, Leibel RL, Ferrante AW. 2003. Obesity is associated with macrophage accumulation in adipose tissue. *J Clin Invest* 112:1796-1808.
- Wiesner J, Vilcinskas A. 2010. Antimicrobial peptides: The ancient arm of the human immune system. *Virulence* 1:440-464.
- Winer DA, Winer S, Shen L, Wadia PP, Yantha J, Paltser G, et al. 2011. B cells promote insulin resistance through modulation of t cells and production of pathogenic igg antibodies. *Nat Med* 17:610-617.
- Woolf AD, Woolf NT. 2005. Childhood lead poisoning in 2 families associated with spices used in food preparation. *Pediatrics* 116:e314-318.
- World Health Organization (WHO). 2015. Obesity and overweight. Available: <http://www.who.int/mediacentre/factsheets/fs311/en/> [accessed October 19 2015].

- Wright RO, Schwartz J, Wright RJ, Bollati V, Tarantini L, Park SK, et al. 2010. Biomarkers of lead exposure and DNA methylation within retrotransposons. *Environmental health perspectives* 118:790-795.
- Wu Z, Xie Y, Bucher NL, Farmer SR. 1995. Conditional ectopic expression of c/ebp beta in nih-3t3 cells induces ppar gamma and stimulates adipogenesis. *Genes Dev* 9:2350-2363.
- Wu Z, Bucher NL, Farmer SR. 1996. Induction of peroxisome proliferator-activated receptor gamma during the conversion of 3t3 fibroblasts into adipocytes is mediated by c/ebpbeta, c/ebpdelta, and glucocorticoids. *Molecular and Cellular Biology* 16:4128-4136.
- Wu Z, Rosen ED, Brun R, Hauser S, Adelmant G, Troy AE, et al. 1999. Cross-regulation of c/ebp alpha and ppar gamma controls the transcriptional pathway of adipogenesis and insulin sensitivity. *Mol Cell* 3:151-158.
- Wulster-Radcliffe MC, Ajuwon KM, Wang J, Christian JA, Spurlock ME. 2004. Adiponectin differentially regulates cytokines in porcine macrophages. *Biochemical and biophysical research communications* 316:924-929.
- Wyde ME, Bartolucci E, Ueda A, Zhang H, Yan B, Negishi M, et al. 2003. The environmental pollutant 1,1-dichloro-2,2-bis (p-chlorophenyl)ethylene induces rat hepatic cytochrome p450 2b and 3a expression through the constitutive androstane receptor and pregnane x receptor. *Molecular pharmacology* 64:474-481.
- Yan Z, Zhang H, Maher C, Arteaga-Solis E, Champagne FA, Wu L, et al. 2014. Prenatal polycyclic aromatic hydrocarbon, adiposity, peroxisome proliferator-activated receptor (ppar) gamma methylation in offspring, grand-offspring mice. *PLoS One* 9:e110706.
- Yang L, Harroun TA, Weiss TM, Ding L, Huang HW. 2001. Barrel-stave model or toroidal model? A case study on melittin pores. *Biophys J* 81:1475-1485.
- Yang W, Omaye ST. 2009. Air pollutants, oxidative stress and human health. *Mutation research* 674:45-54.
- Yang YH, Wu WK, Tai EK, Wong HP, Lam EK, So WH, et al. 2006. The cationic host defense peptide rcramp promotes gastric ulcer healing in rats. *J Pharmacol Exp Ther* 318:547-554.
- Yeh WC, Cao Z, Classon M, McKnight SL. 1995. Cascade regulation of terminal adipocyte differentiation by three members of the c/ebp family of leucine zipper proteins. *Genes Dev* 9:168-181.
- Yu W, Chen Z, Zhang J, Zhang L, Ke H, Huang L, et al. 2008. Critical role of phosphoinositide 3-kinase cascade in adipogenesis of human mesenchymal stem cells. *Mol Cell Biochem* 310:11-18.

- Yun SJ, Kim EK, Tucker DF, Kim CD, Birnbaum MJ, Bae SS. 2008. Isoform-specific regulation of adipocyte differentiation by akt/protein kinase balpha. *Biochemical and biophysical research communications* 371:138-143.
- Zanetti M, Gennaro R, Romeo D. 1995. Cathelicidins: A novel protein family with a common proregion and a variable c-terminal antimicrobial domain. *FEBS Lett* 374:1-5.
- Zebisch K, Voigt V, Wabitsch M, Brandsch M. 2012. Protocol for effective differentiation of 3t3-l1 cells to adipocytes. *Anal Biochem* 425:88-90.
- Zhang JW, Klemm DJ, Vinson C, Lane MD. 2004. Role of creb in transcriptional regulation of ccaat/enhancer-binding protein beta gene during adipogenesis. *J Biol Chem* 279:4471-4478.
- Zhang LJ, Guerrero-Juarez CF, Hata T, Bapat SP, Ramos R, Plikus MV, et al. 2015. Innate immunity. Dermal adipocytes protect against invasive staphylococcus aureus skin infection. *Science* 347:67-71.